UNIVERSITY OF SOUTHAMPTON

Faculty of Physical Sciences and Engineering

Electronics and Computer Science

A Cellular Model of the Electrical Characteristics of Skin

by

Luke Davies

Thesis for the degree of Doctor of Philosophy

May 2018

University of Southampton

Abstract

Faculty of Physical Sciences and Engineering
Electronics and Computer Science

Doctor of Philosophy

A Cellular Model of the Electrical Characteristics of Skin

By Luke Davies

The dielectric properties of skin are of particular interest in the fields of Functional Electrical Stimulation (FES), diagnostic procedures such as Electrocardiogram and cancer treatment. This thesis is concerned primarily with the effect of hydration and electroporation on skin impedance when signals used in FES are applied. Skin impedance has typically been represented by an equivalent circuit of varying complexities in the literature; however this approach does not incorporate the effects of hydration and electroporation. Alternatives to this include simulation of skin cells undergoing electrical stimulation and direct experimentation either in vitro or in vivo. This thesis aims to expand the current understanding in this field with particular focus on the effects of hydration and electroporation through simulation. The stratum corneum (SC) has the most dominant impact on overall impedance of skin, particularly at low frequencies, and therefore was the focus for all of the simulations.

The models representing individual cells showed strong agreement with experimental data in the literature in terms of their impedance when exposed to a variety of frequencies and input voltages. Expanding these models to include a greater number of cells continued to generate agreement with experimental data from the literature. When the conductivity of the SC cells were altered to represent the effect of hydration, the simulations showed a substantial reduction in impedance from 53kΩ to 27kΩ, which can be represented as a double exponential decay. A further model was produced with a cell membrane conductivity dependent upon the voltage across the membrane to represent the presence of electropores. The results showed that when signals typically used in FES are applied, electropores are formed. The presence of electropores causes a decrease in skin impedance from 76kΩ to 22kΩ.

Contents

List of Abbreviations

AC – Alternating Current

DC – Direct Current

ECG - Electrocardiogram

EEG – Electroencephalogram

EMG - Electromyography

FEM – Finite Element Method

FES – Functional Electrical Stimulation

ITV – Induced Transmembrane Voltage

MU – Motor Unit

NMES - Neuromuscular electrical stimulation

SC – Stratum Corneum

TEWL – Transepidermal water loss

List of Figures

List of Tables

Acknowledgements

I would like to thank Dr Paul Chappell for all his support. He was always willing to help and his guidance has been invaluable. I would like to thank my friends Ben, Lewys and Becky for making my time during my PhD so enjoyable. I would like to thank my parents for their unwavering faith and support.

I would also like to give a special thanks to my wife Holly, whose constant encouragement and confidence kept me on track. Finally, I would like to thank my daughter Harriet, whose early arrival helped expedite the completion of this work.

1 Introduction

This thesis will aim to expand upon the current understanding of the skin's response to electrical stimulus, in particular by focusing on factors such as hydration and electroporation. The most recent relevant research has proposed an equivalent circuit model of skin that does not take into consideration factors such as electroporation and hydration. For the purposes of this thesis, hydration refers to the amount of water retained in the skin, specifically the upper layers of the skin from external solutions [1]. Electroporation refers to the creation of pores in a cell membrane by applying an external electric field [2]. This effect can be either reversible or irreversible depending on the strength of the applied field. An aim of this thesis is to help improve Functional Electrical Stimulation (FES) and better understand individual differences in response to electrical stimulation. This could help in any clinical or research setting that aims to use or develop non-invasive techniques. This particular thesis will review existing research into the behaviour of skin in order to best create a finite element model (FEM) to replicate how the skin will behave when electroporation and hydration variants are considered. This is a currently under-researched area which has a substantial impact on the behaviour of skin, therefore impacting on the reliability of applications. Following review of the existing literature the Epidermis was identified as the most relevant layer to be modelled in detail, and therefore became the focus of this thesis. The models completed showed that the signals typically used in Functional Electrical Stimulation result in electroporation in the cell membrane which decreased the impedance of the skin. When hydration was taken into consideration there was also a decrease in skin impedance, however to a much lesser extent than the drop in impedance caused by electroporation. The significance of this is that the previous resistor and capacitor model of skin found in the literature does not encompass all of the relevant factors when considering the effects of FES [3], [4]. These simulation results would benefit from practical experiments to confirm their validity; this thesis will propose what factors an experiment should consider to expand the research. A discussion of the results of the simulations can be found following the models. This thesis will finish by outlining the conclusions that can be drawn from the

simulation results as well as provided suggestions for future work that could expand upon these results.

1.1 Background

There has been a great deal of interest in knowing how the different parts of the body respond to electrical fields, with many uses for such knowledge being found in both theoretical and applied science. One of the earliest examples of this interest is the experiment undertaken in 1910, which aimed to determine the electrical properties of a red blood cell in suspension [5], [6]. The results from this experiment led to the discovery that cells are surrounded by poorly conducting membranes.

A particularly thorough literature review of dielectric properties of the body was produced by Gabriel et al in 1996 [5]. The paper collected the results of many different experimental studies and provides detail about each body part's electrical impedance, including skin, within a range of frequencies from 10Hz to 20GHz. This experimentation has generated a solid understanding of the expected electrical response from different body parts; however it is important to note the variation in results between different studies. This variation has been largely attributed to the different conditions and treatments of the body parts, such as whether the experiments were in vivo or in vitro, the mediums surrounding the organs, the condition of the organs and the variation between species the organs originated from [5]–[8].

The particular focus of this thesis is the dielectric properties of the skin organ in vivo, therefore the existing body of research, in particular experimental data has been reviewed. There have been a number of different experiments carried out on skin samples in order to discover more about their dielectric properties. These tests include using excised skin samples, as well as living samples with different types of electric fields, with a number of different subject types and environmental factors. What has broadly been found is a fairly consistent range of impedances with the exact impedance varying due to number of factors such as hydration and age. Hydration in particular has a substantial impact because it lowers the resistance of the SC, the highest resistance component of skin [6], [7], [9]–[14].

1.2 Uses for Dielectric Properties of Skin

There are a number of different potential applications for which being able to accurately determine the behaviour of the body from an electrical perspective is useful. The applications of this knowledge are relevant to areas such a biochemistry, biophysics and medicine. Being able to send and receive signals from the body without having to do an invasive procedure opens up a number of relatively safe techniques that can be used for diagnosis as well as help treat or even cure conditions, such as certain types of cancer. Of particular interest for use in the treatment of cancer is electroporation. Electroporation is the creation of pores in the cell membrane due to an applied external field. Depending on the strength and duration of the applied signal, these pores will be either irreversible and cause cell death or reversible and the pore will disappear over time. These pores greatly lower the overall impedance of the cell as current can bypass the high impedance cell membrane [15]–[17]. One application is the measuring and recording of skin-surface electrical potentials for the diagnosis of abnormalities and monitoring of organ conditions. Perhaps the most commonly known technique that relies on knowledge of the dielectric properties of skin is Electrocardiography (ECG) that involves using electrodes placed strategically around the body in order to measure the electrical signals from the heart [18]. This is just one technique that involves reading electrical signals directly from the body. Similar techniques include electroencephalography (EEG) which records the electrical signals produced by the brain [19] and electromyography (EMG) which involves measuring the electrical signals produced by skeletal muscles [20]. All of these techniques provide information about how the respective body parts work normally and can be used to identify many of the potential abnormalities present. As all these techniques involve using electrodes attached to the skin to acquire signals non-invasively, it is important to know how skin influences the signals being received in order to improve the accuracy and reliability of these procedures. Of particular interest with regards to this thesis, there is the potential of electroporation and hydration having a considerable impact on the impedance of skin and therefore the results of these diagnostic procedures.

Another area that uses electrical stimulation can be found in the experimental data in the work done by Ud-din et al. In this study they attempted to replicate the signals in the body that naturally occur

in order to aid with wound regeneration. They found that by mimicking and modifying the signals found naturally in the body and applying them externally, wound healing can be improved in the region of 30% over 14 days [21]. This is a relatively unexplored area of research that merits further interest and exploration, in particular by considering factors such as variation in the level of hydration of the skin.

Of particular interest to this thesis is using knowledge of the skin's impedance to improve the accuracy of Functional Electrical Stimulation (FES) [22]–[25]. FES is the process of sending signals into the body through the skin in order to generate contractions in muscle tissues, with an example waveform shown in Figure 1.1. In a typical healthy body in order to voluntarily move a particular muscle an electrical signal is sent from the brain through the nervous system, using neurons as a medium, to the desired motor neurons resulting in a contraction in the muscle fibres. The motor neurons and their associated muscle fibres form a motor unit. Muscles that create large movements such as the leg muscles or arm muscles have relatively few motor units, each containing a large number of muscle fibres. In contrast, the muscles involved in fine movement, such as facial movement, have many motor units with only a relatively few muscle fibres. The total tension in a muscle works out to be the same as the average of the total tension in the different motor units, as shown in figure 1.2. This is of particular significance when considering the aim of FES is to stimulate these motor units.

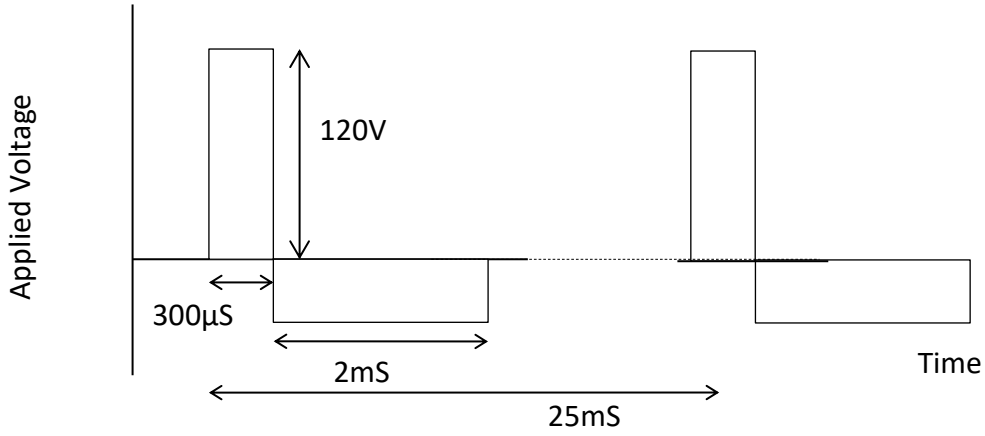

Figure 1.1 An illustration of a waveform used in FES. A typical waveform will have a frequency of 20-40 Hz, amplitude of 100 mA, applied voltage up to 120V and pulse duration of up to 300 µS. A biphasic waveform is used to both introduce and remove charge i.e. charge balance to reduce irritation [24]

By using FES it is possible to externally activate motor units that cannot be activated voluntarily. A common example of where FES is utilised is for individuals who have suffered a stroke resulting in "foot drop". Foot drop is when the individual's foot does not lift properly during the swing phase of walking; the result of this is the toes of the foot dragging on the ground. The individual is unable to successfully fully lift the foot due to either weakness or paralysis in the muscles that usually perform this function. FES can be used to attempt stimulation of the nerves associated with the affected muscles causing the foot to lift [22], [24], [26]. The results of this study could aid in the above research by providing a greater understanding of the impact hydration and electroporation could have.

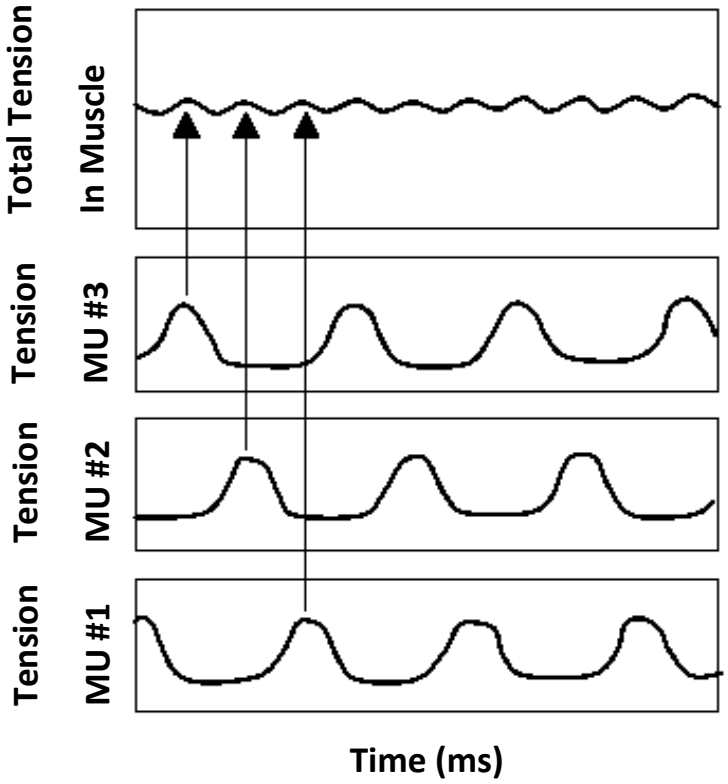

Figure 1.2 Graphs showing how the total tension in a muscle is the combination of the tensed motor units (MU) associated with the muscle [24]

One of the difficulties faced with using FES is being able to activate only the desired motor units and in such a way as to make the muscle tension feel as natural as possible, to ensure least possible discomfort to the individual and greatest benefit to them. To this end knowing how the skin will affect a signal is important to be able to improve the accuracy in activating the desired motor units [27], [28]. Anecdotally, electrode performance can be improved by moistening the electrode with tap water, which provides a good electrical contact with the skin.

There are techniques similar to FES that involve using external non-invasive voltage signals to elicit a response in muscles. One such technique is referred to as neuromuscular electrical stimulation (NMES) with the main difference between NMES and FES being the type of signal used. Typically NMES will use a longer pulse frequency and a higher amplitude signal [25].

1.3 Contributions

The aim of this research thesis is to improve the understanding of how the skin is affected by electrical stimulus through FES. The main areas of focus are modelling the effects of hydrating skin and the effect of electroporation, which is the creation of pores in a cell membrane due to an applied external electric field. The thesis simulates the relationship between the level of hydration in the Stratum Corneum (SC) and its impact on the overall impedance of skin over a range of different input frequencies, as well as when exposed to the levels of voltage often used in FES. Further to this the relationship between the signals used in FES and the creation of electropores is explored to determine if electroporation is a possible unintended consequence of FES.

This thesis has formulated an equation that links the level of hydration of the skin with skin impedance, which was developed from the simulation results. This would benefit from more specific supporting experimental data in future research, as the current literature lacks focus on the effects of hydration on skin impedance. The simulations also found that electroporation should occur when typical FES signals are used. However, due to a lack of relevant experimental data parameters that could be used to determine the full extent of electroporation could not be incorporated into the model.

Some of the work in this thesis has been published in the following journals or presented at conferences:

Davies, L., Chappell, P. and Melvin, T. (2014) Finite element modelling of skin on a cellular level. At Physics Meets Biology, Oxford, GB, 03 - 05 Sep 2014. 1pp.

Davies, L, Chappell, P and Melvin, T. "Modelling the effect of hydration on skin conductivity." Skin Research and Technology (2016). [29]

Davies, L and Chappell, P. "The effects of electroporation on skin impedance." Biomedical Physics & Engineering Express 4.2 (2018): 025012. [30]

1.4 Chapter Summary

This chapter outlines the main focus of this thesis, namely to determine impact of hydration and electroporation on skin impedance and determine whether these factors are necessary inclusions when trying to model the effect of FES on skin impedance. Provided in this chapter are details of the typical waveforms used in FES as well as the major contributions that this thesis has provided. The following chapter explores the structure of skin, the cells found in the skin and sweat glands in order to understand the physical components that need to be represented in a model.

2 Skin Structure

This chapter will review the literature and current understanding of skin structure, with a focus on the individual layers of skin and the make-up of skin cells on an individual and group level. In particular, the epidermis will be focused on in greater detail as the literature suggests that this is the level of skin with the greatest influence on the overall electrical impedance. Also of interest in this chapter is the examination of sweat glands and their influence on the dielectric properties of skin with regards to hydration. This chapter will conclude by exploring the potential interaction between individual cells, with consideration of the importance of this factor being included in the FEM. Of particular interest in this thesis is the epidermis, in particular the Stratum Corneum (SC) is explored in greatest detail.

In order to determine the dielectric properties of skin the structure of skin should first be considered. There are two main layers that make up skin, the epidermis and the dermis. In addition there is a layer between the skin and the underlying bone and muscle called the hypodermis, as shown in figure 2.1. The thickness of skin and its components varies depending on the location on the body being considered. The skin is thickest on the palms and soles of the feet at around 4mm thick and thinnest around the eyelids at 0.5mm. These values are not exact and will vary from person to person, with number of cells in each layer will vary due to factors such skin health and age with each layer's thickness varying independently [31]–[33].

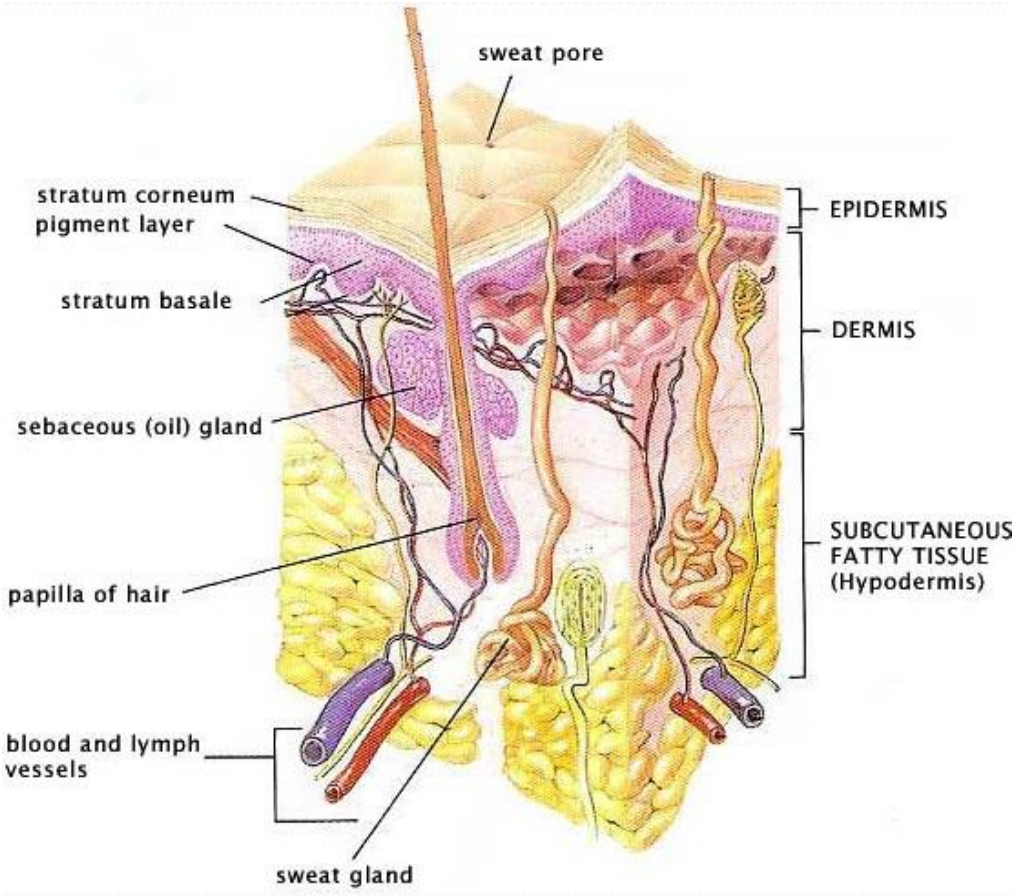

Figure 2.1 Structure of skin [32]

2.1 Epidermis

The epidermis is the outermost layer of skin and serves as a chemical and diffusional barrier to protect the body from potential trauma. The epidermis regulates the amount of water released from the body through diffusion and evaporation processes, known as transepidermal water loss (TEWL) [34]. At its thinnest the epidermis is 0.05mm around the eyelids and this layer of skin is thickest at 1.5mm on the palms of the hands and soles of the feet [35]. It is mainly composed of keratinocytes, accounting for 95% of the cells present. These are the cells that provide the rigid structure of skin and can be considered the “building blocks” of this layer of skin. Other types of cells in the epidermis include melanocytes which are responsible for melanin production, Langerhans cells, which are dendritic cells involved in capture, uptake and processing of antigens, and Merkel Cells which are associated with the sensation of soft touch [36].

The epidermis itself is composed of a number of separate layers, as shown in figure 2.2. Each of these layers serves a different purpose. The most exposed layer is stratum corneum which acts as a diffusion barrier, regulating the hydration of the lower levels of the skin [37]. This sub-layer of particular interest as it has been identified in the literature as having the highest electrical impedance, and will therefore be the subject of this thesis' FEM. The next layer down is the stratum lucidum that exists only in locations that are exposed to substantial friction, such as the palms and soles [9] Below the stratum lucidium is the stratum granulosum that provides the SC with the vital dead cells that contribute to the protection of the body. In the stratum spinosum the Langerhans cells are located [37]. The final layer is the stratum basale, which is a continuous layer of basal keratinocytes that is normally only one cell thick [36].

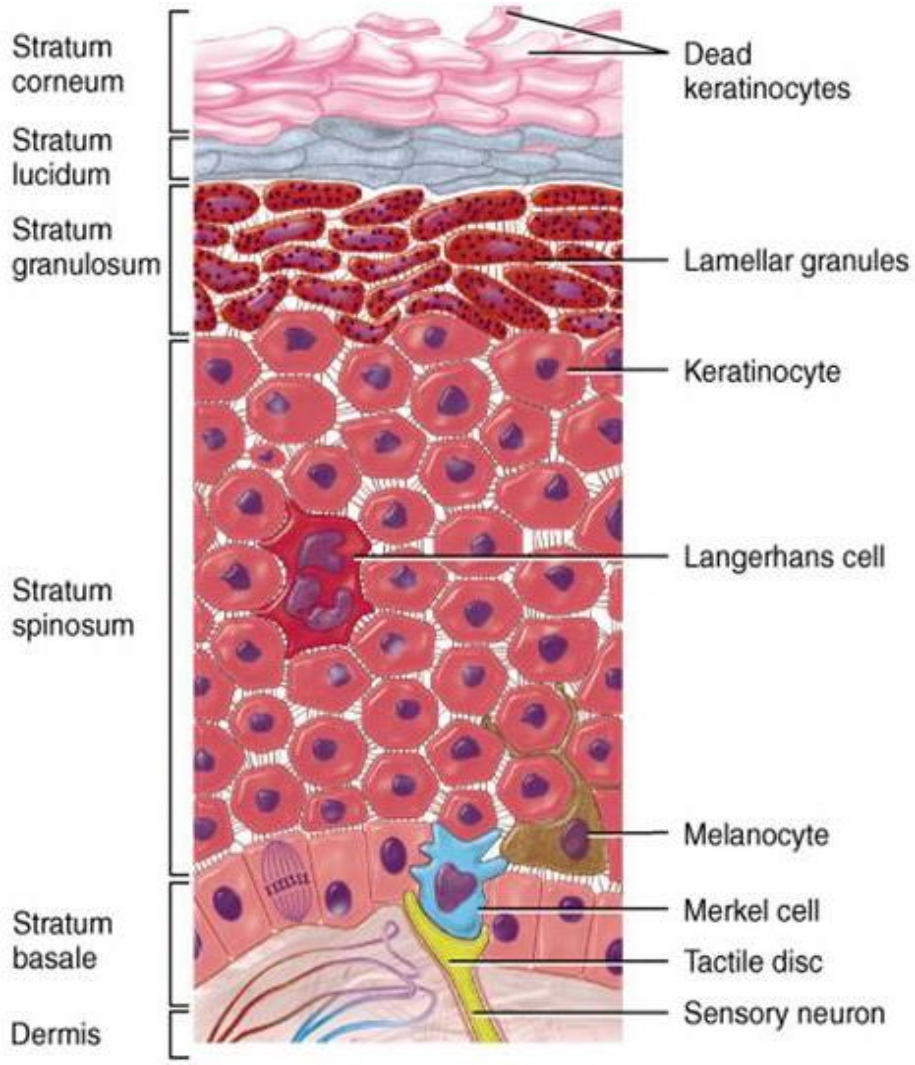

Figure 2.2 Structure of the epidermis [38]

2.2 Stratum Corneum

From an electrical point of view one of the most important sub-layers is the stratum corneum, which will be explored in further detail in this section. The stratum corneum is the top layer of the epidermis and the top layer of skin as a whole. The stratum corneum is made up of dead skin cells that act as a barrier for the body, providing protection from infection, dehydration and other potential threats or trauma [39]. Despite the fact that this is one of the thinnest layers, being only around 20 microns thick on average, it is the most insulating layer due to the lack of moisture in the cells. This high level of insulation causes the stratum corneum to play a dominant role in the skin's electrical response when low frequency electric fields and Direct Current (DC) are applied. However, the dominant effect of the SC is heavily influenced by hydration as well as other factors such as the applied electrode geometry and size [34], [39]–[41].

When hydrated the keratinocyte cells within the stratum corneum can expand to up to 3 times their original size. The amount of time the cells will remain hydrated will vary from person to person, with determining factors including heath, age, disease, climate, genetic variation and the chemical content of the moisturising agent. Hydration has a substantial influence on the dielectric properties of these cells, and in the vast majority of cases will lower the impedance of these cells [1], [9], [42]. Hydrating with water always lowers electrical impedance of keratinocyte cells; however the precise effect will vary depending on the chemical composition of the water and its impurities [43]–[45]. This thesis will examine the impact of different conductivities of different water compositions based on the expected ranges of electrical conductivity of tap water.

2.3 Sweat Glands

Sweat glands are found all over the skin, but are most numerous on the palms of the hands and soles of the feet. These sweat glands aid in temperature regulation by releasing sweat to the surface, thereby cooling the body as the sweat evaporates [9], [35], [46]–[48]. Sweating can also occur as an emotional response; in times of stress, anxiety, fear, or pain sweat may be produced. This sweating can occur all over the body, but is most abundant on the palms of the hands and soles of the feet,

therefore this kind of sweating is unlikely to have a large impact on FES [46]. This is because FES is predominantly used on the larger muscle groups in the limbs and does not currently target fine motor control as found in the palms and soles. In the future as the technology develops this may become more relevant. The typical structure of a sweat gland can be seen in figure 2.3.

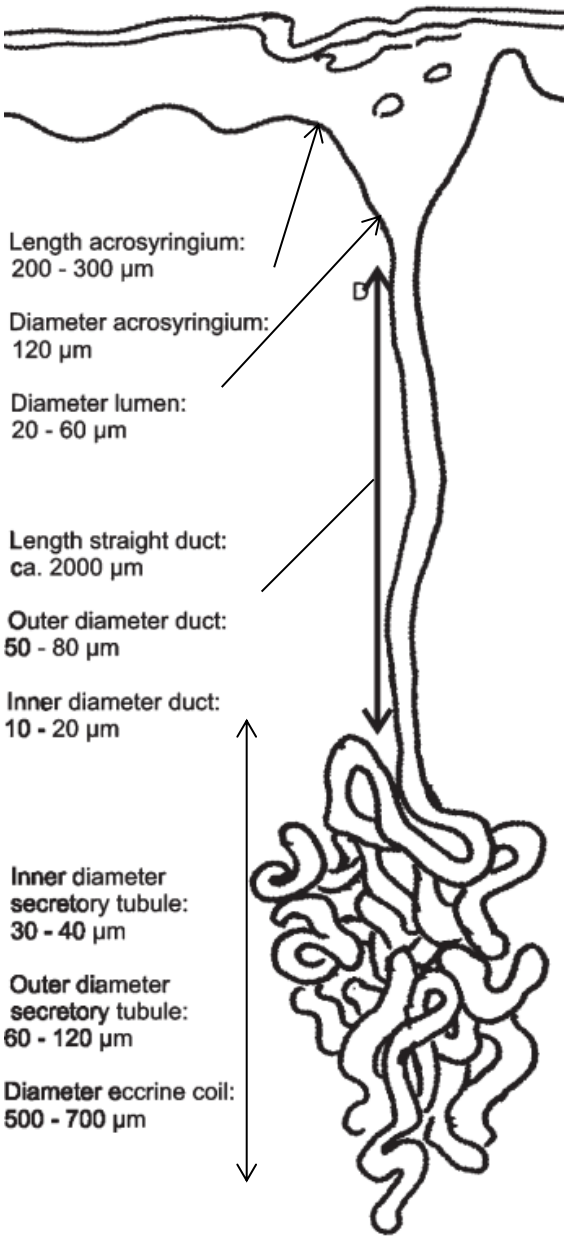

Figure 2.3 Structure of a sweat gland [46]

The impedance of the skin can be heavily influenced by sweat. If the skin is saturated with sweat the impedance will roughly halve within a few seconds since sweat contains ions, particularly sodium ions, and is therefore conductive [46], [49].

2.4 Skin Cells

It is important to consider the structure of skin cells when trying to determine their electrical response, especially important is the cell membrane. The cell membrane is the outermost layer of the cell. Its function is to protect the inner parts of the cell and define its parameters, in a similar manner to how the skin protects the body. The membrane itself is composed of lipids and hydrophilic phosphorus molecules. A variety of proteins are also embedded around the membrane, these proteins act as selective channels and pumps that enable particular molecules to enter and exit the cell. The reason for the membrane being the most important feature from an electrical point of view is that it has a conductivity that is orders of magnitude lower than the internals of the cell and the medium surrounding the cell [50]–[53]. A simplified cell structure is shown in figure 2.4.

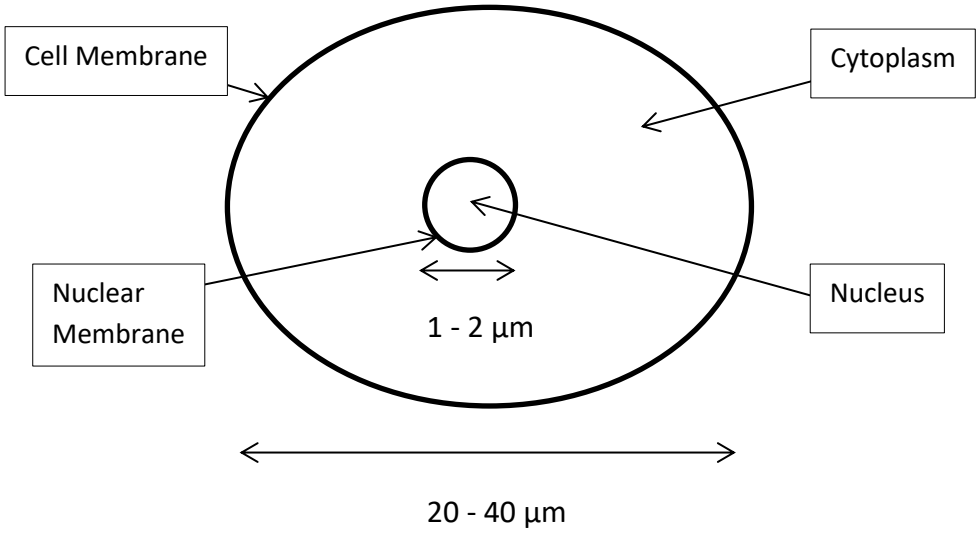

Figure 2.4 Cell structure[52]

The stratum corneum comprises very thin hexagonal or pentagonal cells, called corneocytes that contain very dense keratin, a fibrous structural protein that is extremely insoluble in water [54]. The layers of these cells overlap to create a brick wall like formation and are held together with the corneodesmosomes acting as rivets to maintain the rigid structure, as shown in figure 2.5. Between the cells there is a complex array of lipids, ceramides, free fatty acids, cholesterol and cholesterol sulphate.

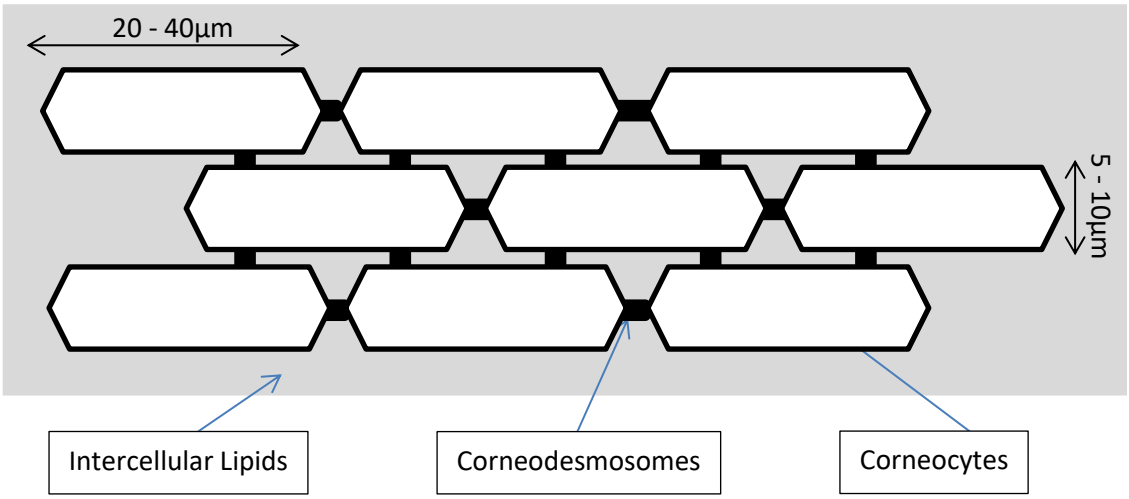

Figure 2.5 Brick like structure of the cells found in the epidermis

While the cell membrane plays the important role in the behaviour of the cell, the inner components also have a substantial impact on the electrical properties of a cell. The inner parts of the cell have a higher conductivity, as previously mentioned. Therefore when effects such as electroporation occur or changes in the physical properties occur in damaged cells due to, for example, trauma, the overall cell impedance drops considerably as the cell membrane is the highest impedance component of a cell [2], [41], [55], [56]. This phenomenon was the subject of simulation within this thesis to further determine the significance of this effect. Initial models within this study included the geometry and electrical properties of the cell nucleus, including its membrane [57].

From review of the literature there have been a number studies looking into how cells interact with one another and what role electrical signals play in these interactions. However, it is generally thought that these interactions have only a small impact on the cells overall electrical behaviour and therefore for the purposes of the modelling in this study, the cell's inner parts are treated as having uniform dielectric properties with no communication between cells. This is because the communication between cells is in the order of microvolts and any variance across the cell cytoplasm is minor when compared with the cytoplasm and the cell membrane [52], [58], [59].

Another assumption that is commonly made is that the cell properties are the same regardless of the cell orientation, which is not the case [60]. This effect is particularly prominent with cells that compose the skin. Epithelial cells, such as the cells found in the skin, feature distinct apical, lateral and basal plasma membrane domains. They are connected to each other by the lateral domain to

create sheets that form cavities and surfaces throughout the body. Each domain has a different protein composition and will therefore have distinct properties, although the impact of these differences on the electrical properties of cells is still unknown [51], [61]. However for the work in this thesis the cells will be treated as being oriented in the same direction, which should negate any expected change in the skin's impedance.

2.5 Chapter Summary

This chapter describes the key features of skin that influence the impedance of skin. In particular, there is a focus on the epidermis, the upper of the two layers of skin, which has been found to have the highest impact on the overall impedance of skin. Within the epidermis there is also a particular interest in the structure and composition of the Stratum Corneum, the layer of skin closest to the surface that is composed of dead skin cells and arranged in a rigid brick-like structure. There is also a look at the sweat glands, due to their substantial influence on the skin's level of hydration. The following chapter provides a review of the current knowledge on the electrical properties of skin and how these properties are influenced with a change in the skin's level of hydration.

3 Electrical properties of skin

This chapter will provide more in depth exploration of the current knowledge of the skin's electrical properties. In particular this chapter begin with a critique of the current simplistic equivalent circuit used to model the electrical behaviour of skin and the attempts to create a more comprehensive equivalent circuit model. There is a review of the literature exploring some factors that affect the skin's impedance, such as age and seasons. Finally, this chapter will provide a more in depth review of the impact of hydration on skin impedance, both the impact of external hydration, such as from tap water as well as the hydration that occurs naturally in the form of sweat.

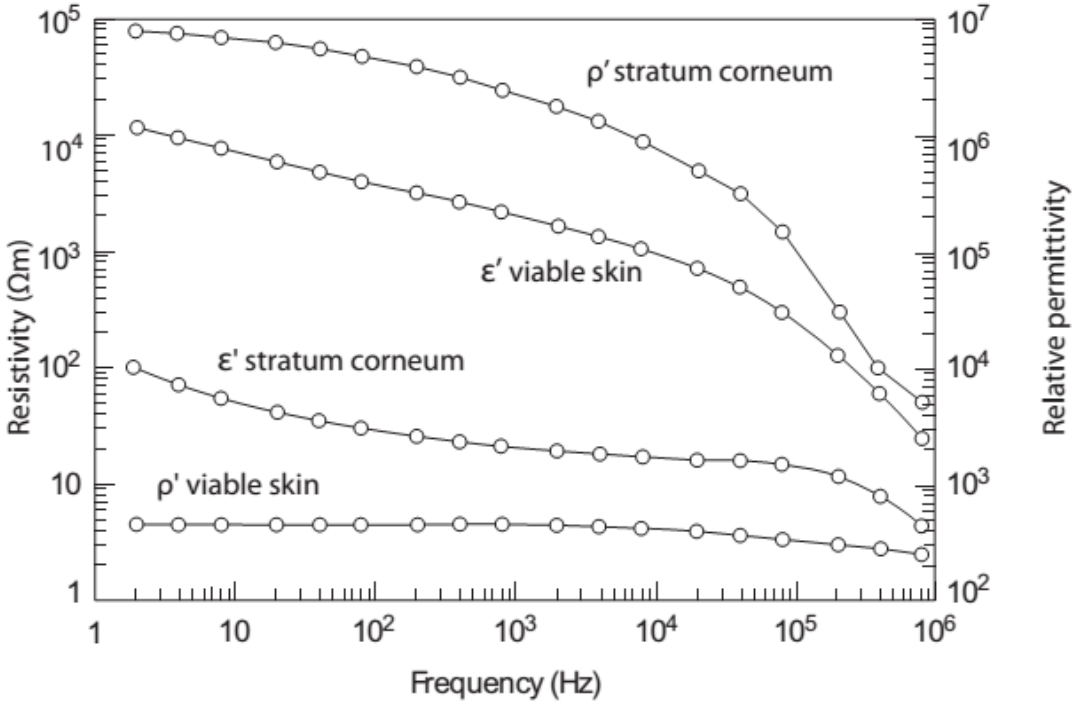

Figure 3.1 Typical values for resistivity and permittivity of the stratum corneum and viable (living) skin, the layers of the skin containing living cells, over a range of frequencies with ρ' being resistivity and ε' being permittivity [9]

Figure 3.1 shows the experimentally found expected impedance variations of skin over a range of frequencies. The initially high level of impedance can be attributed to the stratum corneum, as mentioned previously, and the steady curve down to the lower impedance level is generally attributed to the other layers in the epidermis and dermis [3]–[5].

One of the most common ways to represent the dielectric properties of skin is to simply model it with an equivalent circuit. The advantage of being able to represent skin with an equivalent circuit is that it makes analysis of the signals being sent into and out of the body very simple. This is because the standard circuit analysis techniques can be used.

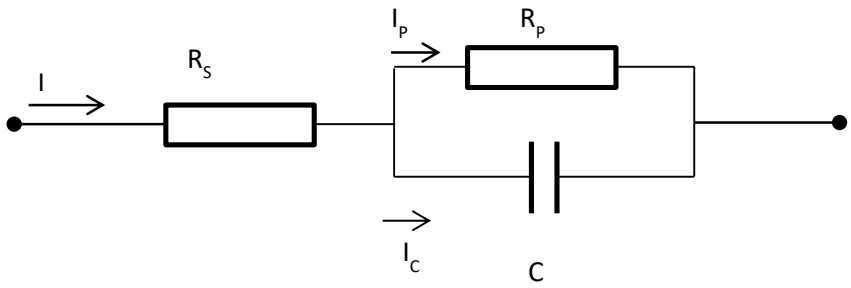

Figure 3.2 Equivalent electrical circuit for human skin [3], typical value for R_s is between 400-700Ω, R_p is between 50-150kΩ and C is between 50-200nF

In the circuit shown in figure 3.2 the combination of Rp, Rs, and C, with selected values, will produce a response that approximately matches those measured experimentally and shown in figure 3.1 [62]. This is not the only circuit capable of producing the impedance change shown in figure 3.1, but is one of the simplest and therefore most commonly used. There are also more complicated circuits that are thought to reflect more accurately the impedance changes of skin, although the circuit in figure 3.2 is still the most common.

The simple circuit described above is adequate to characterise the response of skin for many applications, in particular those that involve reading signals from the body such as EEG, ECG and EMG. However, there are a number of limitations with this circuit as it cannot be easily adapted to reflect the change in skin's response when exposed to a number of factors. These include hydration, as well as individual differences, such as age, genetic variation, disease, gender and environment [8], [13], [14]. Effectively the circuit only provides the general response of skin and the parameter values of Rp, Rs and C need to be altered frequently to maintain an accurate representation [3].

Indeed, this circuit is not able to accurately model some phenomena such as electroporation, which is described in detail in section 4.3.

There are a number of obstacles that are encountered when trying to identify what specific factors are the causes of the large range of values for skin impedance measured experimentally. Some of these factors include exposure to moisture, thickness of the skin, age, race, gender and skin conditions. These have all been recorded to have a noticeable impact on skin impedance [8], [15], [34], [63]–[69]. This makes it difficult to measure the effects of other factors such as blood flow and cell interactions that occur within the skin itself due to the challenge in isolating these effects. For example, any individual subject in an experimental setting will have variations across all factors to any other subject, drastically reducing the ability to control and isolate a single factor. Furthermore, some of factors cause the impedance of skin to change over the course of the day, such as hydration and temperature and as the body ages.

A study into change in the electrical impedance of skin over a twelve year period was undertaken by Nicander et al [7]. An experiment was undertaken whereby 50 subjects had their skin impedance measured at 8 different locations on the body. Measurements were taken at different points in the year in an attempt to incorporate the effect of seasonality on skin impedance, as well as using a mixture of genders and body types to determine if aging effects would occur across all subjects equally. The results of the study showed that there is indeed a change in the impedance of skin due to age, but this effect varies based on the location of the electrode on the body as well as affecting subjects differently based on their age at the start of the study. The reasons suggested for age affecting skin impedance is the change in the SC ability to hydrate and remain hydrated.

A similar study by Nicander et al [14] looked into seasonal effects on skin impedance. 48 subjects of different ages and split into two groups by gender had their skin impedance measured at 10 different locations on the body. The results found from the study were that seasons had a substantial effect on the measured impedance, with the most noticeable reduction in skin impedance occurring in summer. This was linked to the level of skin hydration, specifically related to the amount of sweat present in the warmer seasons.

In order to overcome some of the variations in skin impedance that occur when using a simple equivalent circuit more complicated models have been proposed. One such model takes into account each of the individual layers of skin. It also takes into consideration effects such as blood flow and shows the expected response of skin over a range of frequencies, from 1Hz to 100MHz [5]

. The model considers three different layers of skin based on blood flow and uses a combination of numerical and analytical techniques in order to model the behaviour of skin. The results are promising, being able to produce results that mostly support analytic and experimental data. However, the model still suffers from some of the issues discussed previously, such as age, seasonal change and gender. The researchers were unable to conclusively demonstrate that the increased complexity involved with using such a model produced a significantly more accurate model for practical applications.

3.1 Skin Hydration

One of the most substantial factors that can alter the skin's impedance is hydration. As mentioned previously one of the functions of the skin is to provide a waterproof barrier. In terms of hydration the SC layer can be considered as consisting of two parts, the hydrophilic keratin that composes the corneocytes and the hydrophobic lipid bilayers.

Measuring the electrical impedance of skin can be used in order to determine the water content of the SC *in vivo*. A standard measure for hydration is water activity (a_w) which is the partial vapour pressure of water in a substance divided by the standard state partial vapour pressure of water. Börklund et al [65] found that when exposed to a hydrating solution, $a_w = 0.992$, the resistance of the skin is on average 14 times lower and the effective capacitance is 1.5 times higher when compared with dehydrating conditions, $a_w = 0.826$. These changes are largely reversible and have been tested over a 96 hour period. The results of the paper can be seen in figure 3.3.

In FES it is common practice to use tap water to improve the electrical contact between electrode and skin [25]. Tap water has a substantial range of conductivities that depend heavily on the pollutants contained within, which vary dependent on the source of the water and the treatment it is given. Depending on how the water is treated before it comes out of the tap the range of conductivities that can be expected will range anywhere from 5 mSm^{-1} to 50 mSm^{-1}, an order of magnitude difference [70].

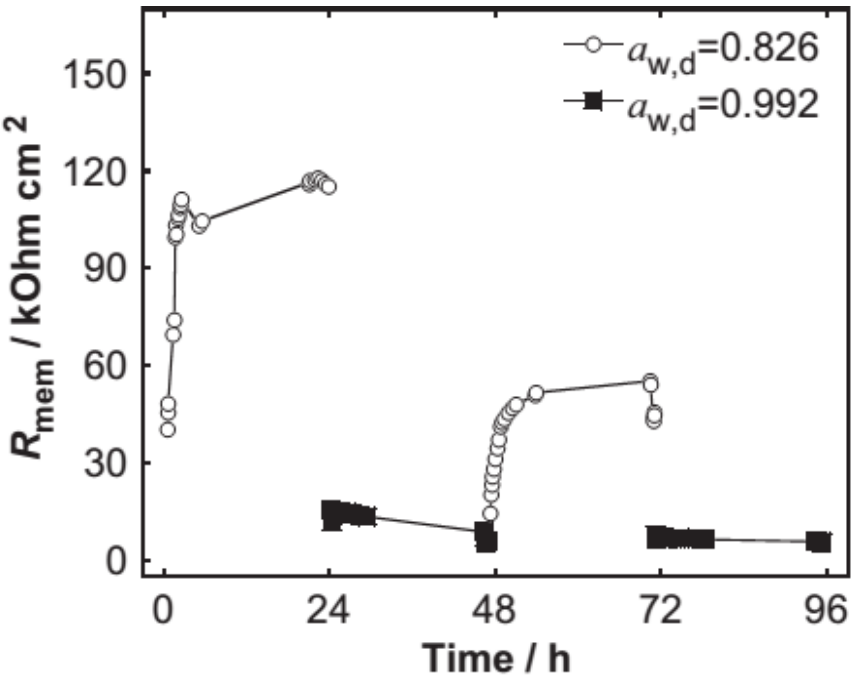

Figure 3.3 Graph showing change in resistance over time with dehydrating conditions ($a_{w,d}$ = 0.826) and hydrating conditions ($a_{w,d}$ = 0.992) [65]

When considering the impact of hydration it is important to consider the impact of sweat. As mentioned previously there are sweat glands located across the body and when saturated they have substantial impact on skin impedance. The two main causes for sweating in the body is temperature regulation and as a response to emotional stimuli. Since sweating caused by emotional response predominantly occurs on the palms and soles of the feet it should have little impact on the parts of the body relevant for FES such as the forearm or lower leg [46], [71]–[73]. Of particular relevance to this body of work is what effect applying an electric field has on a sweat gland as this is directly linked to hydration of skin cells.

A positive surface potential applied to skin will normally repel sweat, causing a decrease in conductivity while a negative potential will attract water, causing an increase in conductivity. The effect of an applied potential on the flux, F, of sweat duct liquid can be seen in equation 3.1, which is a general equation for describing an ionic liquid in a tube [74].

$$F = \frac{\zeta \epsilon I \rho}{4\pi\eta} \tag{3.1}$$

where ζ is the electro-kinetic zeta potential, ϵ, ρ and η are permittivity, resistivity and viscosity of the liquid, respectively, and I is the current [9], [74].

An interesting property of a sweat duct is that it can sometimes exhibit a form of memory, depending on the voltages that have previously been applied to it. This has led to some researchers suggesting that it in some cases a sweat duct is memristive instead of conductive, meaning that the resistance of a sweat gland may be linked to the currents previously applied to it [9]. This effect has been shown by using dry electrodes with a simple harmonic AC voltage as shown in figure 3.4. As the voltage changes from positive to negative the current is increased due to the fact that a negative field attracts water thereby decreasing the resistance of the duct, but what can also be seen is that the current is increasing in subsequent voltage cycles. This effect is thought to be caused by the build-up of fluid which acts as a sort of memory for its electrical history. For the purposes of this study, this meromictic effect has not been incorporated as it occurs over a much larger time scale than those used in the models.

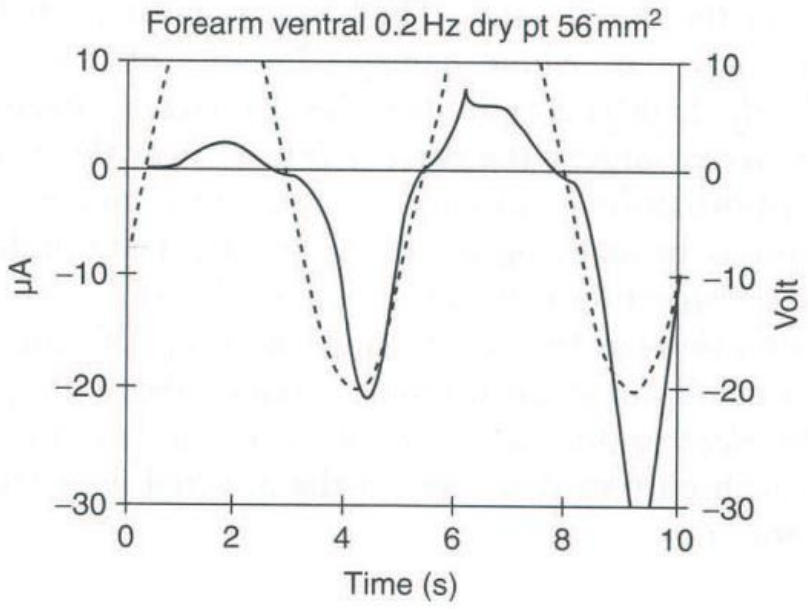

Figure 3.4 Current response (solid curve) and applied voltage (dashed curve) on ventral forearm using dry disc electrodes [9]

One of the most important issues with trying to determine the effect of sweat on the skin's overall impedance is the number of factors involved. The exact chemical composition varies not only

between subjects, but also based on the location on the body. There are a number of studies that have tried to use the conductivity of sweat to try and determine a subject's overall level of hydration, with a higher level of conductivity indicating a higher level of hydration [46], [47], [49], [75].

As mentioned previously one of the factors that causes the body to sweat is temperature regulation [49]. This will naturally cause an increase in the conductivity of sweat due to the hydration of the otherwise dry keratinocytes, however there have also been studies that show the conductivity of sweat will increase with temperature. This effect has been shown to be quite noticeable, increasing linearly in the range tested between 5°C to 50°C, with a 100 kHz signal, with the conductivity ranging from $0.25Sm^{-1}$ to $1Sm^{-1}$. As mentioned in the study these values will vary between individuals as well as over time for an individual as the exact chemical composition of sweat varies due to factors such as hydration, gender and age.

A study undertaken by Birlea et al [76] showed the effect of applying transcutaneous signals through the skin over the period of 6 days. The results of the experiment confirmed what had been previously shown, that the SC is the dominating factor in determining the skin's electrical impedance. The study showed a substantial drop in the SC impedance, changing from 20kΩ to 17kΩ measured between days 1 and 7, a 14% drop over 6 days. There was no substantial change in the value of capacitance over the period of 6 days, although there was an initial variation between subjects. It was noted during the discussion that the most likely cause for this decrease in the resistance of the SC was caused by the accumulation of sweat, although this could not be confirmed as the level of hydration was not monitored in the experiment.

3.2 Chapter Summary

This chapter provides a review of the current understanding of skin impedance by looking at how skin impedance is currently modelled in the form of an equivalent circuit. The circuit provides a response that maps to the expected resistance and capacitance from skin but fails to include factors such as hydration or electroporation and does not easily accommodate for many factors, such as the location of skin on the body being examined. This chapter also takes a more detailed look at

the research available on how hydration effects the impedance of skin, showing the reduction in impedance of around 14% due to high levels of sweat in the skin. The following chapter looks at electrical properties of skin cells in detail with a particular focus on how electroporation causes a significant drop in a cell's impedance.

4 Electrical properties of Cells

The following chapter will provide a review of the electrical properties of the cells that compose the skin. The challenges involved in acquiring the dielectric properties of cells, such how to isolate single cells in vitro, are explored with some experimental results being discussed. In addition, the vast number of cells poses a computational challenge, requiring simplification of some layers of skin in many models in the literature. There is a critique of a proposed cell circuit equivalent, which despite its relative complexity does not take in to account certain phenomenon such as electroporation. An area of particular focus in this chapter is electroporation, its clinical uses and the effect it has on the conductivity of the cell membrane. Much more experimental data is needed on electroporation outside of its uses in cancer treatment.

4.1 Cell Experimental Data

An alternative approach is to consider the skin as a collection of cells instead of the equivalent circuits or the layer level approaches considered so far. By considering the cells themselves it may be possible to produce a model that more accurately represents the electrical response of skin and other parts of the body. There has been a number of papers produced exploring how cells react to an electric field and while most of the cells tested are not skin cells, many of the findings can be extrapolated due to the similarity between the cells. One of the main drawbacks of this approach is that trying to analyse the response of individual cells that are surrounded by large groups of other

cells is difficult, so there has not been much research in the area. In addition, the vast number of individual cells can pose a challenge when trying to produce a model. There are about 60 million cells in one square cm of skin, therefore a model including every individual cell would require a substantial amount of computational power [53]. While it may be theoretically possible to do this, it is nevertheless difficult to validate such a model as there is not enough reliable experimental data in the literature about how the interactions of cells affect their electrical response when grouped. While a completely faithful representation might be of questionable value a smaller model that considers how a small number of cells interact may provide a lot of useful information about the skin's electrical behaviour [77], [78].

In order to produce an accurate model of a cell it is important that there is either analytical or experimental data to compare to the model so that the results can be verified, preferably both. The first values for a cell's electric properties were obtained by applying an electric field to cells suspended in a conducting medium and measuring the resulting impedance [79], [80]. This approach allowed for the isolation and testing of single cells, however the experimental environment was not a true representation of the conditions a cell is usually in. Using cells in suspension also tend to lead to more regularly shaped cells then those that are present in the body, further reducing validity when attempting to use this data to inform usual behaviour of cells.

Attempting to find a means of determining the dielectric properties from cells in the body is extremely challenging for several reasons. Firstly, there are obstacles caused by the small size of the cells, their location and their proximity to other cells. These are also issues involving cells that move, such as blood cells. However, there are techniques available that are able to overcome some of these challenges. One method that can show a change in voltage across a cell membrane uses special dyes. The intensity of the fluorescence of these dyes changes linearly with the induced transmembrane voltage (ITV). The main downside of such a dye is that they tend to also be highly susceptible to noise and the environment, leading to large potential errors in the results [81], [82].

The increasing miniaturisation of technology has allowed for the creation of impedance analysers that can measure the impedance of single cells. These devices are able to find accurate measurements of the impedance of an individual cell, but do require the cells to be extracted from the surrounding cells, ignoring the effects of neighbouring cells [50], [83]. Another recent technology being researched is the use of nanoprobes in combination with an electron microscope. Through the use of these devices the electrical properties of single cells were able to be determined for two types of epithelial cells, live cells and dead cells, with some of the results of the experiment shown

in figure 4.1. The study aimed to measure the electrical properties of individual cells using a nanoprobe on cells exposed to dye as well as cells without dye. This is a beneficial result because using dye can be a very time consuming process. The main issue with this approach is the expense and complexity of the equipment used [59]. In relation to this thesis, being able to determine the electrical properties of individual cells with greater accuracy would help improve future models and experiments.

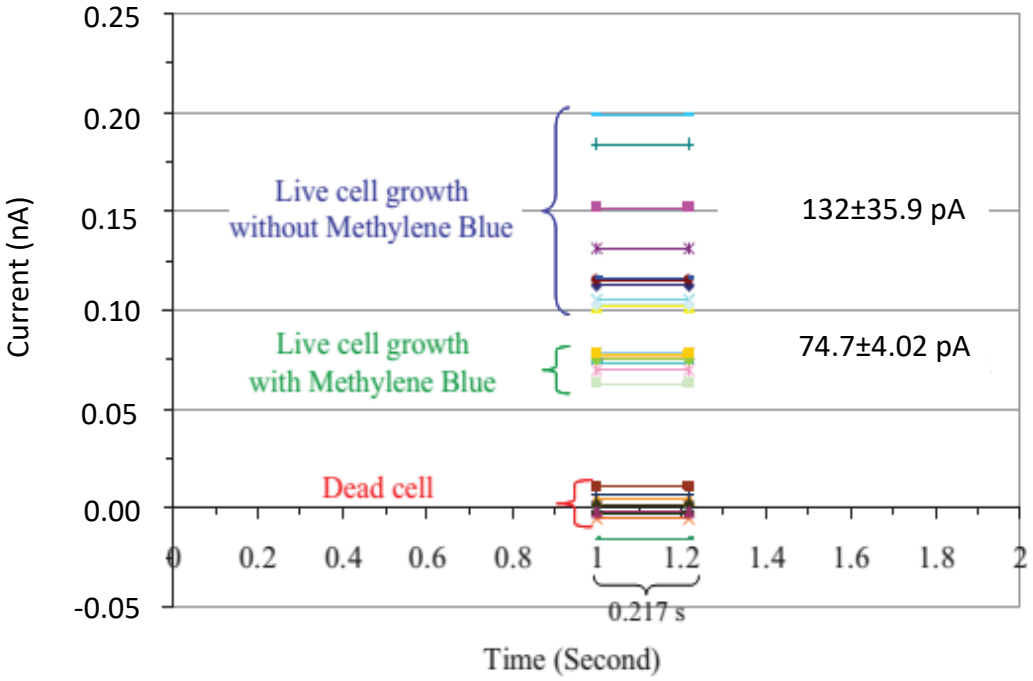

Figure 4.1 Current measurement in individual yeast cells that are either dead, live with dye or live without dye [59].

It is still unknown what mechanical effects are caused by applying a strong electric field to the cell. The vast majority of research into cell's electrical behaviour involves only using fairly low power signals. It is known that a cell will die when exposed to a strong field, due to the effects of electroporation causing the cell to become irrevocably permeable destroying the integrity of the protective outer membrane. This makes testing the cells under strong signals largely unnecessary [78], [41], [84], [85].

4.2 Cell Circuit equivalent

Comparative to the manner in which skin has been represented with an equivalent circuit there are also equivalent circuits that have been developed to represent the electrical response of cells. To determine what components are necessary to accurately represent the response of a cell with an equivalent circuit experiments have been performed using impedance analysers to determine electrical response of a cell over a range of frequencies [58], [78], [86].

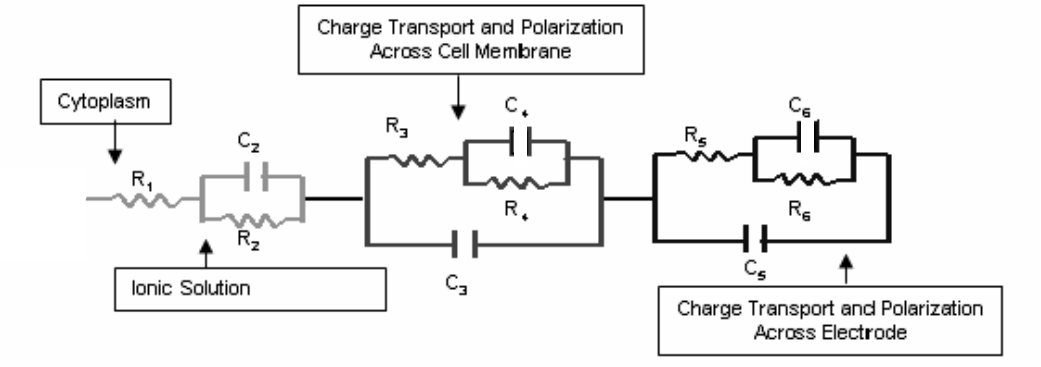

Figure 4.2 Cell Circuit equivalent [58]

Figure 4.2 shows a circuit that can be used to represent the response of a cell, with R_1 representing the inside of the cell, C_2 and R_2 the surrounding medium, R_3, R_4, C_3 and C_4 the membrane and the remaining components represent the electrode. This circuit agrees with the previously suggested idea that the cell membrane has the most influence over the response of the cell. The reason for the membrane requiring more complicated circuitry than the interior or exterior is because it acts as an intermediary between two dissimilar systems [58].

The circuit attempts to take into account a number of different phenomena present but there is no consideration of electroporation in the work. This means the cell model could only be true when the applied electric fields are low enough that electroporation does not occur or high enough that the results take into account the impedance and capacitance changes due to electroporation at all times. The latter may be an acceptable assumption given that electroporation occurs within approximately 1µs of the signal being applied [13]. This circuit model could be expanded to include the effect of electroporation but as has been mentioned previously the exact mechanisms underlying electroporation at the cellular level are not well understood.

The main issue is a lack of direct connection between the components of the circuit model and the physical properties of skin. It is difficult to determine how the models might be changed to incorporate thicker skin, diseased skin and most importantly incorporate the effect of hydration. There is also difficultly in representing the effect of electroporation, due to its sudden and

substantial impact on membrane impedance that may or may not be reversible based on the applied signal. The resulting behaviour of such a model could be converted to a circuit equivalent but the benefit of being able to alter the physical properties such as skin thickness and level of hydration that could be relatively easily incorporated into a FEM model would be more difficult in a circuit model.

4.3 Electroporation

In order to cause a single cell to undergo electroporation, pulses on a microsecond to millisecond time scale must create an induced transmembrane voltage of around 200mV-1V. To create an electropore, an electrical field in the order of 10^8 Vm^{-1} must be applied [87], [88].

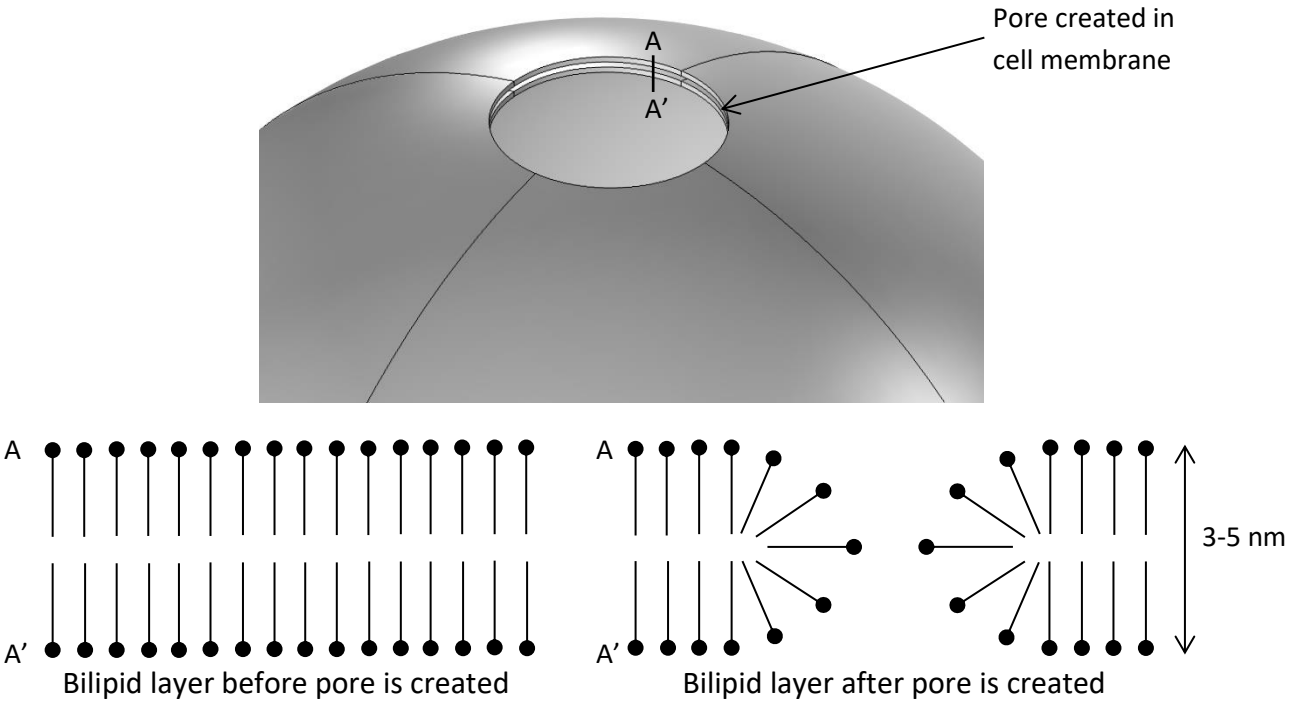

Figure 4.3 3D and 2D diagrams showing the creation of a pore due to an applied electric field [16]

While there is not a lot of experimentation that suggests that electroporation is relevant to FES one of the big areas where cell models involving electric fields are being developed is electroporation. Electroporation is the process of changing the permeability of a cell membrane by applying an electrical field with a high enough intensity for a long enough period of time, with the effect shown in figure 4.3. This process has been shown to be either reversible or irreversible, depending on the intensity and duration of the applied electric field. The signal used is also normally in the form of

short pulses, which allows for a higher level of control over the electroporation process than a continuous signal [26], [53], [56], [58]–[60].

One of the main uses for electroporation that is currently being researched is for treating cancer. This can be done with electroporation in two ways, either by introducing drugs into targeted cancer cells [84] or by causing the cancer cells to die by using an irreversible permeability change. This process can also be used in other applications that involve gene therapy or cell based therapy.

Procedures involving the use of irreversible electroporation have been in use since 2000 and have had a number of successes, being used to remove over 76% of tumour tissue present in some instances [16], [17], [89]. The basic idea is to use targeted signals to cause irreversible electroporation in the desired cells, causing cell death. The process requires a lot of knowledge of the electric field in order to target on the desired cells and the level of voltage used to produce irreversible electroporation (IRE) raises a number of potential concerns, such as ohmic heating due to the field strengths involved. One of the advantages to this approach is that as long as the field is kept to around 2000Vcm^{-1} [17], depending on the length of pulses used, the process is non-thermal and can be used next to major blood vessels which would be difficult to perform direct surgery on. This applied voltage for irreversible electroporation is significantly larger than the 0.2-1V required for reversible electroporation. As mentioned earlier this approach requires an in depth knowledge of the electric field generate and the fields are strongly influenced by the local environment and the different dielectric properties of the tissues present. Knowledge of the dielectric properties of the cells present can be particularly difficult to determine as the properties of tumour cells vary substantially to those of healthy cells, with cancer cells having a lower conductivity and higher capacitance when compared with the corresponding non-cancerous cells [50], [84].

Because the situations in which electroporation is used require a highly targeted signal it is important to have as much information as possible as to how a cell will react to an applied electric field. In order to do this without direct experimentation models have been designed to determine a cell's electrical behaviour to single cells and groups of cells with a variety of parameters, although this is still a growing area of research with many areas that have yet to be explored [88], [89].

In most of the literature the idea of electroporation occurring is not discussed unless it is the focus of the work. However there are papers that show that electroporation might occur as an unintended result of sending a signal into the body. Specifically the experiment undertaken by Al-Khada et al [92] shows that electroporation occurs during defibrillation, in the cells directly surrounding the

electrode as well as in the bundles at trabeculas throughout the endocardium. While this paper provides a source of comparison for the electroporation model there are some important differences that should be taken into account. The properties of the skin at both locations will vary slightly, with the number of layers in the SC of the upper arm being around 1 more than found in the SC covering the chest. This is a minor difference so the expected behaviour should be similar but the dielectric properties will vary at different locations for reasons other than number of layers in the SC, such as level of hydration due to sweat, which could lead to a difference in the skin impedance measured. The signals used are also different, voltages upwards of 150V being used in defibrillation, much higher than typically used in FES.

To produce an electropore an electric field in the order of 10^8 Vm^{-1} must be applied. The induced voltage across a cell membrane, ITV, can be determined by equation 4.1.

$$\text{ITV} = fs\ E\ R\cos\phi \qquad (4.1)$$

In the equation E is the applied electric field, fs is a function that relates the different specific conductivities affecting the cell and is defined in equation 4.2, R is the distance from the centre of the cell to the edge and ϕ is the angle from the point on the cell being measured and the direction of the field. This equation only holds true for a steady state simulation where it is assumed the cell has had time to settle after being exposed to the electric field [82]. More detailed equations that include the effect of time exist and determining which equation should be used depends on the need for accuracy compared to the computational power available.

$$fs = \frac{3\lambda o\,[(3dR^2\,\lambda i) + (3d^2\,R - d^3\,)]\,(\lambda m\, - \lambda i\,)}{2R^3(\lambda m + 2\lambda o\,)\,(\lambda m\, + \frac{1}{2}\lambda i\,) - 2\,(R-d)^3(\lambda o - \lambda m\,)(\lambda i\, - \lambda m\,)} \qquad (4.2)$$

The value of fs is calculated using equation 4.2 where λo, λi, and λm are the specific conductivities of the extracellular medium, cytoplasm and the membrane, respectively, and d is the thickness of the membrane [82]. Using the same parameters as those used in the model produces a value for fs of approximately 1.5. The equation for fs combines the specific conductivities across the 2D slice of the cell by taking into account the radius of the cell and the thickness of the cell membrane. A more detailed analysis of how the equation for fs is derived can be seen in Kotnik et al [93].

While equation 4.1 is suitable for a single cell model it is difficult to produce a model containing multiple cells. While the equation may still hold true for each cell it is difficult to determine how each of the cells influences the effects of the applied field when they are in close proximity and so

determining the effect of applying a uniform electrical field becomes difficult to predict and difficult to verify.

One of the main problems in determining the cell's influence on each other is that the cells' response to an electric field will change when electroporation occurs. When its permeability is increased it also becomes more conducting due the release of ions from within the cell. This problem is further exacerbated by the fact that the point at which a cell undergoes electroporation is not precisely defined but instead there is a known range of intensities in which a cell will undergo electroporation, which introduces non-linearity. A model produced recently was able to overcome these issues to some extent as it was able to show behaviour that matched that found experimentally, and was able to predict the proportion of cells that are likely to undergo electroporation for a given electric field [81]. The study modelled a group of irregularly shaped cells and compared these to the results of an experiment in which cells were injected with dye and exposed to a steadily increasing electric field. The percentage of cells undergoing electroporation in the model was within the margin of error of the number of cells undergoing electroporation in the experiment. However, the margin of error was in the region of ±25% for certain electric fields and the cells being used being very different in shape and formation to those found in the skin.

4.4 Chapter Summary

This chapter outlines the expected behaviour of a skin cell when exposed to an electric field. A skin cell is characterised by the low impedance cytoplasm and surrounding medium and the high impedance cell membrane. A look at how the electrical properties of cells can be measured is explored, looking at the difficulties of acquiring accurate properties from cells in vivo. An equivalent circuit model for a skin is discussed describing the limitations of such a circuit when trying to consider how numerous different factors might influence skin impedance. One of the main focuses of this chapter is on how the cell membrane is effected by an applied electric field in the form of electroporation. An applied signal of sufficient voltage and pulses can cause the membrane to form pores that will either recover over time or become permanent cell damage. These pores significantly reduce the overall cell impedance.

The next chapter describes the models produced for this thesis. This includes a review of work done by Pucihar et al and Walker et al upon which the models are based. Of particular interest are the results of the hydration model that looks at how a change in the conductivity of the SC will lead to a substantial drop in the skin's impedance as well as the impact of electroporation based on a number of different applied voltages.

5 Models

This chapter starts with an overview of the types of models for representing the electrical properties of skin currently available in the literature, including critique of validity and lack of incorporation of factors such as electroporation and hydration. A description of all the models produced for this thesis is provided, stating how the model was produced, what parameters were used and what simulations were run. A range of results from these simulations are shown that best demonstrate the noteworthy behaviours of the simulations. Of particular focus in this chapter is the development and results of the hydration model, which has been designed to simulate the effect on skin impedance of hydrating the skin. Also of particular interest in this chapter is the electroporation model, developed to determine whether electroporation occurs during the application of signals typically used in FES.

5.1 Model Development

While reviewing the literature a number of approaches to modelling the electrical properties of skin have been used. As discussed previously one such method was the model skin as an equivalent circuit. The way in which this is done typically is to replace different elements of the skin, typically the SC and the lower layer, sometimes incorporating circuitry for sweat glands or other features as well incorporating circuitry for electrodes.

In practical situations this can be very helpful, as standard circuit analysis tools can be used to work out how the skin’s impedance will affect an applied signal. This approach was not used for this thesis for a number of reasons. One the main disadvantages of using an equivalent circuit is that it requires that all factors other than those specifically represented by circuitry are not a significant influence on the skin's impedance. This may be the case under specific conditions, and with enough

experimental data these models can provide a good approximation of expected behaviour, as shown in the work by Martinsen et al [94].

The main aim of this thesis was to determine whether or not factors that were not typically modelled might influence FES signals used in standard operation. In particular, trying to determine the influence of hydration and electroporation would not have been possible using an equivalent circuit. This is because it was not known before simulation exactly what circuitry would be able to reproduce these effects, or even if these effects would be relevant for the types of signals used in FES.

A model created by Huclova et al [62] represented the skin as distinct layers with the relevant dielectric properties representing each of the layers. The results of the simulation were in strong agreement with the predicted skin impedance when exposed to high frequencies above 10 kHz, however large discrepancies were found at frequencies below this value. It was thought that while this approach might be a more faithful representation of reality when compared to an equivalent circuit model, it still did not include a lot of factors that would influence the electrical behaviour of skin. The effects of factors such as hydration and electroporation were not considered during the creation and simulation of the model. While electroporation might not be a factor it has been well established that hydration, either through external application in the form of water or other hydrating solution, or through sweat can play a very noticeable effect on overall skin impedance [1], [95], [96].

Other than using an equivalent circuit model or trying to represent the skin as distinct layers another approach was to use finite element modelling at a cellular level [82]. Typically this was to explore how different features of a cell might affect the creation of electropores. One model in particular was using FEM to determine how cell shape would affect the measured ITV and includes simulation, experimental and analytical results for comparison. A logical extension to the layer level model produced by Huclova et al [77] would have been to model the impact of hydration, and could have been used to explain some of the discrepancies between their modelled results and their measured results from experimental data. The advantage of the layer model over the circuit model for this is that hydration should only impact the SC as it forms a barrier to the lower layers of skin, meaning that only the SC would need to be included in the model [97]–[99]. However, trying to determine the effects of cell shape or electroporation would have been difficult as these effects occur at cellular level [100]–[102].

FEM was selected for the models in this thesis in order to try to incorporate as many of the potential physical factors available, whilst keeping the level of complexity in the model as low as possible to reduce the computational power required. Throughout the literature review in this thesis there have been several references to the large volume of factors that could be included in any model of the skin from an electrical perspective. Factors such as age, season, temperature, sweat, gender and location on the body are all factors that have been shown to have a measureable impact on conductivity [8], [13], [14], [34], [42], [75], [103], [104]. Using FEM allows for the creation of cells that fit to the pentagonal or hexagonal shape of the cells typically found in the skin and to provide these structures with the same dielectric properties as they would be expected to have in reality.

Another advantage of using FEM is that different features such as hydration and electroporation can be explored by determining firstly how they would influence the individual cells of the skin. Following this the model could then be expanded in scale to determine how these factors would affect the layers of the skin. This could have been done in an equivalent circuit, however when attempting to incorporate all the influencing factors validation would be very difficult. This is due to the variances in thickness and composition of different layers, the disparity of extracellular lipids, as well as the influence of hydration [32], [79], [94], [105]–[107]. It would also be particularly difficult to incorporate the effects of electroporation, as they occur at the cellular level. In addition, the exact field strength and duration required for electroporation are not well understood except in specific highly researched areas, such as cancer treatment.

One of the issues with FEM modelling is that it can be very difficult to predict whether or not a simulation will converge beforehand. Whether or not a model will converge and how long it takes for a model to converge are influenced by a great number of factors, such as element size and number, geometry used, the smoothness of the applied signals and the types of physics being modelled. The approach typically used to aid convergence is to use a coarse mesh and the least number of geometries possible and to then increase model complexity slowly. In this thesis a course mesh was used initially for the models, and a finer mesh then generated.

In order to analyse the effects of electric fields on cells, algorithms based on the finite element method were used in this thesis. The finite element method is a technique used for finding approximate solutions for certain types of differential equations. The technique involves breaking down large domains into small elements that can require less time and computational power to solve. The COMSOL® Multiphysics software uses FEM by representing physical objects as a mesh of finite elements which can then be analysed to find the behaviour of the whole system. The mesh

elements attempt to match the shape of the original objects as much as possible, although some approximations are required for curved surfaces. The size of each mesh element will vary within a certain range in order to ensure that a mesh is created without any gaps. The choice of mesh element size is important; too large and the results will not show an accurate representation of what is occurring; too small and the simulation will require a lot of time to compute. Also, using smaller mesh sizes does not always provide more information, as small mesh elements in areas with little or no activity provide no extra insight into the system as a whole. The issue with this is that it is not always possible to know which parts of the system will provide interesting results beforehand; therefore testing with different meshes can be informative. The mesh densities used for each of the different models is provided in Appendix B although the element sizes will vary based upon what is being modelled.

Simulation solutions are calculated by using built in algorithms that perform multiple iterations until the answer has converged within a predetermined tolerance. Specifically, for the models in this thesis COMSOL® Multiphysics software uses equations defining electrical behaviour as shown in Appendix A. All the solutions produced by the software are approximations, so some level of error is expected, however the tolerances used for all the models produce results with an error within 0.1% of the simulated answer which is accurate enough to draw conclusions from. It is important to note that all results are based on simulation, therefore not independently valid without supporting experimental data. It is possible for the simulated solutions to converge on incorrect values, however the results have been compared to analytical and experimental data in the literature to promote validity.

5.2 Single Cell Boundary condition

The first stage in creating the model was to look at an existing model produced by Pucihar et al [82]. The model they produced was able to determine the induced transmembrane voltage (ITV) across a cell in order to improve the understanding of electroporation. The model produced by Pucihar also introduced a novelty by using a boundary condition to model the membrane, instead of representing it as a thin layer surrounding the cell in their model. It was shown that such a substitution not only saved a lot of computational power, but was able to produce results that were

accurate when compared to the predicted output using the analytical solution. The reason for this was attributed to the fact that using membranes that accurately reflect reality requires a substantial number of mesh elements, so many that the only feasible method of producing a viable model is to increase the thickness of the membrane and alter its properties so that a model can be run in a reasonable timeframe. However, such an approach introduces errors and while the boundary condition is not a true reflection of reality the way it is derived provides a very accurate substitution [81].

$$J = \frac{\sigma_m(V_o - V_i)}{d} \qquad (5.1)$$

The equation used to replace the membrane in the model is given by equation 5.1 where J is the normal component of the current density, σ_m is the specific membrane conductivity which is 50 μSm^{-1}, d is the membrane thickness which is 5 nm, and Vo, Vi are the electric potentials at the outer and inner surface of the membrane.

The model in this thesis was produced using the COMSOL® Multiphysics 4.4 modelling software. The model contains a cuboid block of material with dimensions 100x100x100µm which is then given the properties of the conducting solution used by Pucihar et al [82]. To simulate the electric field one of the sides is set as a constant 1V voltage source while the other side is treated as ground. The remaining sides are set as insulating surfaces. This produces a uniform electric field of $100Vcm^{-1}$ across the block which is considered to be a large electric field.

The cell itself is represented with a sphere of radius 10µm. In Puchihar's original paper the model was then extended to include an irregularly shaped cell, but because of the relatively uniform shape of keratinocytes implementing this step is unnecessary [38], [53], [108].

The inside of the cells was given a specific conductivity to represent all of the content inside of each individual cell. The electrical behaviour of the cell membrane is set by applying equation 5.1 on the boundary of the sphere. The sphere is placed on the centre of an insulating plane with the bottom of the cell 5µm from the surface. Figure 5.1 shows an image of the geometry of the model for a spherical cell, with the large block representing the suspension solution used in the cell shape experiment.

The shape and the location of the cells are assumed to be constant for the model. This assumption seems valid given the tightly packed nature of the skin cells which keeps them from moving and changing shape. The mesh was created automatically by COMSOL® Multiphysics, with an example

mesh shown in figure 5.2. The mesh elements were set to have maximum dimensions of 10µm and minimum size of 1.8µm.

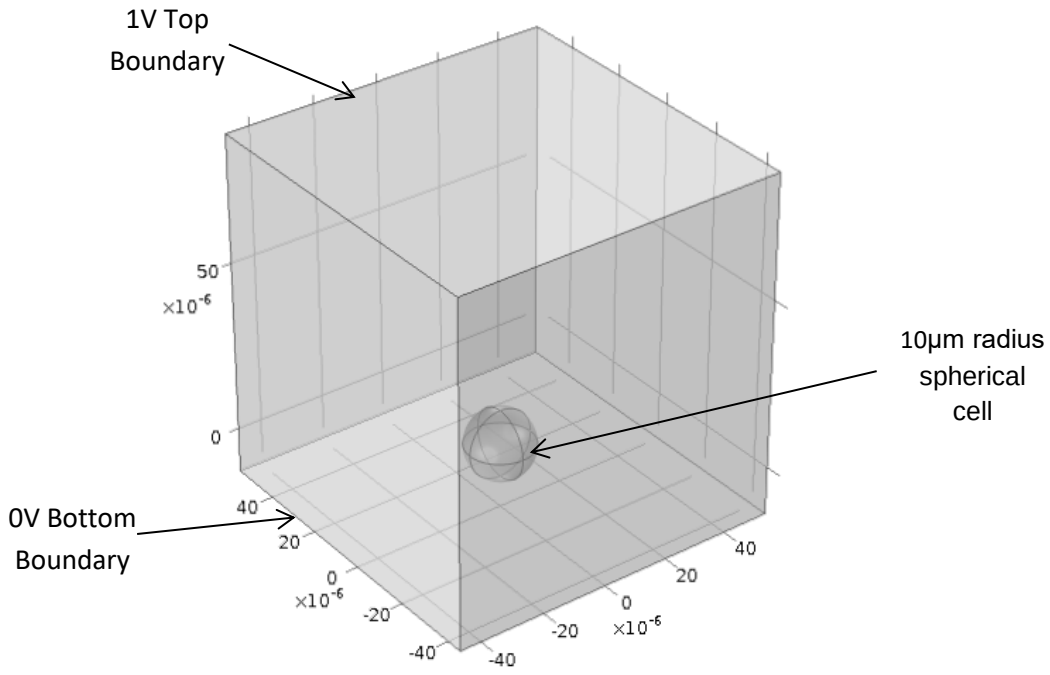

Figure 5.1 Geometry of model showing the conducting medium and spherical cell with the measurements in microns

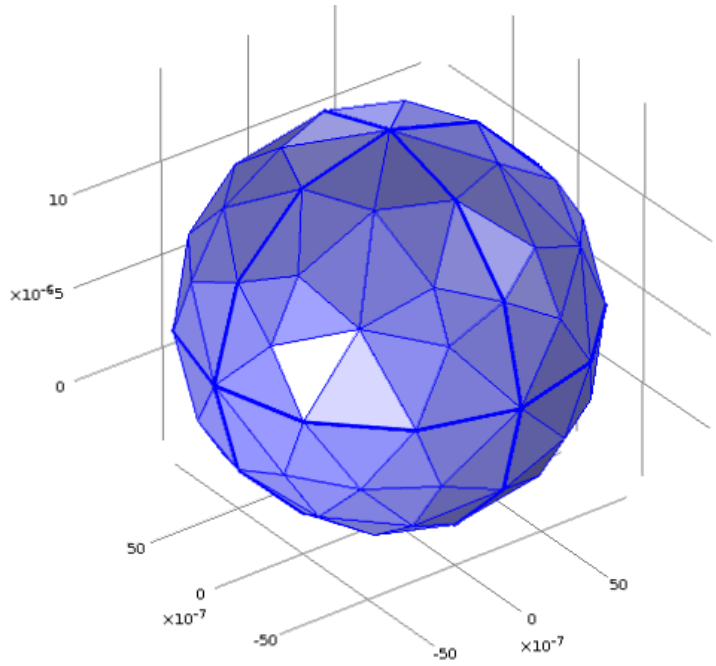

Figure 5.2 Image of the mesh elements used to represent the spherical cell produced by COMSOL® Multiphysics

The result of the simulation that is of interest is the ITV along a 2D slice of the cell, through the centre of the sphere. The analytic solution used for comparison is provided using equation 5.1 where the value for fs is calculated by using equation 4.2.

Parameter	Value
λo	1 Sm^{-1}
λi	0.2 Sm^{-1}
λm	50 μSm^{-1}
R	10 µm
d	5 nm

Table 5.1 Parameter values used in single cell boundary model

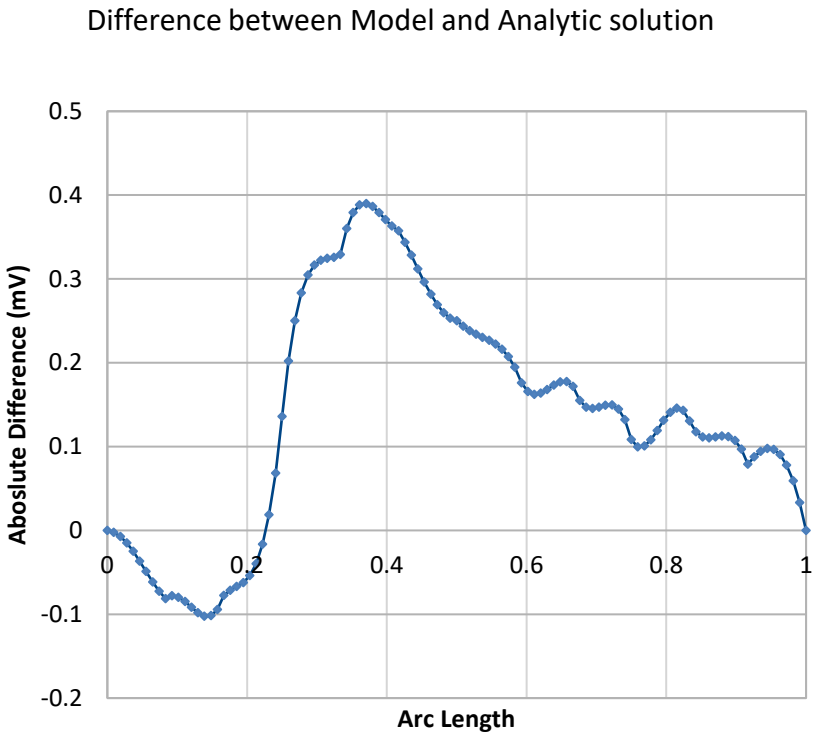

Figure 5.3 Spherical model results showing the absolute voltage difference between analytic and simulated voltage where arc length is the normalised distance from top point on the cell's surface and the point on the cell's surface being measured

A simulation of a cell using equation 5.1, the parameters shown in table 5.1 and COMSOL® Multiphysics was carried out. The plot on the bottom of figure 5.3 shows that the absolute difference between the simulation using COMSOL® Multiphysics and the analytic solution is very small. The results range between -150mV to 150mV and the biggest difference at any point is around 0.4 mV. This shows that the spherical model provides an accurate representation of a cells electrical response and that using a boundary condition to substitute the cell membrane leads to a very small difference between simulated and analytic results.

5.3 Epithelium Model

A second model was developed based on the work of Walker et al [109]. The model was designed to represent the electrical properties of cervical epithelium with the aim being to investigate

whether changes in electrical properties of these cells can be an indicator of cancerous cells. The model was chosen because it used cells with almost identical properties to the cells found in the skin; the parameter values used in the model were in fact obtained from skin cells. The model simplifies the cell interior substantially, using a uniform material to model the cytoplasm and a small cuboid to model the nucleus. However, there are some key differences between the cervical epithelia model and the desired skin model in this thesis. While the cervical epithelium cells are very similar in shape and properties to those found in the dermis and epidermis there is no analogue for the corneocyte found in the SC present in the model. There is also no experimental data to compare the simulated results against. Another factor that might have been important was that the model developed by Walker at al [109] does not include sweat or hair glands, due to their absence in the cervix, although these features are also not in the final skin model due to the difference in scale.

As with the previous model COMSOL® Multiphysics 4.4 software was used. The model was set up as a frequency dependent study using the electric currents module. Using the inbuilt CAD tools a 3D model of the nucleus cytoplasm and surrounding medium was created, the resulting cuboidal cell can be seen in figure 5.4. Each element was then given a relative permittivity and electrical conductivity in keeping with the values for their biological counterparts, with the exact values shown in table 5.2.

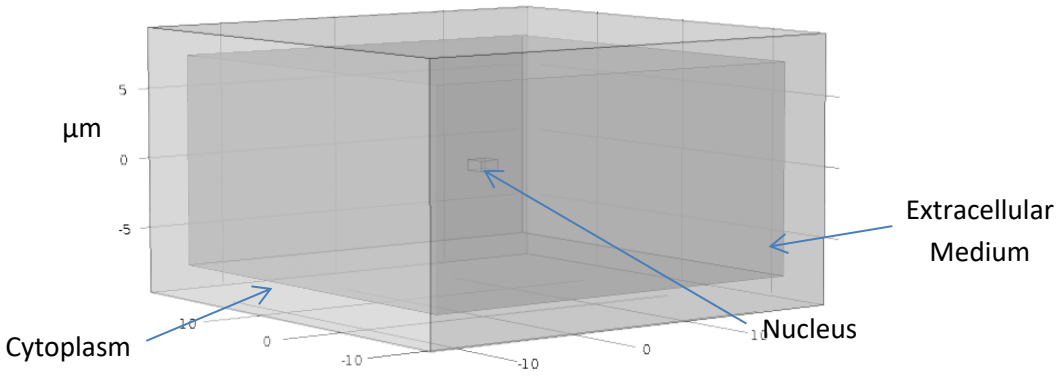

Figure 5.4 Single cell created in COMSOL® Multiphysics with scale in microns

In order to reduce the computational power needed to run the simulation, the cell membrane and the nuclear membrane were not created as part of the geometry of the cell but were instead replaced with a boundary condition in the same way the cell membrane was replaced in the spherical cell model. Unlike in the previous model where this was achieved by manually inserting the equations into the model, an equation for the contact impedance was applied to each of the

nuclear membrane and the cell membrane boundaries. The contact impedance is part of the electric currents physics package and is shown in appendix A. This substitution removes the need for a much finer mesh for the nanometre scale membrane compared to the other micrometre scale elements. The thickness of the cell membrane was set to 8nm and the nuclear membrane to 40nm with the electrical properties shown in table 5.2. The reason for the change in the cell membrane thickness from 5nm in the previous model to 8nm is that the model produce by Walker et al used 8nm for the membrane thickness. This is due to the type of cell used by Walker et al for their experiments.

The mesh elements were set for a size between 0.612µm and 3.4µm with a smaller mesh size between 1.19µm and 0.051µm for the nucleus, with the exact sizes and shapes being determined by COMSOL® Multiphysics. This was chosen because the nucleus is only a small volume compared to the entire cell and so a fine mesh would not dramatically increase the simulation time and the large mesh size may not be able to provide a reliable estimate for the small nucleus.

	Dimensions (µm)	Relative permittivity	Conductivity (Sm^{-1})
Extracellular medium	34x34x19	72	1.1
Cytoplasm	30x30x15	86	0.6
Nuclear Interior	1.5x1.5x1.5	145	0.8
	Thicknesses (nm)	Relative permittivity	Conductivity (Sm^{-1})
Cell Membrane	8	90	$1x10^{-7}$
Nuclear Membrane	40	31	$2x10^{-3}$

Table 5.2 Parameters for the single cell model as used in the model by Walker et al [109]

One of the sides of the extracellular medium was set to be the input signal with the opposite side grounded as shown in figure 5.5. The remaining sides are set as electrical insulators. The input signal

was set up as a sinusoidal voltage that varies between 0V and 10V peak to peak and tested at 11 frequencies: 100Hz, 1kHz, 10kHz, 20kHz, 50kHz, 100kHz, 200kHz, 500kHz, 1MHz, 5MHz and 10MHz.

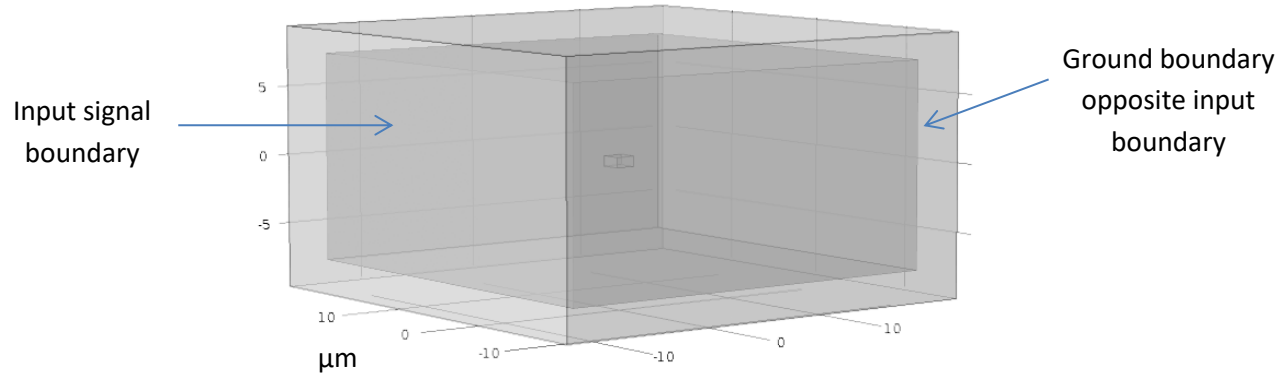

Figure 5.5 Single cell model geometry

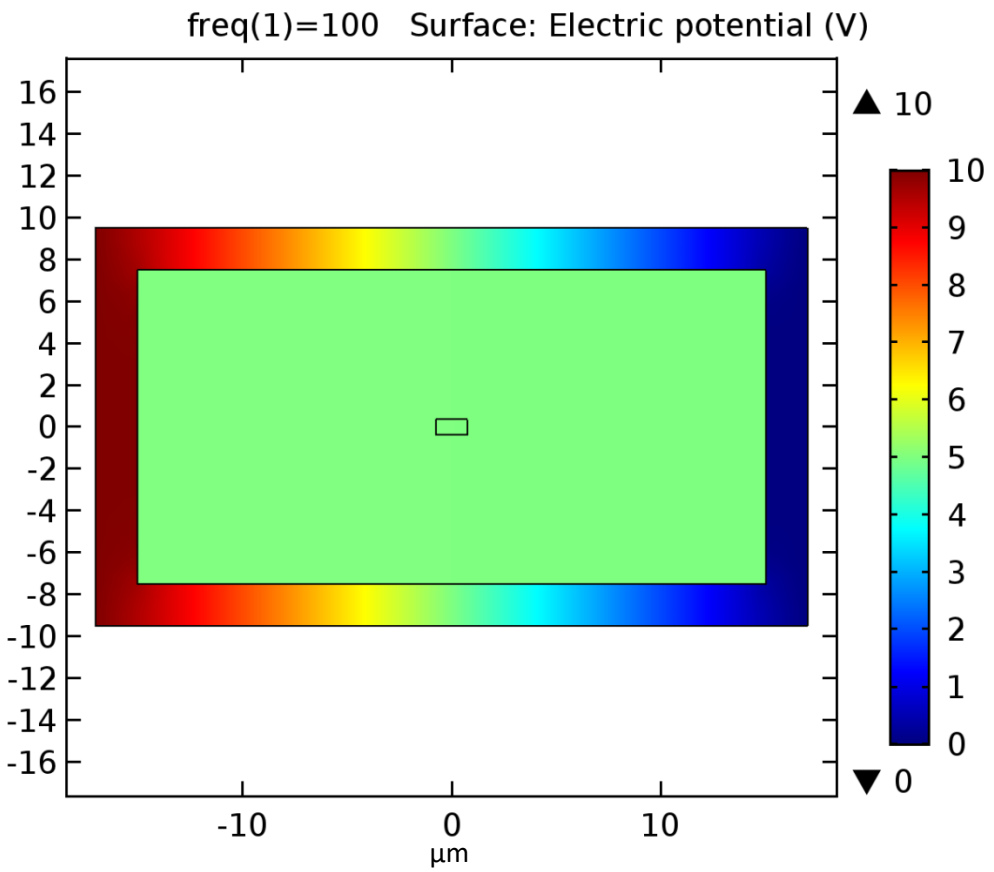
freq(1)=100 Surface: Electric potential (V)
16
14
12
10
8
6
4
2
0
-2
-4
-6
-8
-10
-12
-14
-16
-10
0
10
µm
▲ 10
10
9
8
7
6
5
4
3
2
1
0
▼ 0

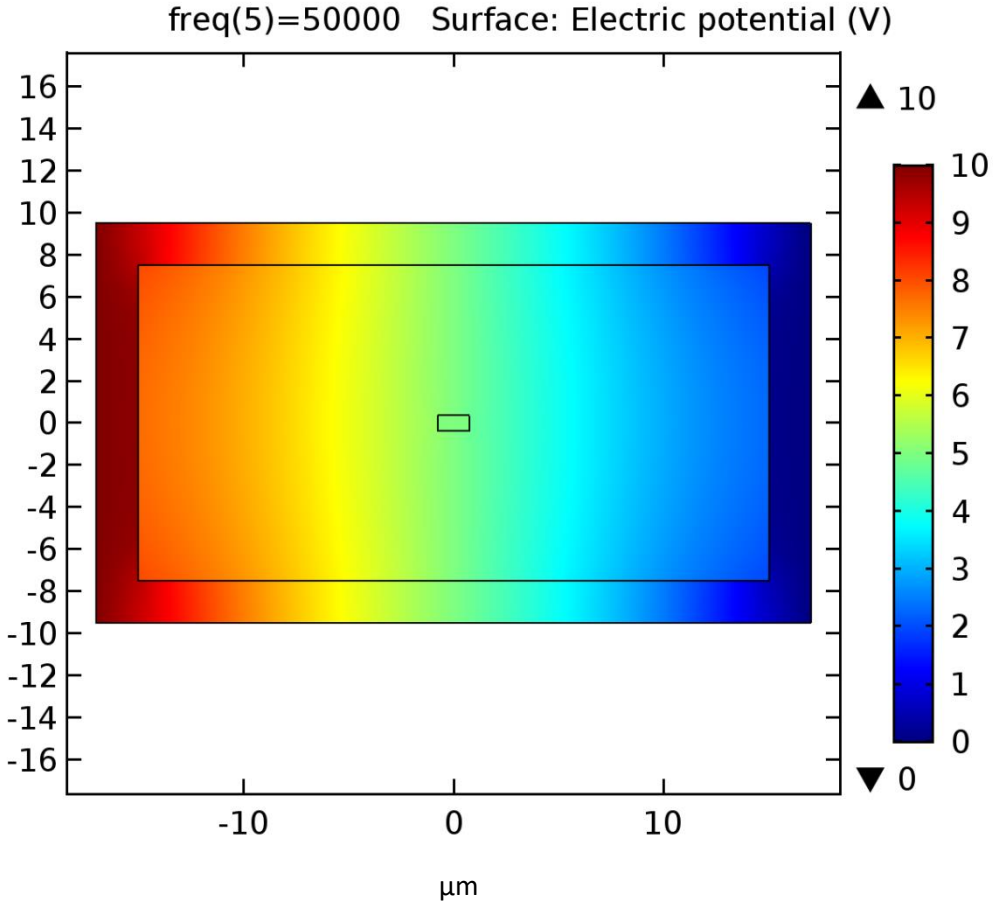
freq(5)=50000 Surface: Electric potential (V)
16
14
12
10
8
6
4
2
0
-2
-4
-6
-8
-10
-12
-14
-16
-10
0
10
µm
▲ 10
10
9
8
7
6
5
4
3
2
1
0
▼ 0

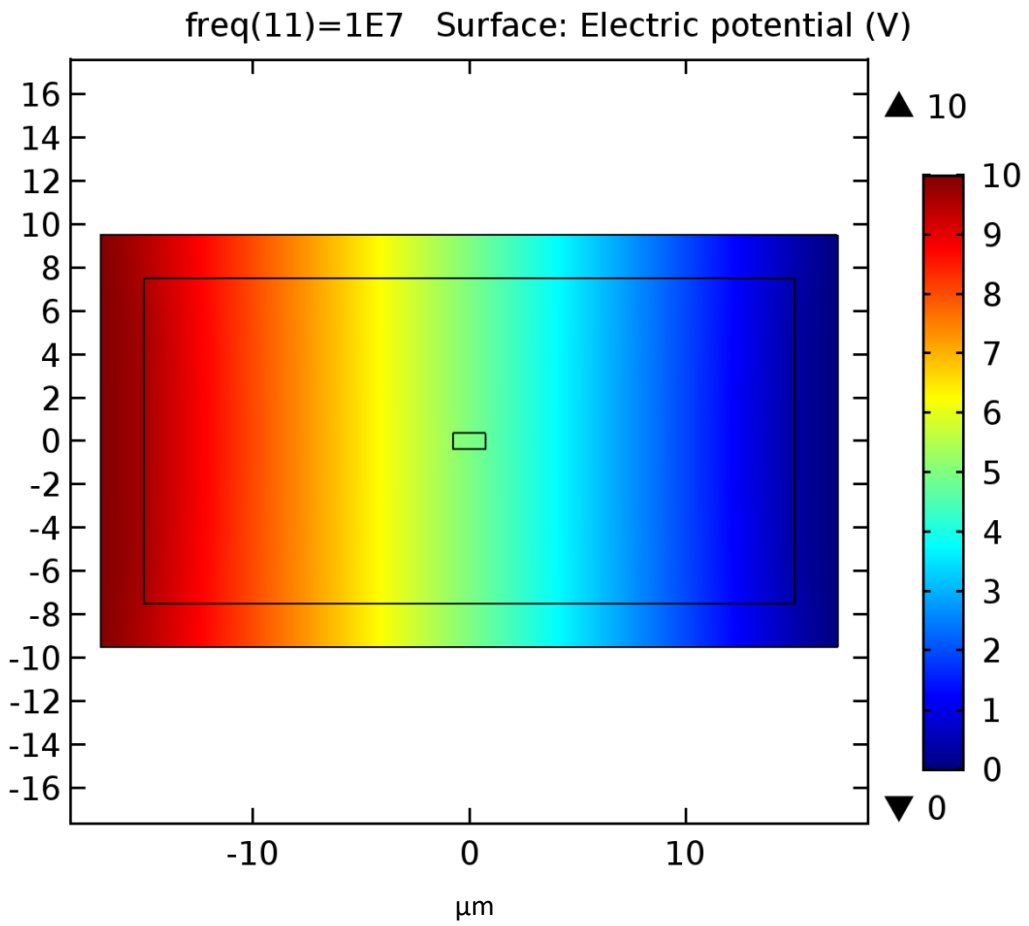

Figure 5.6 A plane through the centre of the cell shown in figure 5.4. Shows the voltage across the plane at 100Hz (top), 50kHz (middle) and 10MHz (bottom) with 10V input voltage.

Figure 5.6 shows the voltage gradient across the cell and the extracellular medium at the lowest and highest of the 11 frequencies.

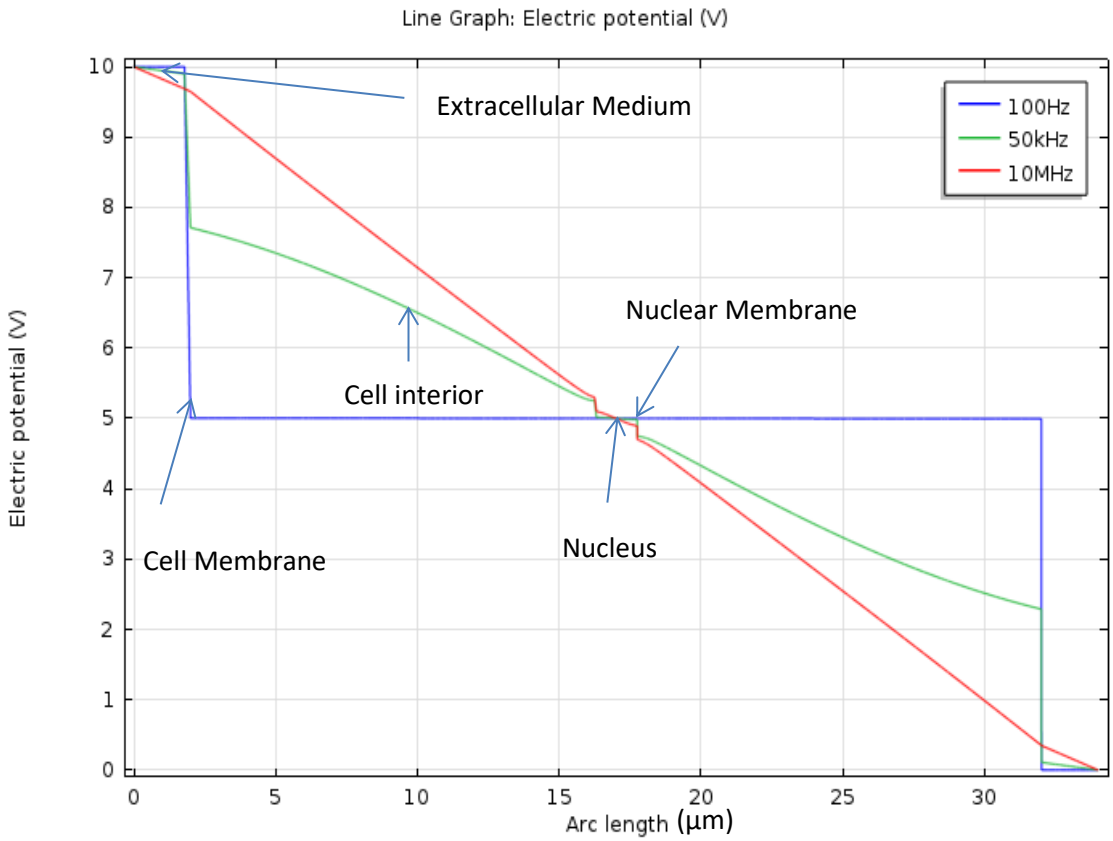

Figure 5.7 Voltage gradient across single cell and extracellular medium at 100Hz, 50kHz and 10MHz

What can be seen is that at the lowest frequency the cell membrane prevents current flowing into the cell, creating a uniform voltage across the cell interior. As the frequency increases some of the current passes through the membrane, this creates a voltage gradient across the inside of the cell. At a frequency of 1MHz and above the membrane stops influencing the current entirely, the voltage gradient across the extracellular membrane and across the cell interior is identical, except for the nucleus. This effect can be seen more clearly in figure 5.7 where the plot shows the difference in voltage between each end of the cell interior.

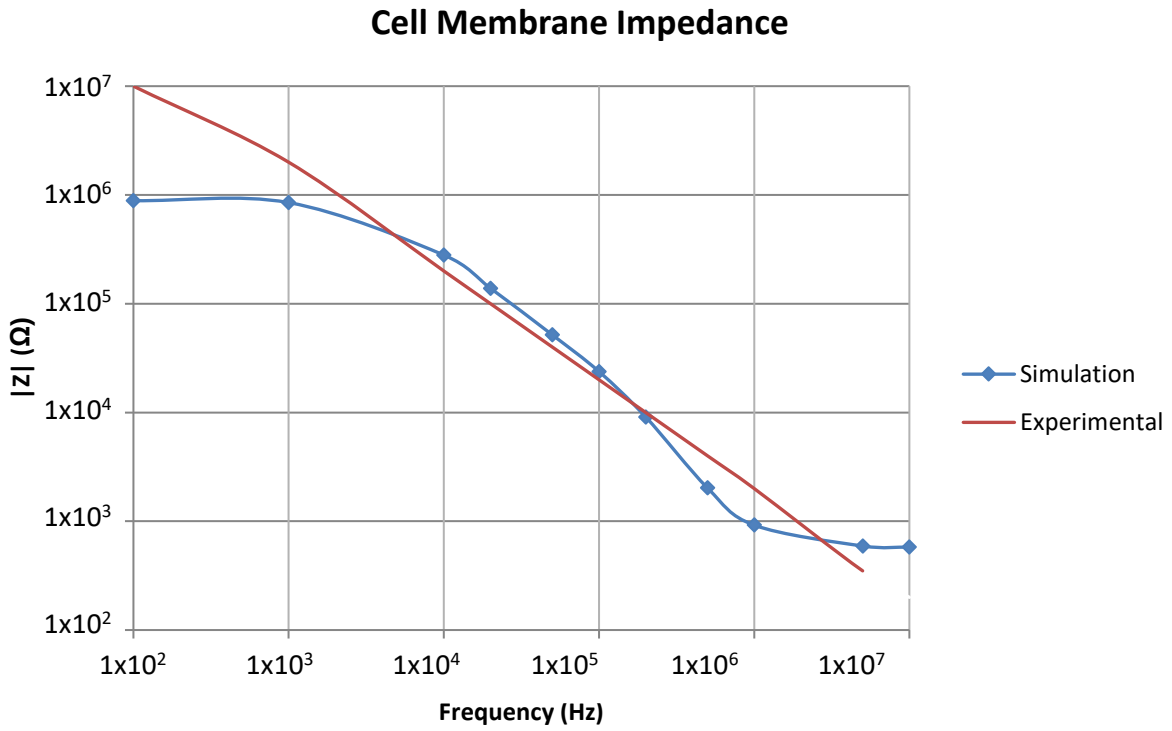

Figure 5.8 Impedance of cell membrane across all frequencies simulated

The plot in figure 5.8 shows the impedance of the cell membrane calculated from the model and the experimental results of cell membrane impedance for a rat fibroblast cell measured by Bai et al [55]. The behaviour shown by both sets of results shows high impedance at a low frequency that drops off as the frequency increases, which is to be expected from the experimental data found in the literature [4], [110]. What is interesting is that while there is only a small difference in the 1kHz to 100kHz region there is a noticeable difference between the experimental and simulated impedances at the high and low frequencies. The exact cause for the difference is unknown, possible factors could be the influence of the surrounding medium in the model, the cell's dielectric properties changing in the experiment while remaining constant in the model or due to the different dielectric properties of the rat fibroblast cell measured and the skin cell being modelled. A factor that likely plays considerable role in the differences measured is the different shape of the cells in question. Keratinocytes tend to have a fairly fixed cuboidal shape while the fibroblasts tend to be more spherical [60].

5.4 Three by Three Cells Model

The single cell model was expanded to include more cells. The first extension was done by creating an array of 27 cells with the same properties as the single cell and expanding the extracellular medium appropriately. The 3 by 3 cell array can be seen in figure 5.9. The array of cells was tested at the same range of frequencies and using the same electrical properties shown in Table 5.2 as for the single cell.

The frequency response shows that even with more cells present the change in the cell membranes' impedance with an increase in frequency is the same as was found in the single cell model. This means that when scaling the model by adding more cells that it can be ignored as a potential factor in changes in behaviour in later models.

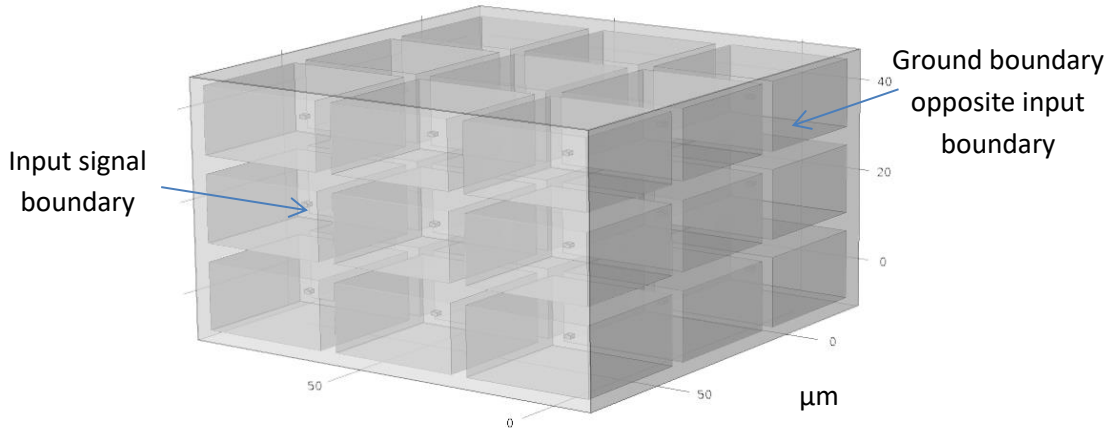

Figure 5.9 3x3 Array of cells with scale in microns

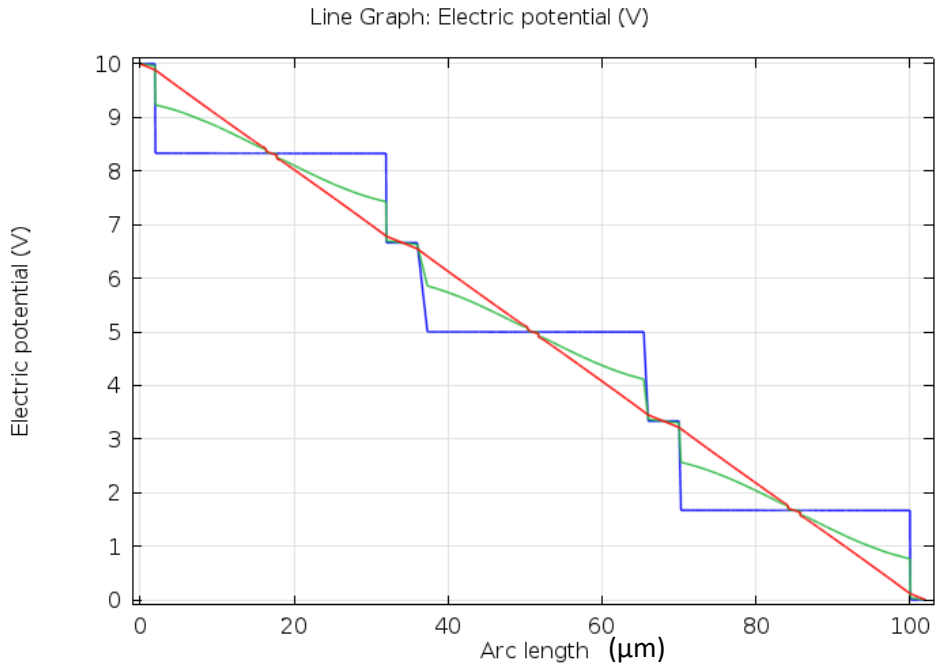

Figure 5.10 Voltage across a line through the centre of 3 cells in the array, the blue line is at 100Hz, the green line at 50kHz and the red line at 10MHz

The results in figure 5.10 show that the array of cells has a very similar behaviour to what was found with a single cell. At the low frequencies, the cell membrane has very high impedance that decreases at the higher frequencies. The sharp drop in voltage shown between the less steep sections is due to the surrounding cell medium, which has a much lower impedance than the cell membrane. This result was the expected outcome as the individual cell properties had not changed. However, it was important to ensure that scaling up the number of cells did not change the behaviour in an unexpected way.

5.5 Three by Six Cells Model

The next step was to incorporate more cells but also to include cells of a different shape because skin cells at the higher levels such as the SC are much flatter than those found at the lower levels of the epidermis. This model extension is the first step towards incorporating two layers of skin, with the upper thin cells representing the shape of the dead keratinocytes found in the SC and the cells below similar to those found in the stratum spinosum. This extension only alters shape; the electrical properties of the cells are still the same for both layers. The other main difference between models is that the input signal is at the top of the model and the ground boundary at the bottom.

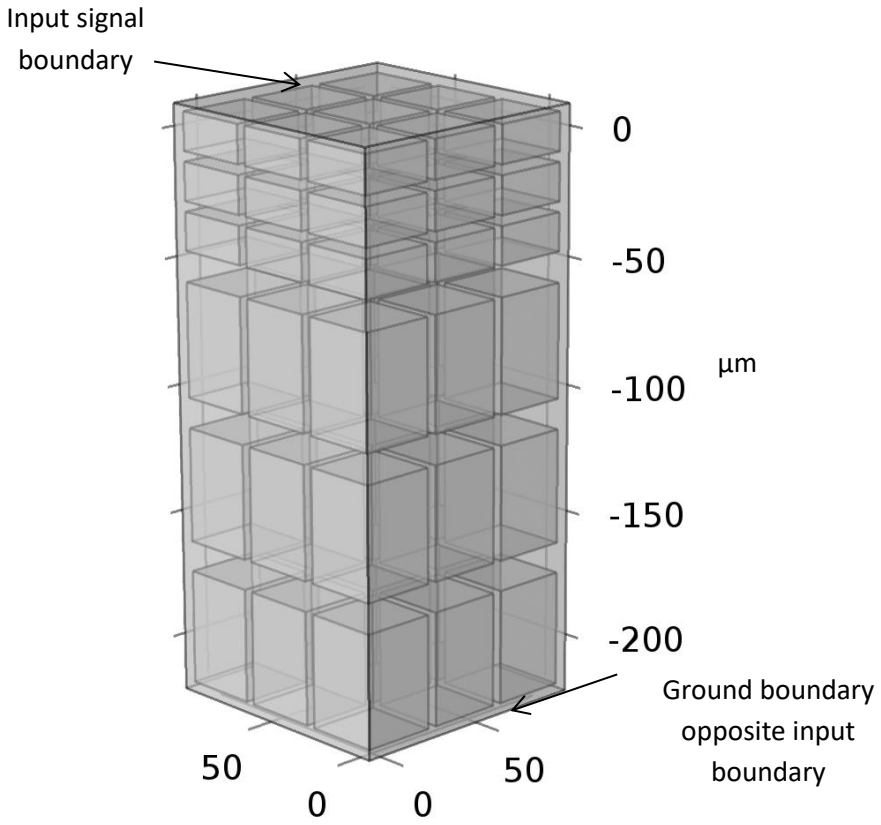

Figure 5.11 3x6 Cell Array with scale in microns

The other substantial change in the 3x6 model was to change the location of the voltage source and the ground planes, as shown in figure 5.11 to represent sending signals through the skin. For this change the mesh elements had a reduced limits in the smaller cells. In the large cells the elements had a maximum size of 2µm while they had a maximum of 1.5µm in the smaller cells. This change was determined by checking the results of the simulation at 100Hz and 1MHz with mesh elements with a maximum size of 0.3µm and increasing until the difference in simulated results change by more than 0.1%. At lower frequencies there is a very similar behaviour to the results found from the 3x3 model, with the cell membrane acting as a barrier to the flow of current and at higher frequencies there is also a substantial drop in the cell membrane's impedance. There is a voltage drop of 5V across the smaller cells as well as a 5V drop across the larger cells. This suggests that even at high frequencies the membrane is still having an impact on the overall behaviour of skin impedance.

(a)

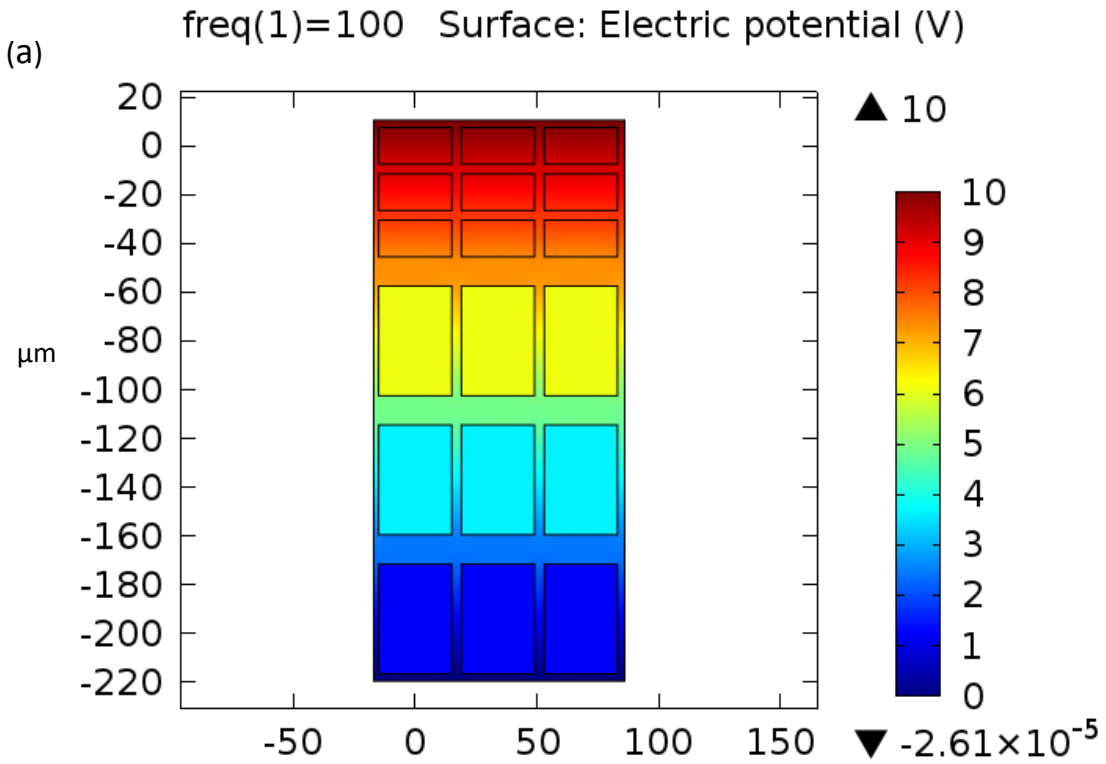
freq(1)=100 Surface: Electric potential (V)
µm
20
0
-20
-40
-60
-80
-100
-120
-140
-160
-180
-200
-220
-50
0
50
100
150
▲ 10
10
9
8
7
6
5
4
3
2
1
0
▼ -2.61×10-5

(b)

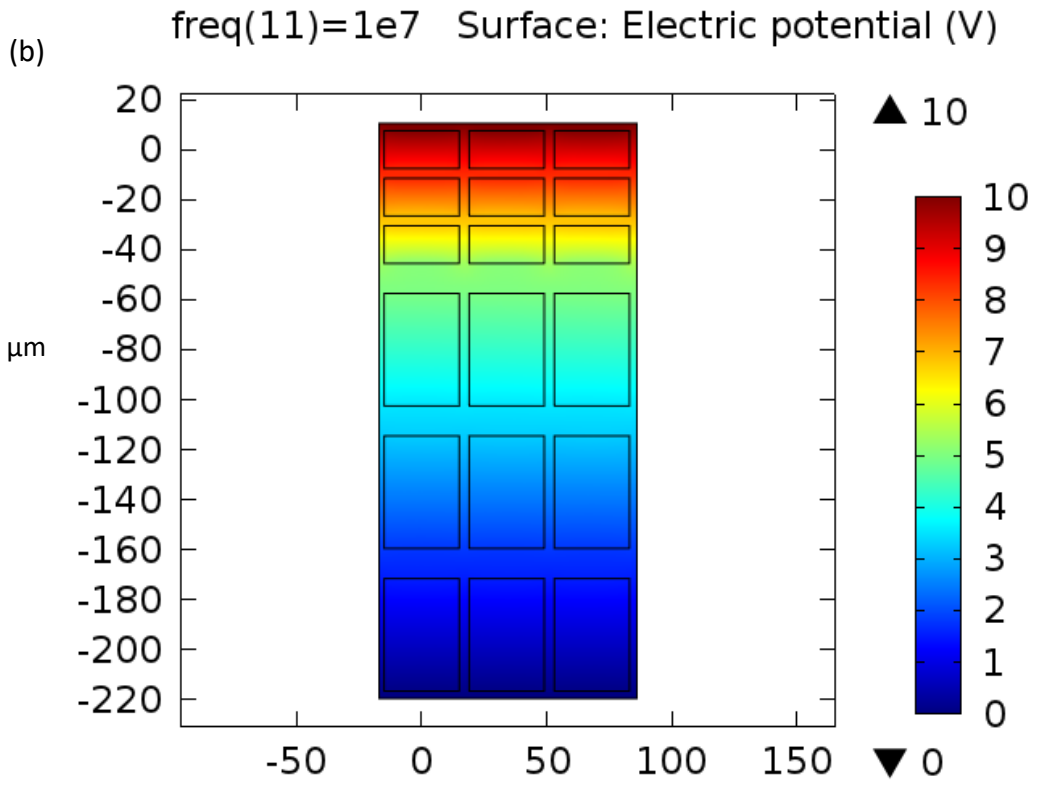
freq(11)=1e7 Surface: Electric potential (V)
µm
20
0
-20
-40
-60
-80
-100
-120
-140
-160
-180
-200
-220
-50
0
50
100
150
▲ 10
10
9
8
7
6
5
4
3
2
1
0
▼ 0

(c)

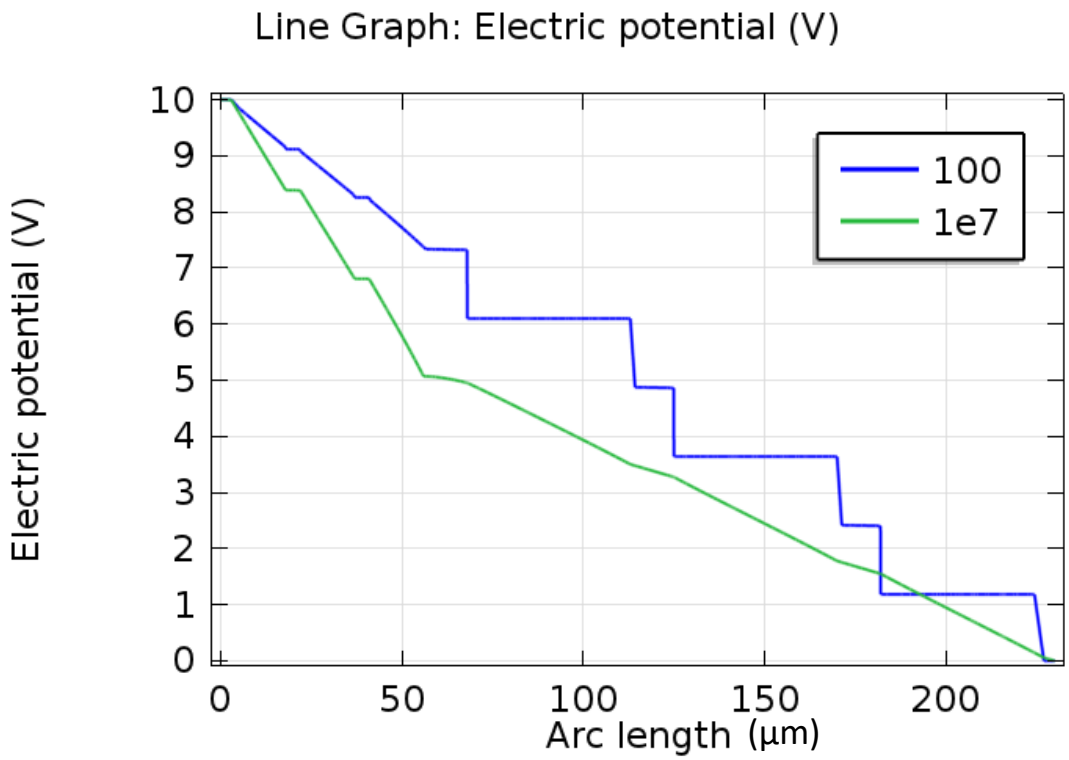

Figure 5.12 Voltage across a cut plane through the cell array at 100Hz (a) 10MHz (b) and voltage across a line through the centre of 6 cells in the array (c) where the blue line shows 100Hz and the green line 10MHz and arc length is the distance in microns from the 10V boundary

What can be seen in Figure 5.12 is that the change in cell shape shows a greater drop in the voltage in the smaller cells, however due to the uniform dielectric characteristics used the cell's frequency response is unaffected by cell shape. This does not mean that cell shape will not have a substantial impact for irregularly shaped cells, as was found in work done by Pucihar et al [81] because this change still used regularly shaped cells. What the model shows is that for the purposes of this and future models extending or shrinking the dimensions of a cuboidal cell without any other associated changes, will not influence the frequency response of the impedance of skin. In later models the shape of the cell may play a more substantial role as the dielectric properties of the cells are changed.

5.6 Hydration model

A finite element model was produced in order to analyse the effect of hydration of epidermal cells. The model consists of a layer of cells designed to represent the electrical properties of skin cells and

a layer of cells that represent the collective behaviour of the other epidermal layers. The number of cells used to represent the depth of the SC was 15 [61], [104]. Because of the comparatively less important role played by the lower levels of the epidermis 4 larger cells were used with the same electrical properties.

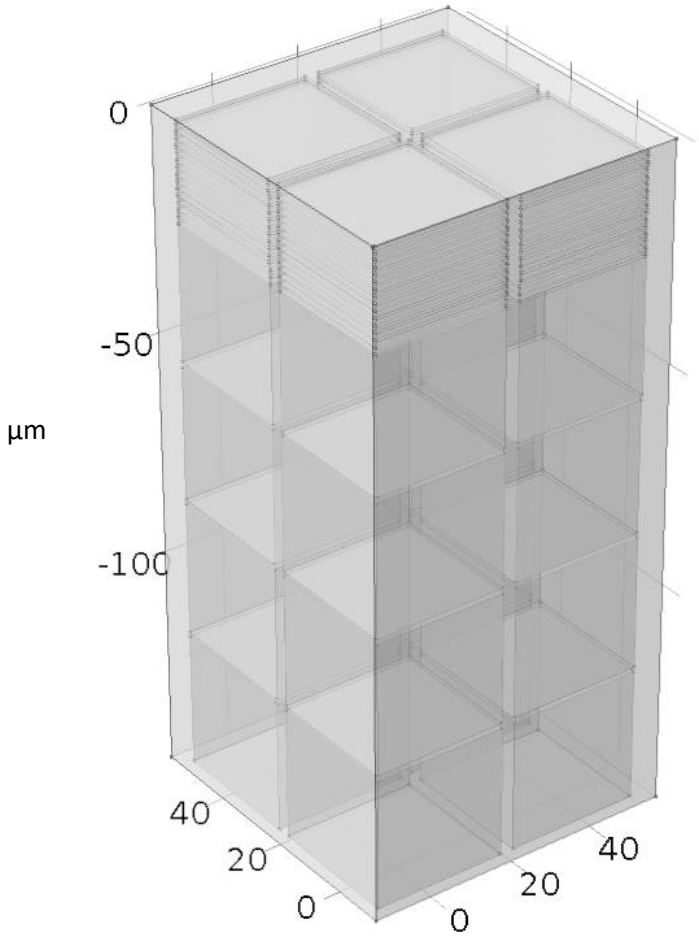

Figure 5.13 Geometry of the model showing the extracellular medium and the two types of cell used

Using the inbuilt CAD tools in COMSOL® Multiphysics a 3D model of the surrounding medium was created, the resulting cuboidal cell can be seen in figure 5.13. Each element was then given a relative permittivity and electrical conductivity in keeping with the values for their biological counterparts, with the exact values shown in table 5.3.

Object	Dimensions (µm)	Relative permittivity	Conductivity (Sm^{-1})
Extracellular medium	34x34x19	72	1.1
Cytoplasm	30x30x30	86	0.6
SC Cytoplasm	30x30x1	86	$1x10^{-7}$
	Thicknesses (nm)	Relative permittivity	Conductivity (Sm^{-1})
Cell Membrane	8	90	$1x10^{-7}$

Table 5.3 Parameters used in the hydration model

In order to reduce the computational power needed to run the simulation the cell membrane was replaced with a boundary condition. The contact impedance is part of the electric currents physics package. This substitution removes the need for a much finer mesh for the nanometre scale membrane compared to the other micrometre scale elements.

One of the sides of the extracellular medium was set to be the input signal with the opposite side was grounded. The remaining sides are set as electrical insulators. The input signal was set up as a sinusoidal voltage that varies between 0V and 10V and tested at 11 frequencies: 100Hz, 1kHz, 10kHz, 20kHz, 50kHz, 100kHz, 200kHz, 500kHz, 1MHz, 5MHz and 10MHz. This frequency sweep was repeated for 3 different values of SC cytoplasm conductivity.

In order to measure the impact of hydrating the skin specifically the SC cytoplasm was simulated with a variety of different conductivities starting from $5x10^{-3}$ Sm^{-1} increasing in steps of $5x10^{-3}$ Sm^{-1} up to and including $50x10^{-3}$ Sm^{-1} to represent the typical conductivity of water [70]. An additional conductivity of $1x10^{-7}$ Sm^{-1} was used to represent the lowest conductivity that might be expected from a corneocyte. Only the conductivity of the cells in the SC were changed because work done previously has shown that as long as the SC is intact then there is no substantial effect of hydration on skin impedance due to tissue fluid below the SC.

Once the simulations had been run the voltage gradient across the cells as well as the current flowing through the cells were recorded at each frequency in order to calculate the overall

impedance of the model. An example voltage gradient can be seen in Figure 5.14 and the impedances and phase angles recorded for the 3 different values of SC cytoplasm conductivity are shown in Figure 5.15.

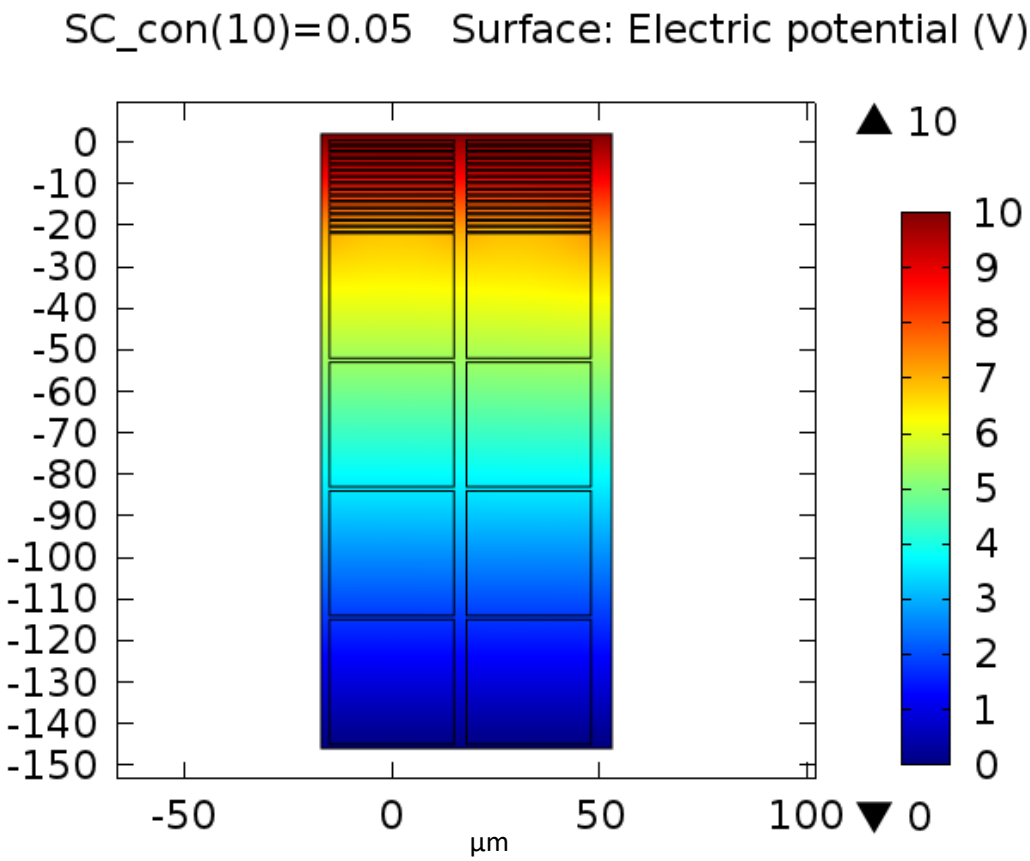

Figure 5.14 Voltage gradient across model with SC conductivity of 0.05Sm^{-1} at a frequency of 100kHz

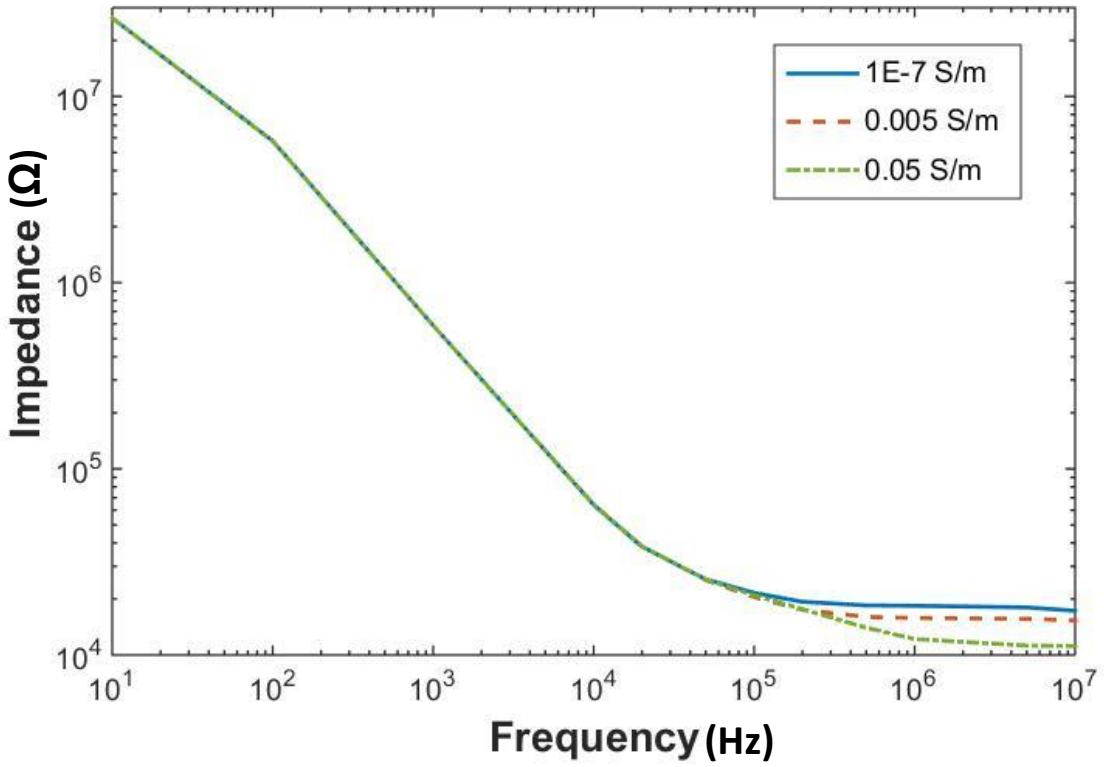
1E-7 S/m
0.005 S/m
0.05 S/m
Impedance (Ω)
Frequency (Hz)

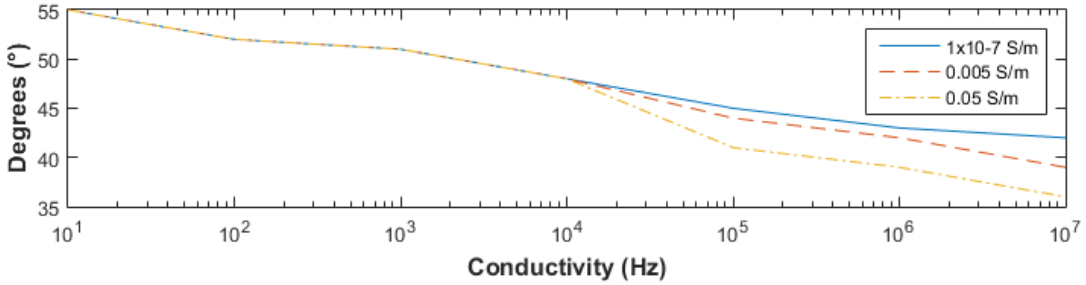
1x10-7 S/m
0.005 S/m
0.05 S/m
Degrees (°)
Conductivity (Hz)

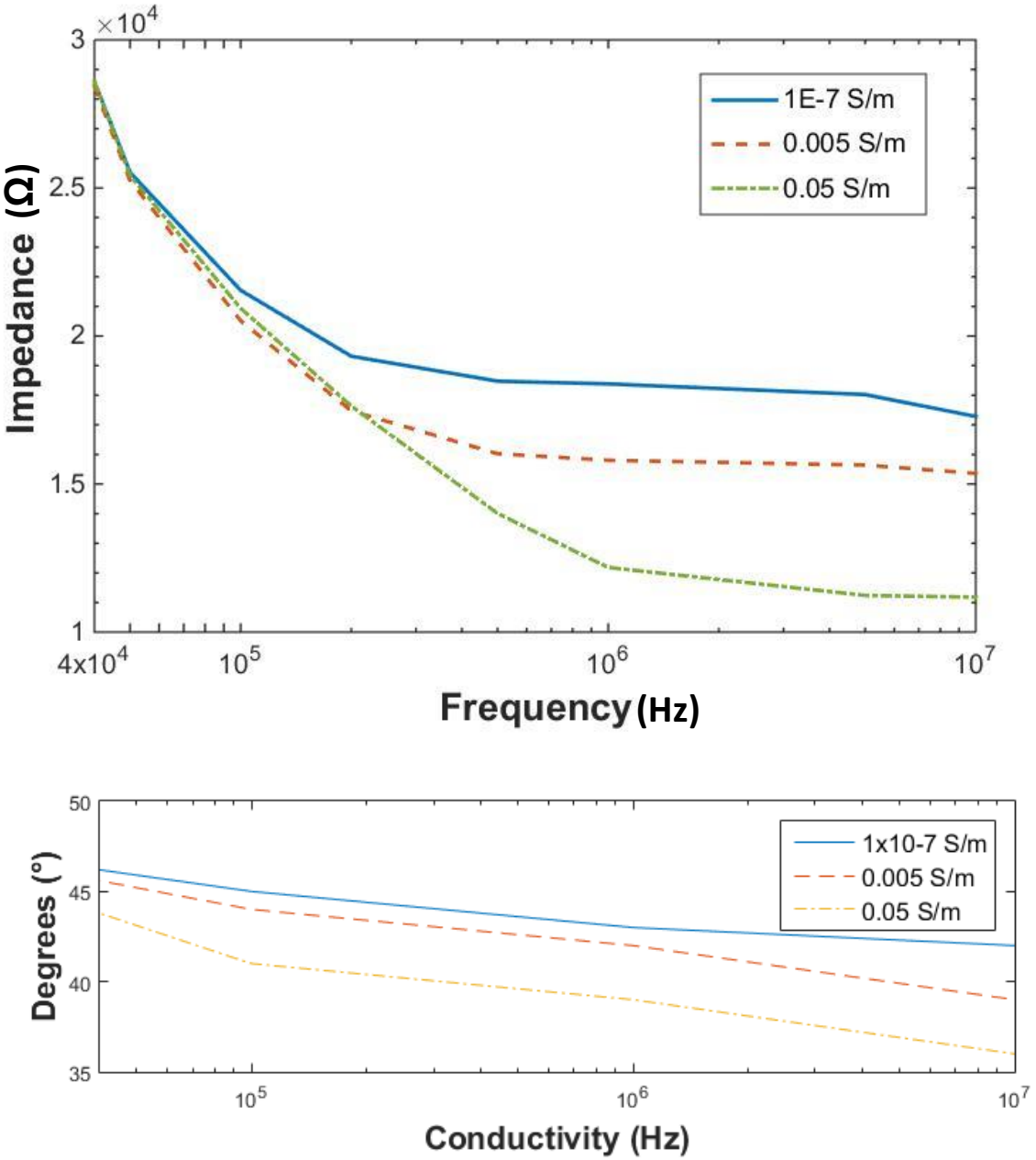

Figure 5.15 Top graph shows a loglog plot of the variation in impedance and phase angle of cells with increasing frequency (Hz) with 3 different SC cytoplasm conductivities (Sm^{-1}) for signal frequencies between 100Hz and 10MHz, bottom graph shows an expanded view of the impedances and phase angle at the higher frequencies between 40kHz and 10MHz with linear impedance and phase angle axes

The results in figure 5.15 show that at lower frequencies the conductivity of the cell has no impact on the overall impedance. Above 10^4Hz the impedances diverge, with the impedance decreasing with a lower conductivity. There is also a decrease in the phase angle measured, with the angle reducing as the frequency is increased, which is likely due to the reduction in resistance.

In order to explore the effect of hydration at the higher frequencies the simulation was changed to be run at a set of frequencies with a range of different conductivities. The results show that between 50kHz and 2MHz there is a change in the impedance of the model that decreases by around 200Ω. When looking specifically at the typical conductivities of tap water the results show that for each frequency there is a very slight curve, shown in figure 5.16 that can be fitted to a quadratic equation

$$Z = A\sigma^2 - B\sigma + C \qquad (5.2)$$

using the parameters shown in table 5.4, where Z is the overall skin impedance and σ in the conductivity of the solution applied.

Frequency (MHz)	A	B	C	R^2	Average Difference (Ω)
1	361363	66760	18440	0.9999	0.72
2	324048	64502	18368	0.9999	0.55
3	295464	61981	18283	0.9999	0.62
5	246291	56697	18067	0.9999	0.57
7	204627	51358	17802	0.9999	0.29
10	150657	43391	17337	0.9999	0.41

Table 5.4 Parameters for $A\sigma^2 - B\sigma + C$ with R^2 and average absolute difference between simulation results and the fitted curve

This behaviour was further explored by expanding the range of conductivities tested to include up to 5Sm^{-1}, the typical conductivity of sea water [70]. This shows a very different behaviour with the change in conductivity decreasing considerably slower at above 0.05 Sm^{-1}, with almost constant impedance at 50kHz, shown in figure 5.17. This change in behaviour can be modelled as an offset double exponential decay,

$$Z = Ae^{B\sigma} + Ce^{D\sigma} + E \qquad (5.3)$$

with parameters shown in table 5.5, where Z is the overall skin impedance and σ in the conductivity of the solution applied.

Frequency (kHz)	A	B	C	D	E	R^2	Average Difference (Ω)
500	2275	-9.11	2271	-23.7	14030	0.9998	3.09
750	2070	-3.87	3833	-15.7	12550	0.9999	2.07
1000	2490	-2.82	4238	-13.8	11670	0.9998	2.54
2000	3053	-1.70	4805	-11.3	10430	0.9998	2.97
3000	2776	-1.33	4609	-8.24	9963	0.9999	2.23

Table 5.5 Parameters for $Ae^{B\sigma} + Ce^{D\sigma} + E$ with R^2 and average absolute difference between simulation results and the fitted curve

The equation and parameters were determined using the curve fitting provided in MATLAB® with a double exponential decay providing the best fit. The offset is most likely due to the lower layer cells being unaffected by the change in conductivity and therefore providing a minimum overall impedance. While experimentation would be necessary to determine the accuracy of the equation a likely explanation is that the initial steep drop in impedance is due to the high impedance of the SC cells dropping as the hydration causes the impedance to drop to a level similar to the surrounding medium. The other, far less steep decay might then be due the cells becoming more conductive then the surrounding medium. As previously stated this requires verification from experimentation. This equation represents the expected change in skin impedance with a change in hydration as soon as a solution is applied, but a physically realistic equation would need to inlcude additional components. There are time related factors due to the changing level of skin hydration as an applied solution leaves the skin. There is also the impact of sweat which is time, temperature and signal dependant, although in practice sweat does not have a substantial impact at room temperature in the short term but will acculumlate under electrodes over time [75]. While the change in hydration and the impact of sweat might not be relevant in the short term a factor that would need including for a physcially realistic equation would be the location of the electrodes. Different parts of the body can absorb varying amounts of water based on the number of layers of skin, and will therefore having an impact on the equations described above.

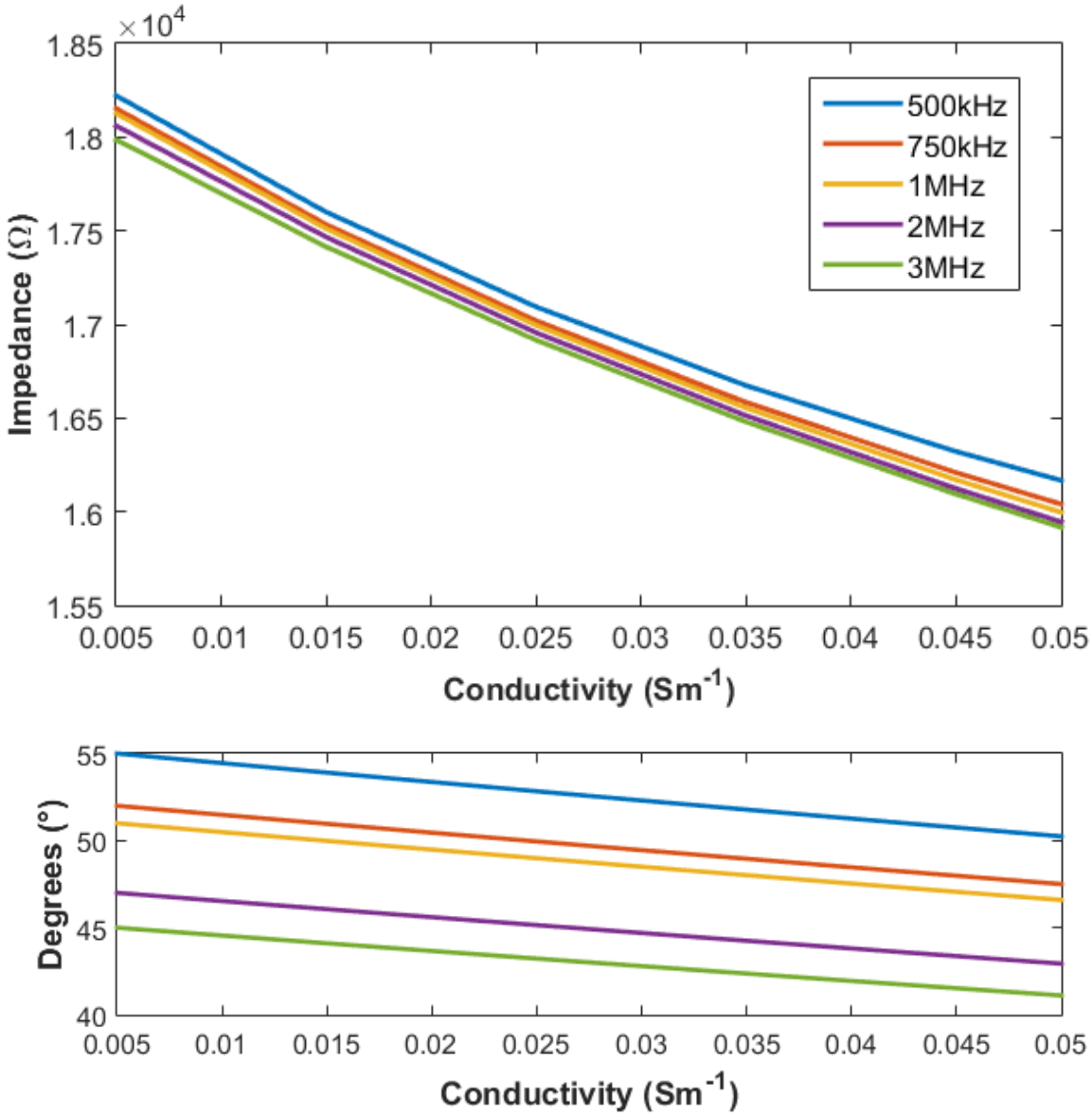

Figure 5.16 Change in Impedance and Phase Angle due to varying SC cytoplasm conductivity between 0.005 Sm^{-1} and 0.05 Sm^{-1} at 5 signal frequencies

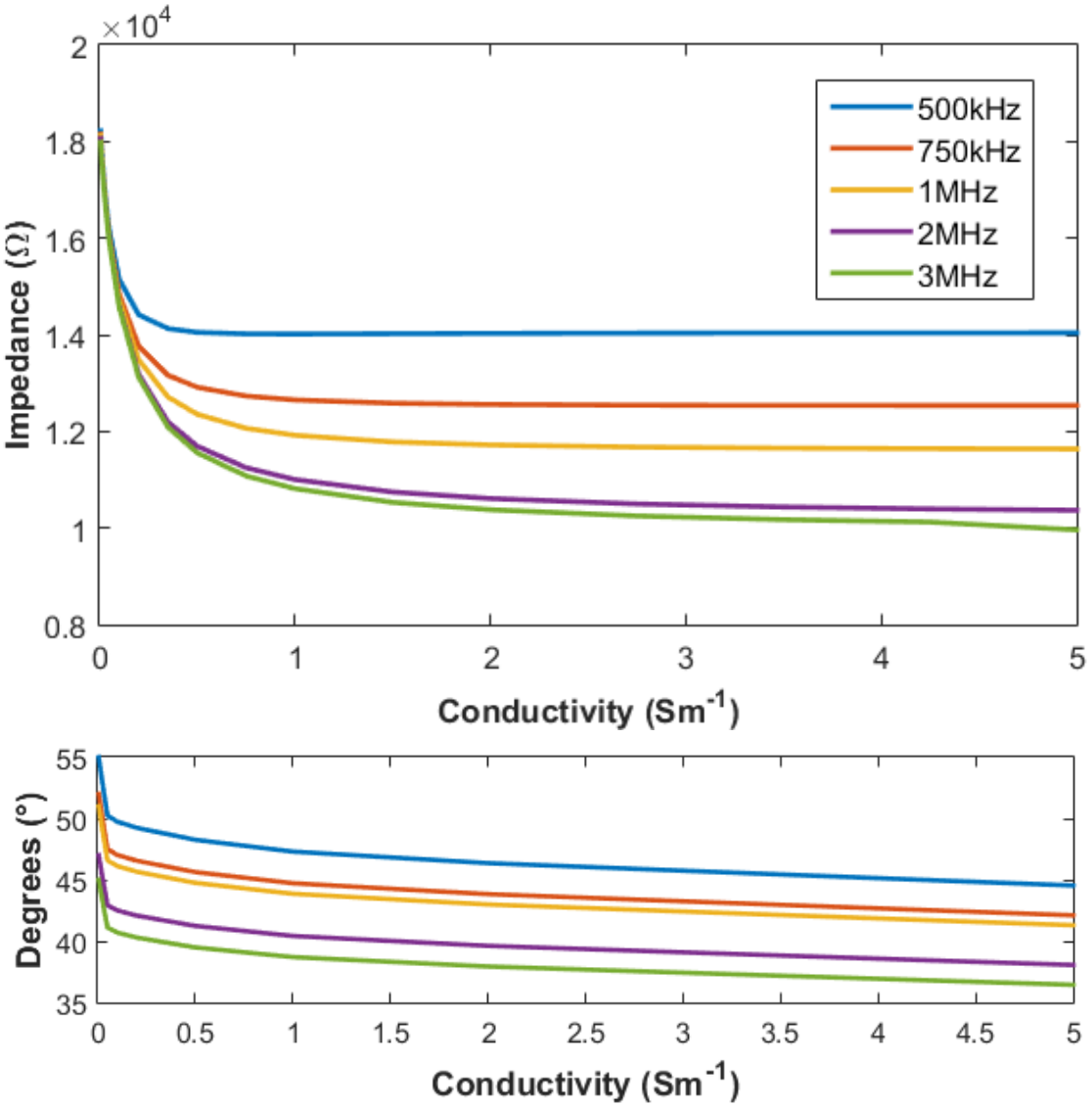

Figure 5.17 Change in Impedance and Phase Angle due to varying SC cytoplasm conductivity between 0.005 Sm^{-1} and 5 Sm^{-1} at 5 signal frequencies

The results of the model show that at higher frequencies there is a noticeable change in impedance with an 11% increase between the typical SC conductivity and highly conductive water being applied. There is also a drop in the phase angle, which is likely due to the increase in the overall conductivity, although there is noticeable lack of experimental data in the literature for comparing the phase angles. The results of this model support the idea that hydrating the skin under the electrodes using tap water can improve the results obtained clinically by reducing the skin's impedance. Because of the wide range of conductivities that standard tap water can possess it may be that this effect will vary across locations depending on the type of water available [42], [43], [70]. It should also be noted that the hydration of skin will change over time so reapplication of water is necessary for consistent results. Depending on the length of the applied signals and on how frequently the signals are applied there may also be a change in impedance caused by the accumulation of sweat in the sweat glands [49], [75].

Lowering the conductivity of the SC cytoplasm creates an almost linear drop in impedance. This shows that the effect of SC conductivity in the model diminishes very slightly, which suggests that the higher the conducting material used on the skin the better in order to lower impedance. However this changes once the conductivity is high enough, around $0.02Sm^{-1}$, where the impedance decreases very slightly and at lower frequencies does not change. This is likely due to the lower levels becoming the dominant factor in determining the cells overall impedance creating a lower limit for the impedance. Knowing that this lower limit exists has implications for treating people who have been exposed to highly conducting liquids, such as sea water, that might create hazards e.g. in defibrillation [92].

There are a number of areas outside of FES that could benefit from knowing how skin impedance affects conductivity. For example, the model could be expanded to look at the effects of applying a much larger voltage to the cells similar to the voltages used in defibrillation. This would also require looking at the effect of high voltages on the electrical properties of skin cells.

It should also be noted that the effect of hydrating skin would not affect all the SC equally as the outermost cells are the driest and will have a more substantial impact on the impedance than the innermost cells in the SC. This variation in hydration in the model could be explored

further, although a lack of experimental data in this area makes a comparison with practical data difficult. It is also important to note that if the SC has been removed then the model does not reflect the how the impedance would change since only the hydration of the SC is being taken into account.

5.7 Hydration Model with Hexagonal cells and Corneodesmosomes

In order to make a model that is a more faithful representation of the cells found in the skin hexagonal prisms were used instead of the cuboid shaped cell and corneodesmosomes were included, as shown in figure 5.18. The computational disadvantage of such a model is that by including the corneodesmosomes a comparatively fine mesh must be used increasing the time need to run the simulation, with typical run times shown in Appendix B.

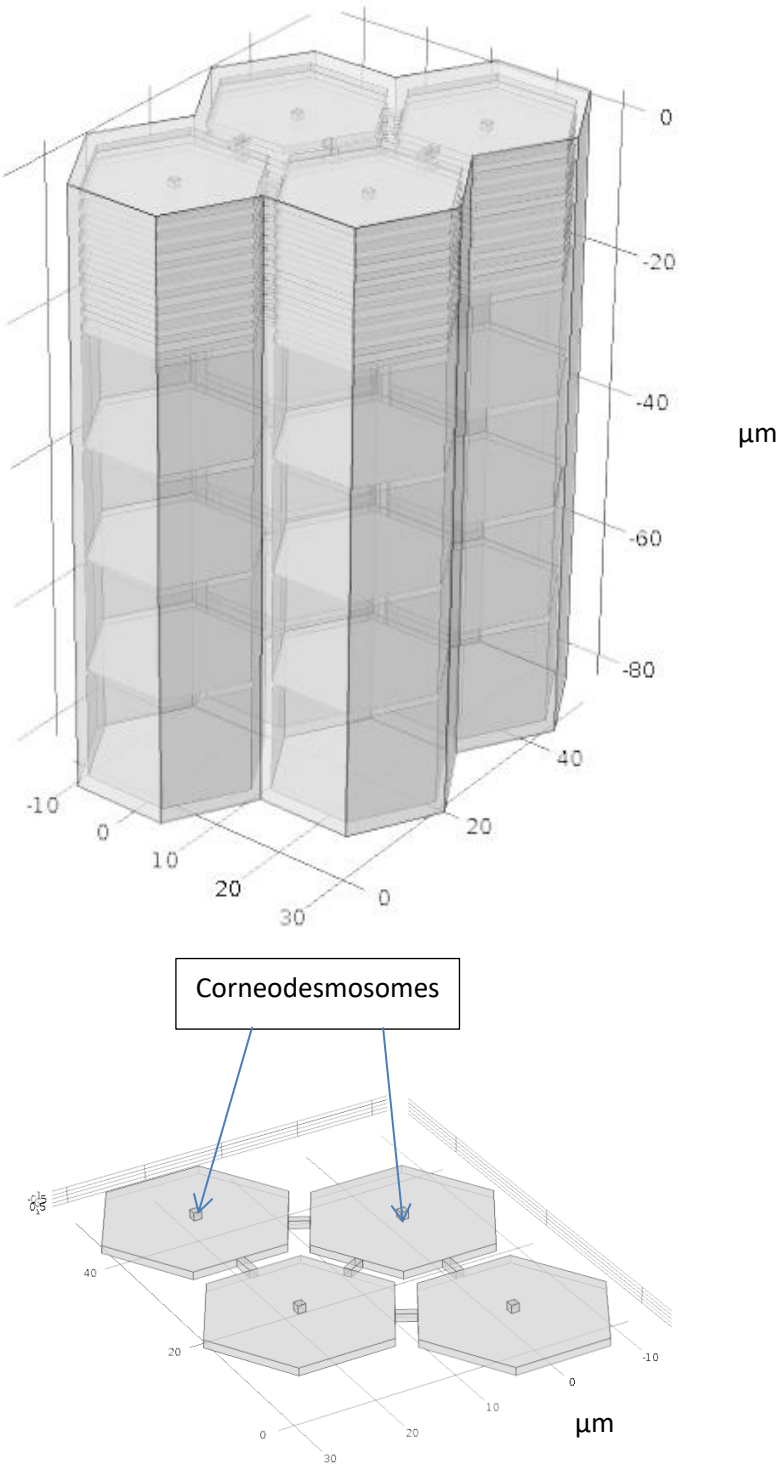

Figure 5.18 Geometry of the model showing the extracellular medium and the hexagonal cells and the corneodesmosomes with a single layer of the SC shown on the right

The hexagonal model shares the same electrical properties as the block model. The corneodesmosomes have dimensions of 1x1x1µm with a relative permittivity of 86 and a

conductivity of $1x10^{-7}$ Sm^{-1} and a cell membrane with parameters shown in table 5.3. The hexagonal cells for both the SC and the non-SC cells are based on a regular hexagon with edge length 12µm.

The simulation was run using SC conductivities of $1x10^{-4}$ Sm^{-1}, $2x10^{-4}$ Sm^{-1}, and $5x10^{-4}$ Sm^{-1} and then repeated with these SC conductivities increasing by a factor of 10 with the final SC values used being 1 Sm^{-1}, 2 Sm^{-1} and 5 Sm^{-1}. For each SC conductivity the simulation was run at frequencies of 10kHz, 100kHz, 200kHz, 500kHz, 750kHz, 1MHz, 2MHz, 3MHz and 5MHz. The results of the simulation can be seen in figure 5.19.

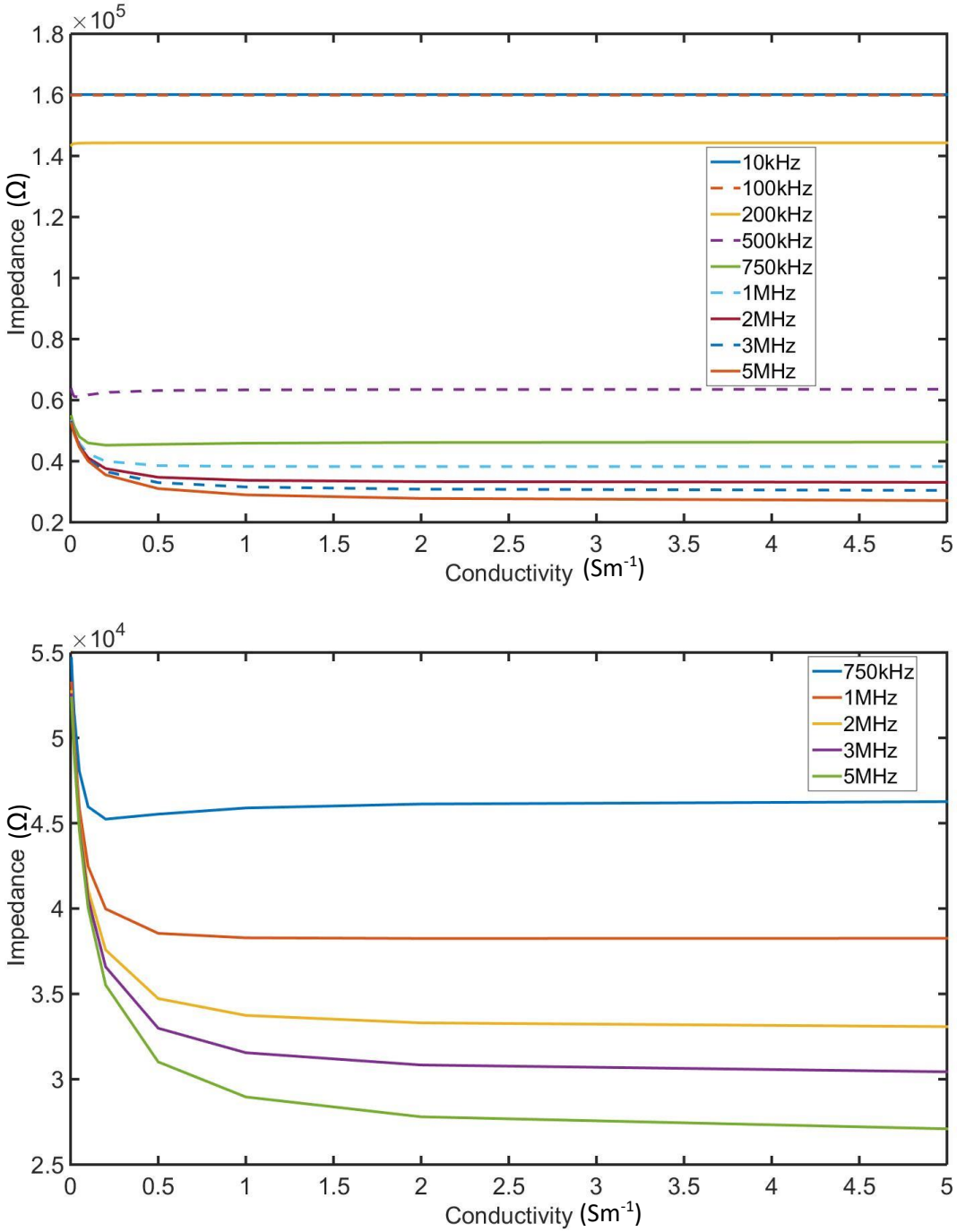

Figure 5.19 Change in Impedance due to varying SC cytoplasm conductivity between 0.005 Sm^{-1} and 5 Sm^{-1} at 9 signal frequencies (top) and the 5 highest signal frequencies (bottom)

The absolute values vary considerably with the impedance being at around 3 times larger in the hexagonal model when the conductivity is above 2Sm^{-1} while below this conductivity the

hexagonal model impedance decreases with conductivity until the impedance in the hexagonal model is 5 times smaller than the original model. This can be in part explained by the additional space added between the SC cell in order to accommodate the corneodesmosomes, as well as due to the change in dimensions overall with the altered shape. However, the results of both models share similar characteristics. At low frequencies the change in conductivity has no impact on the overall impedance of the cells while at higher frequencies the change in behaviour can be modelled as an offset double exponential decay with parameters shown in table 5.6. These results support the findings of the previous model that hydration has much greater impact at higher frequencies and that there is a limit to the effect of increasing hydration.

Frequency (MHz)	A	B	C	D	E
1	5862	-6.261	10530	-22.19	38270
2	7184	-3.025	13430	-16.92	33230
3	8615	-2.465	14340	-15.34	30640
5	10390	-1.953	15600	-13.55	27340

Table 5.6 Parameters for $Ae^{B\sigma} + Ce^{D\sigma} + E$

5.8 Sweat gland model

As mentioned previously an important factor in the natural hydration of the skin is sweat. In order to analyse the effect of sweat on the dielectric properties of the skin a model was designed to represent the sweat glands. This model varies considerably to the previously developed model in terms of scale in order to include full length sweat glands. The model contains sweat glands uniformly distributed within a surrounding bulk and assigned the electrical properties of the cells found in the epidermis. There is also a thin layer added to the top of the model to represent the high impedance SC. The geometry of the model is shown in figure 5.20. The parameters used in the model are shown in table 5.7. To model the sweat ducts filling and emptying the conductivity of the glands is varied between 100µSm^{-1} and 5Sm^{-}

[1], with the lower end representing dehydrated cell conductivity and the upper end being the conductivity of sweat [47]. The properties used for the physical dimensions are chosen to most accurately reflect the thickness and composition of the skin found on the fore arm. This is because FES is often used on the arm to aid with movement. The number of sweat glands found in the fore arm is approximately 155 per cm^2 [111] and this will vary across the body and from person to person but for the purposes of the scale of this model this value was considered to be appropriate. The sweat glands in the forearm are evenly distributed across the skin. The resulting mesh for the model used elements of varying sizes between 1.5 µm and 3µm. An extra fine mesh was used to model the SC as the thickness is only 8nm but is thought to be the layer to have the largest overall impact on the skin impedance.

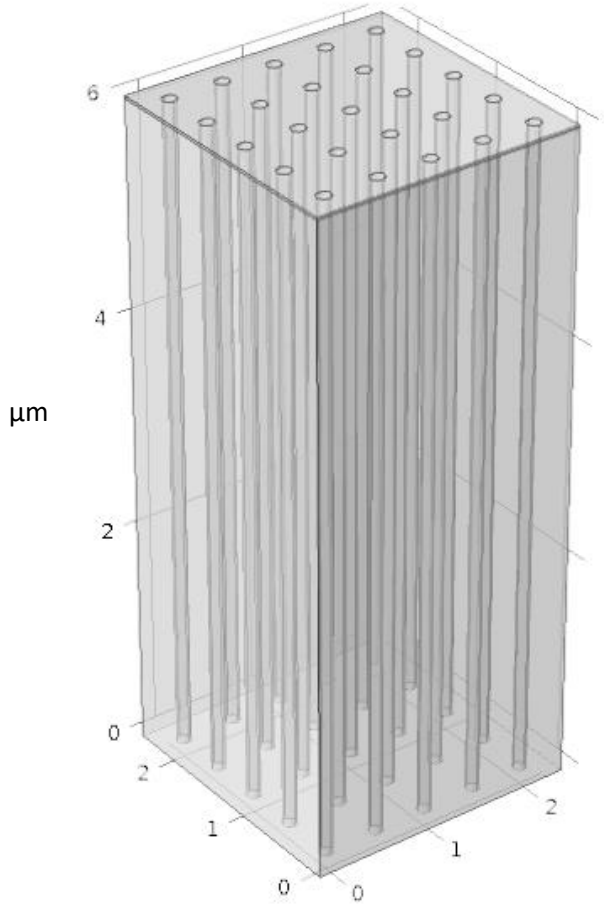

Figure 5.20 Geometry of sweat gland model

Object	Dimensions (µm)	Relative permittivity	Conductivity (Sm^{-1})
Sweat gland	Radius: $65x10^{-3}$ Length: 6	2	$100x10^{-6}$
Epidermis Cells	6x2.5x2.5	5	$07.69x10^{-4}$
SC Cells	$25x10^{-3}$x2.5x2.5 Thicknesses (nm)	2.5 Relative permittivity	$1x10^{-6}$ Conductivity (Sm^{-1})
Cell Membrane	8	90	$1x10^{-7}$

Table 5.7 Parameters used in the sweat gland model[49]

A simulation was run using frequencies of 100Hz, 1kHz, 10kHz, 100kHz, 500kHz, 1MHz, 2MHz and 5MHz, with the results shown in figure 5.21 and 5.22. The results for 100Hz and 1kHz have been excluded because the values of the results were within 1Ω of the results for 10kHz.

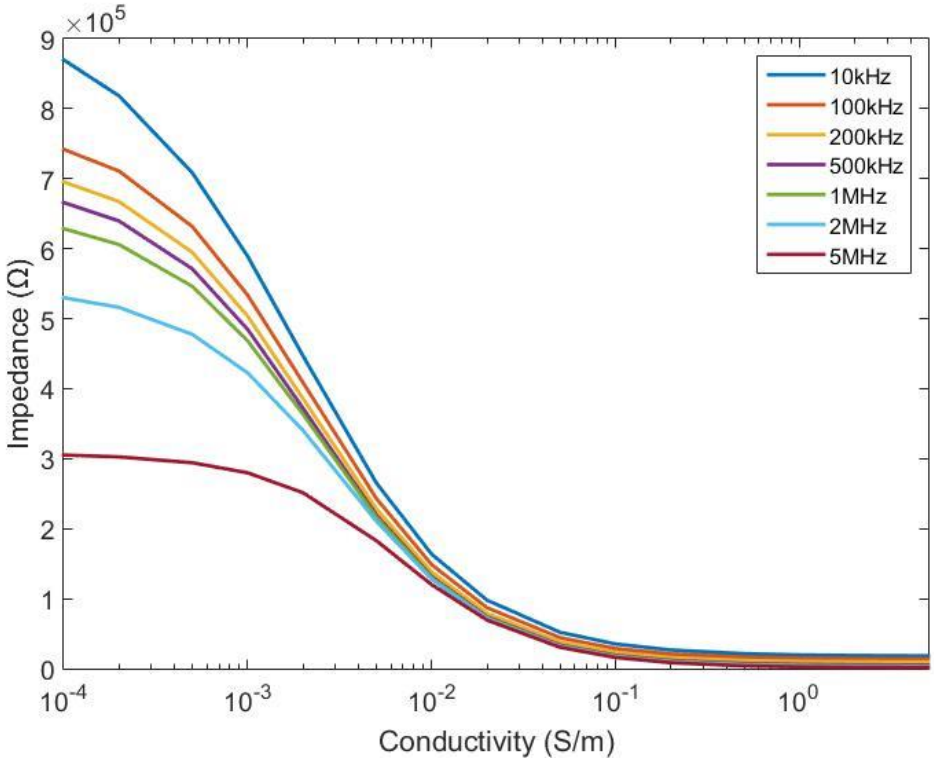

Figure 5.21 Change in Impedance due to varying sweat gland conductivity between 0.005 $Sm^{-1}$and 5 Sm^{-1} at seven frequencies

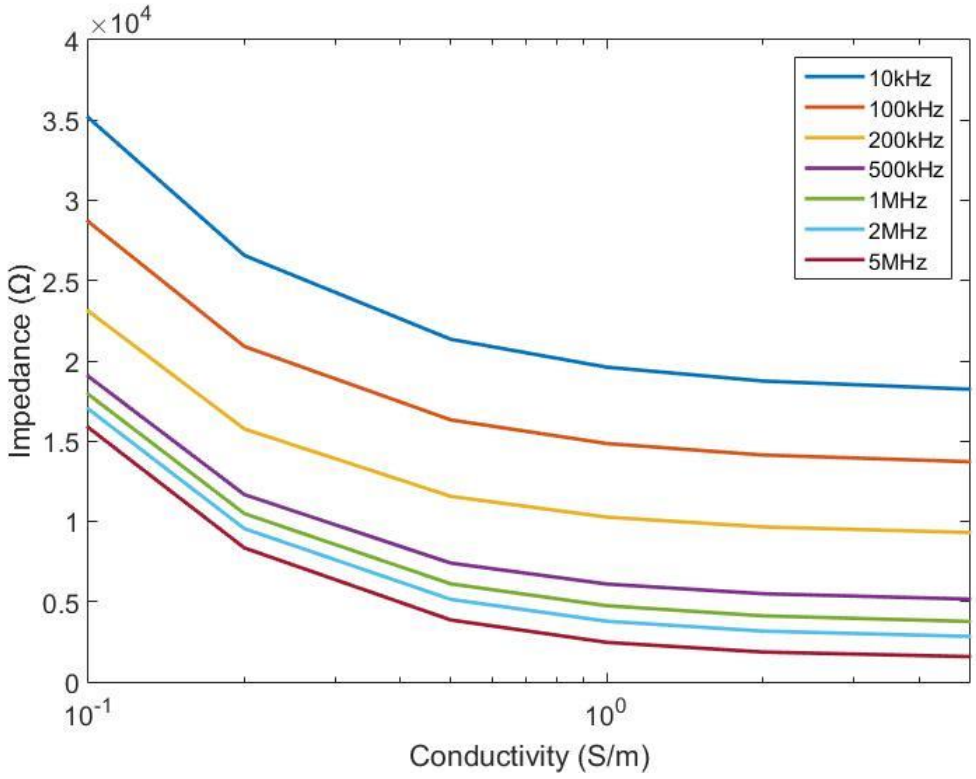

Figure 5.22 Change in Impedance due to varying sweat gland conductivity between 0.1 Sm^{-1} and 5 Sm^{-1} at seven frequencies

The results displayed in figure 5.21 and 5.22 show that the effect of sweat is substantial upon the overall impedance of the model. The curves show a considerable drop in impedance with an increase in conductivity that starts to level out above 0.1Sm^{-1}.

As mentioned previously, when the frequency of the applied signal is below 10kHz the impedance changes by less than 1Ω due to changes in SC conductivity. However, above 10kHz the frequency has a much more noticeable effect on impedance. From figure 5.22 it can be seen that at 5MHz with a sweat gland conductivity of 5Sm^{-1} the impedance is 1.5kΩ which is less than 10% of the 18.3kΩ impedance at 10kHz for the same conductivity.

The behaviour of the separation of impedances at low conductivities is mostly likely due to the effects of the high impedance SC. The high level of impedance that is caused by the upper layer of skin creates a barrier that prevents the flow of current through a large area of skin and causing the sweat glands to be the most conducting path. However, as the conductivities of the sweat in the sweat glands increase the SC no longer impedes the flow of current until it has almost no effect on the overall impedance of the skin cells.

This is the expected behaviour from the literature; sweat glands will affect the skin impedance in a very similar way as hydrating the skin does. There is a noticeable difference in the behaviour in the lower frequencies, around 10^{-4} Sm^{-1} where the difference in impedance levels are highly divergent in the sweat model. However the hydrating model had much more similar levels of conductivity.

5.9 Electroporation model

Given the amount of research in the literature the next stage of simulation was to determine the impact of electroporation on the cell model. Throughout the research a common theme for non-invasive use of electrical signals is in the detection and treatment of different types of cancer. These studies have been very informative for expanding the understanding and mechanisms involved in electroporation although the signals typically involved in these procedures vary greatly from those used in FES.

Membrane thickness was chosen as one of the parameters to be altered due to the role it plays when considering electroporation. In previous models a fixed thickness of 5 nm was used because this thickness was determined in the experimental data. It would have been suitable to keep a fixed membrane thickness as this has been the case in the literature. However, as the switching function is directly linked to the voltage measured across the membrane, and there are sources that suggest different membrane thicknesses are possible, it would be beneficial to simulate the potential impact of membrane thickness on the results [2].

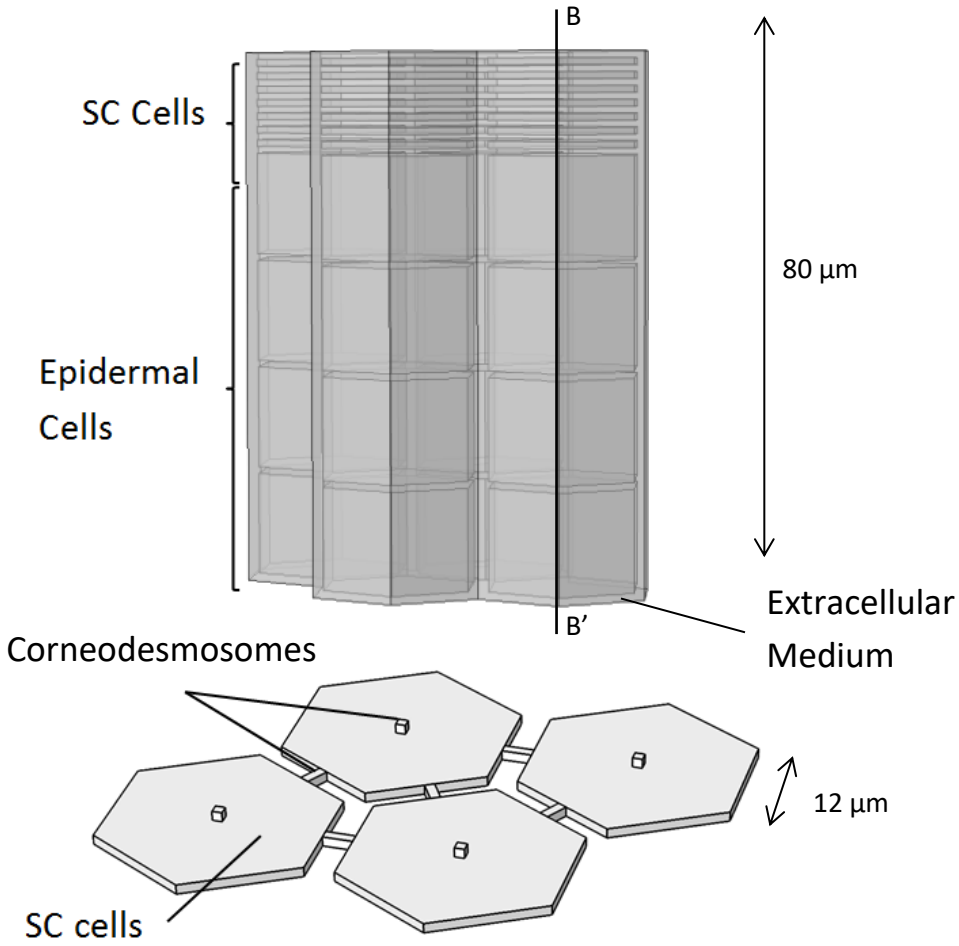

Figure 5.23 Geometry of the model showing the extracellular medium and the three types of cell used with one layer showing the corneodesmosomes

In order to reduce the computational power needed to run the simulation the cell membrane was replaced with a boundary condition. The contact impedance is part of the electric currents physics package. This substitution removes the need for a much finer mesh for the nanometre scale membrane compared to the other micrometre scale elements.

One of the sides of the extracellular medium was set to be the input signal with the opposite side grounded. The remaining sides are set as electrical insulators. The geometry used for the model can be seen in figure 5.23

The input was created using a rectangle function with a peak voltage of 0.1V, 10V, 100V and 1000V. The pulse had a period of 300µs and a rising edge of 80µs, with an example shown in figure 5.24. The input voltages were simulated with membrane thicknesses of 3, 4 and 5nm,

to cover the thickness shown in literature and with a threshold ITV required to create an electropore set to values between 0.2V and 1V, with an interval of 0.1V.

To model the effect of electroporation a switching function was used to determine the conductivity of the cell membrane. When the voltage across a cell membrane is below a threshold ITV the conductivity is $1x10^{-7}Sm^{-1}$ and when the voltage is above the threshold it is $0.6Sm^{-1}$ as shown in table 5.8. When the voltage across the membrane was above the threshold voltage the conductivity would increase to match that of the cell interior, replicating the effect of creating an electropore.

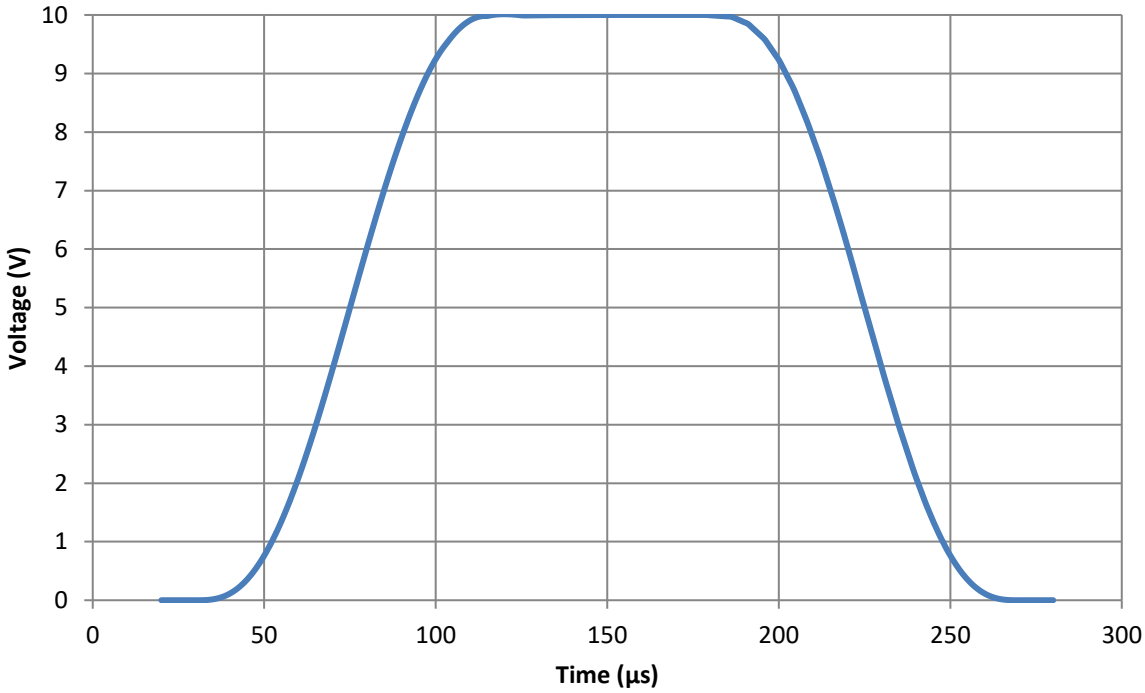

Figure 5.24 Input Voltage used in 10V simulation

Object	Dimensions (µm)	Relative permittivity	Conductivity (Sm^{-1})
Extracellular medium	34x34x19	72	1.1
Cytoplasm	30x30x30	86	0.6
SC Cytoplasm	30x30x1	86	$1x10^{-7}$
Cell Membrane	3-5(nm)	90	$1x10^{-7}$

Table 5.8 Parameters for the single cell model

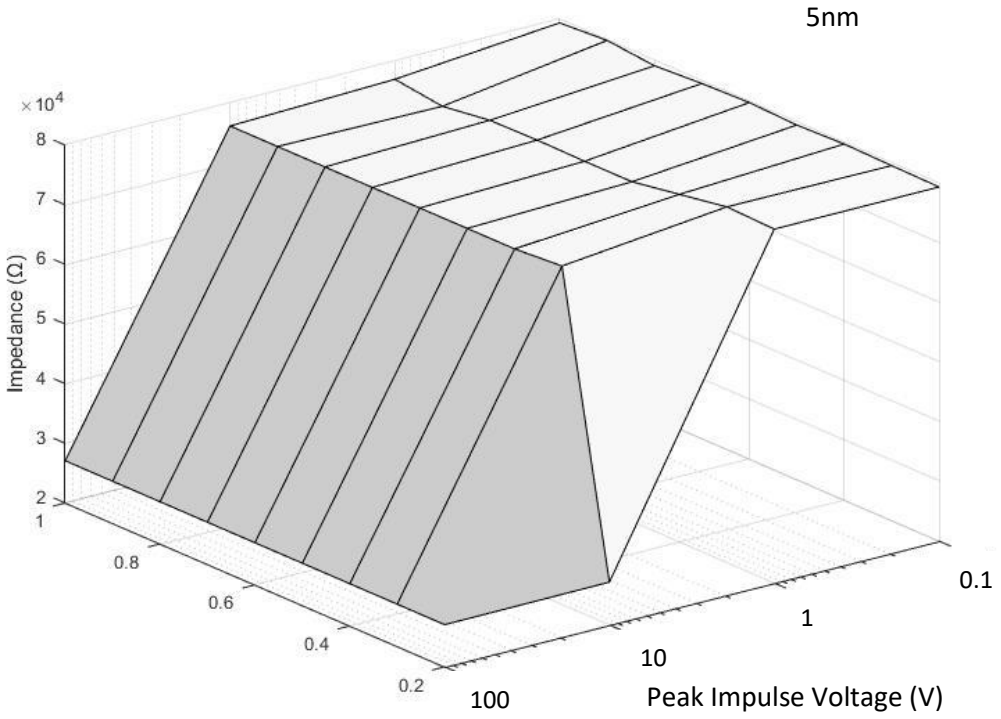
5nm
×10^4
Impedance (Ω)
8
7
6
5
4
3
2
1
0.8
0.6
0.4
0.2
ITV Threshold (V)
0.1
1
10
100
Peak Impulse Voltage (V)

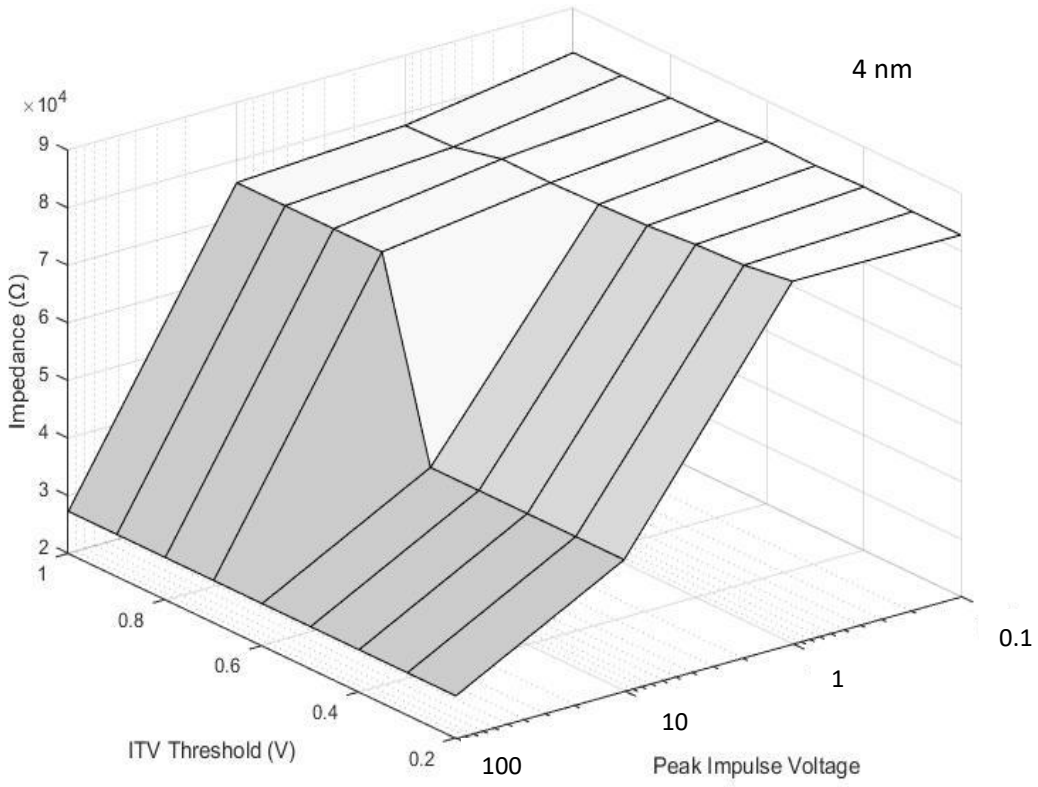
4 nm
×10^4
Impedance (Ω)
9
8
7
6
5
4
3
2
1
0.8
0.6
0.4
0.2
ITV Threshold (V)
0.1
1
10
100
Peak Impulse Voltage

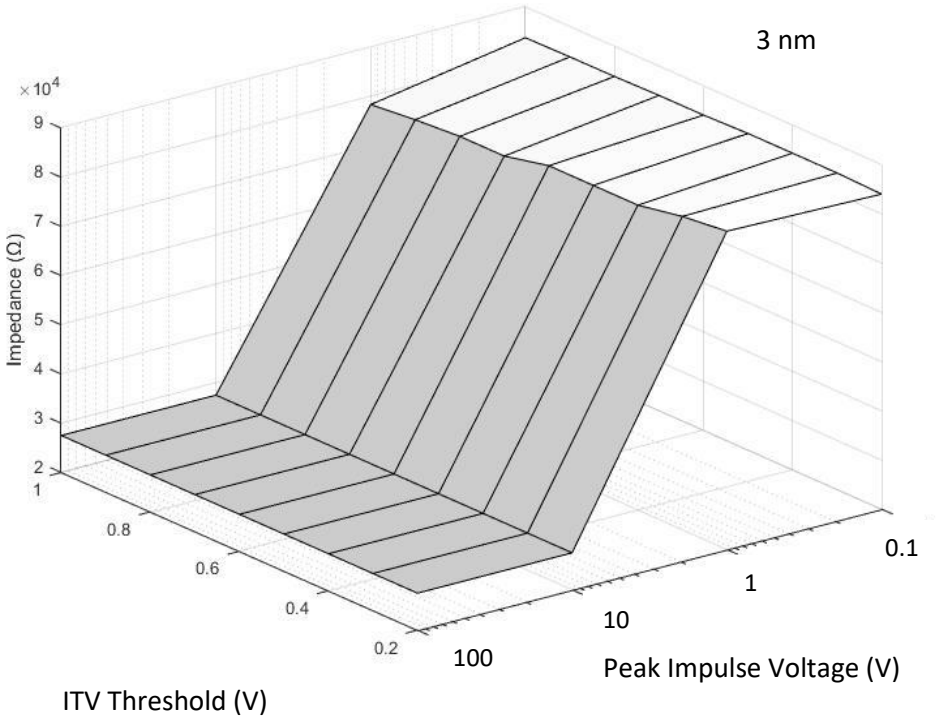

Figure 5.25 Impedance measured at time step 150µs, the centre of the pulse shown in figure 5.24, showing changes due to peak impulse voltage (using a logarithmic scale) and ITV threshold voltage required to create and electropore. The surface at the top plot shows the impedance with a membrane thickness of 5nm, the middle plot with a membrane thickness of 4nm and the bottom plot with a membrane thickness of 3nm

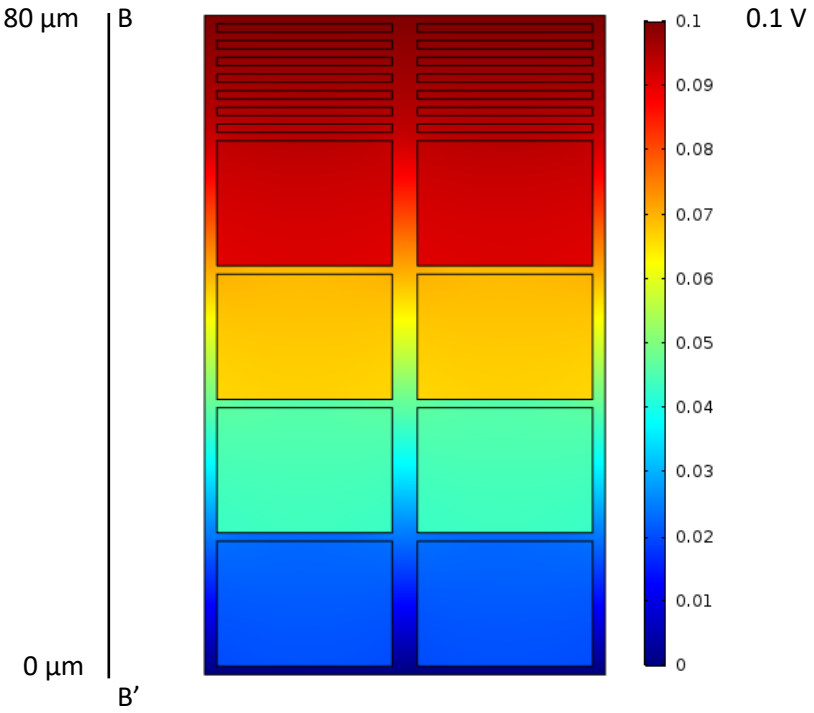

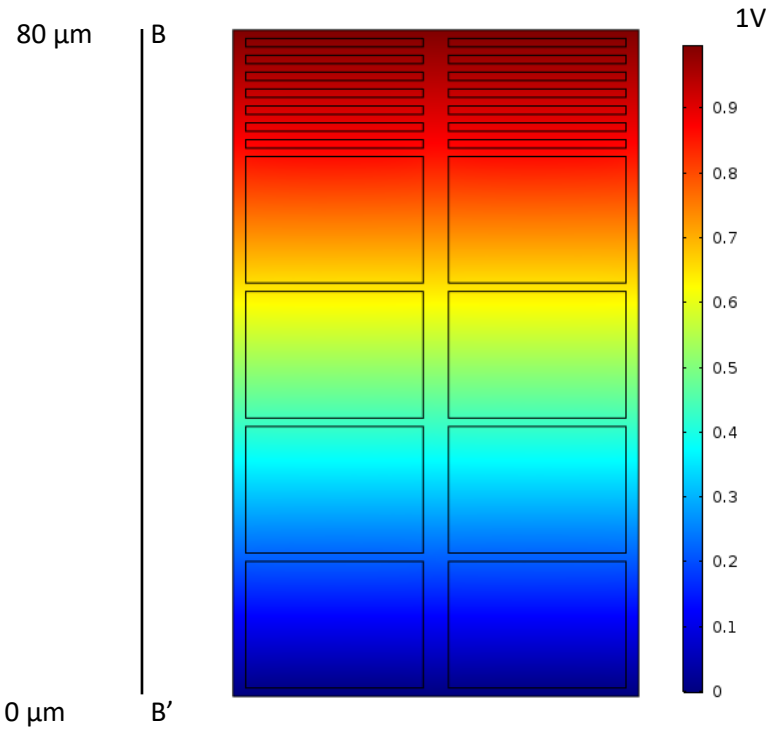
80 µm
B
1V
0.9
0.8
0.7
0.6
0.5
0.4
0.3
0.2
0.1
0
0 µm
B’

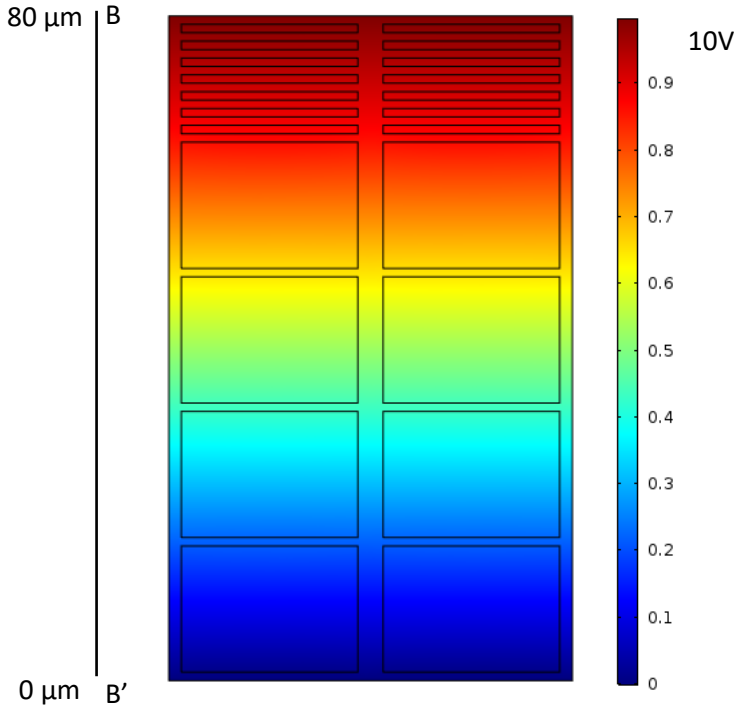
80 µm
B
10V
0.9
0.8
0.7
0.6
0.5
0.4
0.3
0.2
0.1
0
0 µm
B’

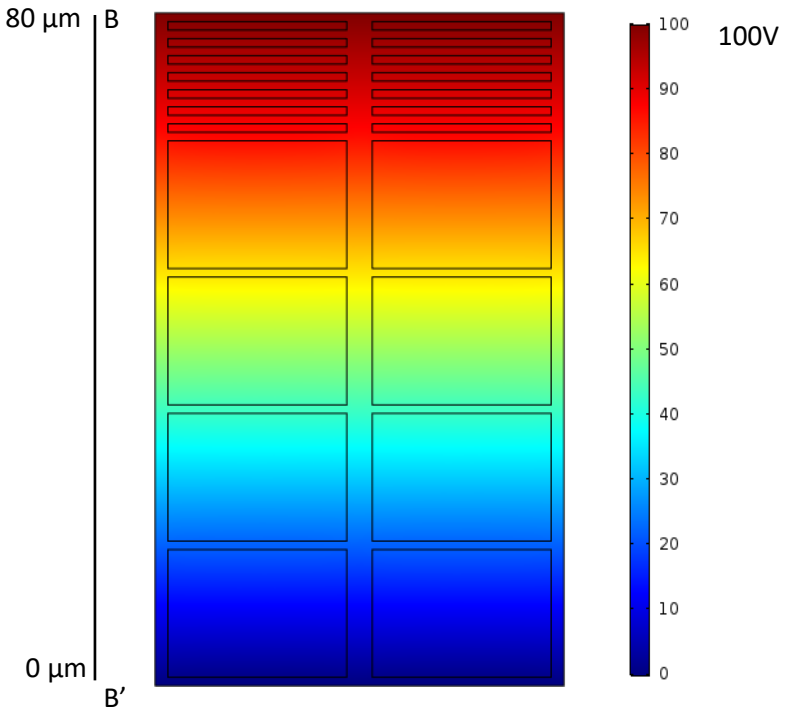

Figure 5.26 Voltage gradients across the model at 150µs with different peak impulse voltages. The plots show a cut in a plane of the model at the section B to B' as shown in figure 3 with a 0.1V, 1V, 10V and 100V peak voltages. Shown on the right hand side is the colour scale for voltage in each cell with respect to the zero voltage at the base of the cells (B')

The results of the simulation, Figure 5.25, showed that for most of the parameter values electropores are being created, as there is now a current flowing through the cytoplasm due to the reduction in cell membrane impedance. This suggests that in general there will be electropores being formed when FES is used, especially since typical FES signals have an amplitude of 30-100V [25], a value at which electropores were formed for all values of the ITV value or the membrane thickness that were simulated. Figure 5.26 shows that when the peak impulse voltage is 0.1V there are no electropores being formed and when the input amplitude is 10V electropores are formed at all membrane thicknesses. Finally, when the amplitude is 1V electropores are formed with a membrane thickness of either 3nm or 4nm, depending on the ITV threshold.

The effect on impedance of electropores being created is substantial, with a drop from 76kΩ to 22kΩ. This shows that if voltage signals of at least 1V are used and the threshold voltage is 0.2V there will be a considerable reduction in the overall impedance of skin. The top plot in figure 5.26 shows that when the peak input voltage is 0.1V there is no change in voltage within the cells, shown by the colour not changing within the cells, which indicates that there is only a small current flowing through the cells and creating the overall impedance of 76kΩ. When the peak voltage is 1V, 10V or 100V pores are formed in the membrane, which can be seen from the colour gradient changing in the same way as the surrounding cell medium, meaning that current can now flow freely through the membrane, greatly reducing the skin's overall impedance.

The simulation shows that using the experimentally determined properties of skin cells and the equation used to model a localised drop in membrane impedance; electropores will form in the voltage ranges that would be expected from experimental observations, from 1V and upwards, depending on the thickness of the membrane and the ITV threshold.

5.10 Chapter Summary

This chapter details the creation of the models produced and the key results of simulations performed with these models. Of particular interest to this thesis is the substantial impact that hydration has on the overall impedance of skin. It also shows the limitation of hydration as the SC becomes more conducting then the lower layers of skin and shows a similar reduction in impedance to what was found in literature. The results in this chapter also show that when electrical pulses of 1V are applied directly to skin a transmembrane voltage necessary to create electropores can be produced, depending on the number of layers in the SC. These results support the idea that an equivalent cell model would need to incorporate the impact of skin hydration to model the effects of FES and that further experimentation is required to determine the impact of electroporation on FES. The following chapter outlines

the key results found from each of the models created, with a particular focus on the results of the hydration model and the electroporation model.

6 Discussion

The results of the single cell modelled based on the work by Pucihar et al [82] showed a strong agreement between the simulation results and the expected results from the analytic results, with a difference no greater than 0.3% at any point. While this spherical cell model was the least related to the later models in terms of cell shape, input signals used and results measured it was able to provide direct comparison with analytic results. While experimental results were provided in this work, these suffered from issues with significant variance due to the dyes used, therefore the simulation results were only compared with analytic results. From this model the substitution of the very thin cell membrane with a boundary condition in COMSOL® Multiphysics was shown to provide an exceptional representation of the membrane without requiring a very thin mesh, which has been used for all the models simulated in this thesis.

Following on from the single cell boundary condition model was the epithelium model based on the work by Walker et al [109]. While the intent of the model created by Walker was to model the properties of epithelium cells as an indicator for cancer, the work provided a valuable set of results to use against the simulated results for comparing the frequency response of the individual cells. The impedance of the modelled cell showed a close agreement with the experimental results within the frequencies of 1 kHz and 100 kHz. The difference in impedance above and below these frequencies may be due to differences in the parameters used. Expanding upon this model to introduce the additional cells as well as changing the orientation of the applied signal produced a model with characteristics much more closely representative of the cells found in the skin surface. When including a larger collection of cells in the model the voltage gradient was closer to what would be expected from the experimental data found in the literature, with a larger drop in voltage across the

smaller cells representing the stratum corneum. This suggests that part of the SC's dominance with respect to skin may be in part due to the more compact cells present.

An area of particular interest for this thesis is the impact of hydration on the skin's impedance. The SC acts as a barrier to water for the skin and the hydration model reflects this by changing the conductivity of the cells found in the SC. The change in impedance due to altering the conductivity of the SC is similar to the results found experimentally in the work done by Birlea et al [112] in their study of the week long effects of neuromuscular electrical stimulation (NMES). They found that the level of resistance found in the skin dropped by about 14% and linked this to the accumulation of sweat in the body, very similar to the 11% reduction in skin impedance found in the model due the changing the SC conductivity between 100nSm^{-1} and 1.5Sm^{-1}.

The results of the experiment by Birlea et al [76] showed that hydration has an overall impact that has similar effects on skin impedance as aging [104] and season [14], both studies showing changes in impedance in the region of 10%-15%. This supports the idea that the root cause of this difference is the body's ability to maintain the level to which it can be hydrated with changes due to aging, which causes the associated increase in impedance. To validate the results of this model experimentation would be necessary, as there is a current deficiency of experimental data available in the literature.

An assumption is made in the hydration model that there is a uniform absorption of water across all the SC layers; it is known that hydration is not uniform and hydrates most at the upper layers of the SC [44], [68]. However, given the wide range of conductivities used it was assumed that changing the conductivity as an average for all the SC layers was an acceptable simplification, especially as the overall skin impedance is of interest.

A switching function was used to represent the creation of electropores based on the parameters found in the literature. An electropore is formed when the induced voltage across a cell membrane is in the range of 200mV – 1V with the properties that determine the exact voltage required for a pore to form being currently unknown. As the length of time required for an electropore to form is approximately 10^{-6} seconds [88] it seems reasonable to suggest that unless experimenters were actively trying to incorporate the possible influence of electroporation it may have an impact on the results that is not being accounted for. Once

the effect occurs the time it can take for a cell to return to its original behaviour can range from minutes to hours, depending on the cell membrane, the length of time the signal was applied and the voltage of the applied signal [88], [100].

The way that an applied voltage creates a pore in the cell membrane that enables current to move through a cell is very similar to the behaviour shown in the epithelium and hydration models about how frequency impacts a cell. At low frequencies the cell membrane acts like a barrier to current, but as the frequency increases the cell membrane allows for a flow of current through the cell until a frequency of 1MHz where the current can flow freely through the cell membrane without impedance. The results in the behaviour at low frequencies below 100Hz being very similar to cells with no electropores present while above 1MHz the behaviour is similar to when a pore is present in the membrane.

Given that FES signals will use voltages of 30-100V and upwards the results of the electroporation model implies that there will be some amount of electroporation occurring. The voltage was applied over a larger section of skin than has been modelled, however the results of the model show that a voltage in the order of only 1V is required for electropores to form. As the epidermis is the layer with the highest impedance, it is therefore possible for electropores to form when a voltage of 30V upwards is applied. The electric field produced by FES is not uniform but it has been found that around 20%-50% of voltage applied is dropped across skin [113], depending on the location it is reasonable to suggest that a field strength in the order of $10^8 Vm^{-1}$ could be produced across some cells membranes and therefore create electropores. Electroporation is not likely to affect all cells exposed to an FES signal as the ITV required varies between cells. However, it is most likely to affect the cells close to the electrode, as found in the paper by Al-Khadra et al [92] looking at the impact of electroporation in defibrillation.

An assumption in all the models in this thesis is that the thermal effects of FES signals are negligible. As discussed previously, when irreversible electroporation is being used there is some possibility for ohmic heating due to the field strengths being used. This is especially a concern if small electrodes, around 20mm, are being used. However, for this to occur in irreversible electroporation (IRE) the signals required would need to be above $2000 Vcm^{-1}$ [16], substantially higher than the voltages used in FES.

While the results of the electroporation model show the impact if all cells were to undergo electroporation it should be noted that in practice when electrodes are being used and there is not a uniform electric field being applied to all cells there would be a much smaller number of cells undergoing electroporation. The range of values for the applied field strength required for electroporation, 200mV - 1V, is also very wide. Therefore it may vary not only between different types of cell, but also due to small differences between cells of the same type. While this has not been researched directly it might be a substantial factor in skin cells, particularly as the cells approach the stratum corneum where they are dead and have considerably different electrical properties to the live cells found in the lower layers.

One assumption that is made in the model is that the electropores can form anywhere in the membrane and there is no size limit. This is similar to the approach taken in other electropore models, although most other models are based on spherical cells. Since the exact mechanisms of electroporation are still unknown there may be some limiting factor that prevents electropore of certain sizes from being produced, however the aim of the model was to determine if any electropores might form in these circumstances. The results of the model show that when the input voltage is over 0.1 V then there is the potential for electropores to form.

The sweat gland model shows that the SC has a very dominant influence on overall skin impedance when sweat is not present. However, by changing the conductivity of the sweat glands to represent the expected behaviour when the glands are filled shows that in the cases of substantial sweating the overall impedance can drop to around $1x10^3\Omega$ at 100kHz, a much more substantial drop then was found in the hydration model. This is due to the sweat glands passing through multiple layers of skin and they are therefore providing an alternative low impedance pathway when compared to the other skin layers.

A number of behaviours discussed in the literature review, such as temperature dependence and individual difference are incorporated by using a large range of possible sweat conductivities. However, time dependent factors, such as the attracting and repelling of sweat from the sweat gland due to an applied electric field have not been incorporated. This is due to the time being considered for the models as only a short time period in the order of

milliseconds were analysed and the time dependent effects take hours to be noticeable in terms of impedance [46].

It was found that the impact of the nucleus and the corneodesmosomes is minimal. The nucleus affects the current flow as shown in the results of the epithelium cell model, but contributes less than a 0.1% difference to the measured overall impedance. Therefore, these elements were removed from the model in order to help to reduce the number of mesh elements required thereby reducing run time, seen in appendix B.

The results of the simulation support the idea that an equivalent circuit, such as the one produced by Martinsen et al [3] would not be appropriate for use with FES. This is due to the potential impact of a substantial drop in overall impedance at a wide range of voltages that will vary based on at least skin thickness and the ITV required for electroporation that will vary between different cell types [114].

The parameters for the shape of the cells and surrounding medium, as well as the dielectric properties possessed by these cells, was determined from what was found in the literature. For the most part there was only a small amount of discrepancy between different sources, with parameters varying only slightly. The number of layers that compose the SC remains fairly consistent in the upper limbs and while the lower layers can vary substantially these layers have less impact on the overall impedance as previously discussed.

In terms of the dielectric properties of the cells and cellular medium there was solid agreement from multiple sources of experiment data for the permittivity of all model components as well as for the conductivity of the cell membrane and cellular medium impedance. However, there was recently some debate over the value of the conductivity of the cell's cytoplasm. It is generally agreed that the cytoplasm can be represented as a uniform material with constant dielectric properties and the exact value for the cytoplasm conductivity was calculated to be $0.6Sm^{-1}$ based on using a saline solution to represent the cytoplasm [2]. However, in work done by Denzi et al [115] the value of $0.32Sm^{-1}$ was been found from direct experiment on a cell. As this was found after running the simulations for many of the models the hydration model was modified to use this potentially more accurate value, with the results shown in Appendix C. What was found was that the overall change in impedance was at most an increase in impedance of 150Ω. What the results of the parameter

changes show is that while the parameters may not be exact, such as the cytoplasm conductivity, the dominant effect at low frequencies is still the order of magnitude of difference between the conductivities of the cytoplasm and extracellular medium and the high level of impedance possessed by the cell membrane even though the membrane is only around 5nm thick.

7 Conclusions

The induced transmembrane voltage measured in the spherical cell model shows a very similar induced transmembrane voltage from that obtained using an analytical solution. This suggests that the model is valid for determining ITV of a spherical cell in a constant electric field. This can clearly be seen by the results shown in figure 5.3, which shows a difference in the order of millivolts for a signal with a 1V peak value between the analytical and simulated results. This ensured that the properties used for the subsequent skin cell models were as accurate as possible.

The results for the epithelium model show that at low frequencies, below 100Hz, the cell membrane will prevent current flow through the cell; this can be seen in figure 5.6 as the cytoplasm showed no variation in voltage. As the frequency of the applied voltage increases this effect becomes less dominant until it reaches 1MHz, where the membrane has very little impact on current flow. The simulation results have very similar values for skin impedance to the experimental results in the 1kHz to 100kHz range, however outside this range there are some minor differences between the simulation results and experimental data from the literature. This further reinforces the accuracy of the parameters used as the cell responds to difference frequencies as expected from previous experimental data found in the supporting literature.

The hydration models in this thesis show that within the range of conductivities from $0.005Sm^{-1}$ to $0.05Sm^{-1}$ for a constant frequency above 40kHz a quadratic model describes the variation of impedance with conductivity. Within the range of conductivities from $0.005Sm^{-1}$ to $5Sm^{-1}$ for a constant frequency above 40kHz a double decaying exponential model describes the variation of impedance with conductivity. At frequencies above 3MHz the

exponential model parameters become constant. The hydration simulations show that at high frequencies above 200kHz, and with good hydration, the skin impedance is almost constant and is approximately halved with a stratum corneum conductivity of $5Sm^{-1}$ from 19kΩ to 11kΩ for the base model and from 53kΩ to 27kΩ for the hexagonal model. This is supported by some experimental data in the literature[110], however the relationship found from the simulation is unique in this field of research. This is an important finding as it is common practice to hydrate skin when attaching electrodes but there is little research exploring the relationship between hydration and skin impedance. The results of these simulations were published in the Skin Research and technology peer-reviewed journal [29].

The sweat gland model results presented in figure 5.21 and figure 5.22 shows conductivity having a substantial impact on the overall impedance of skin. This is most evident at higher frequencies, at 5MHz there is an impedance of 1.5kΩ, which is less than 10% of the 18.3kΩ impedance at 10kHz.This is in line with both the results of the hydration model as well as experimental results found within the literature. This model stands apart from the other models in this thesis in terms of scale. Specifically, this model does not differentiate individual cells, rather gave collective dielectric properties to the distinct layers of the skin. The results of this model demonstrated that signals typically used during FES can be heavily influenced by sweat, which is the expected result based on the literature.

One of the more noticeable results came from the final set of models created. The results of the electroporation model show that when electropores are formed there is a significant decrease in overall skin impedance, with impedances of 76kΩ at 0.1V, 74kΩ, 24kΩ at 10V and 22kΩ at 100V, membrane thickness of 3nm and ITV of 0.2V. The creation of pores occurs when input voltages above 1V were used depending on the membrane thickness and exact input voltage used, meaning that during the typical use of FES the effects of electroporation should be taken into account. This can be done by assuming a significant decrease in impedance approximately 1µS after a signal is applied or by using a signal with a peak voltage lower than 1V. These results were published in the IOP Biomedical Physics & Engineering Express [30].

The fact that electroporation is a phenomenon that can occur within the range of voltages used in FES has been mentioned in studies not specifically using FES, but there is a lack of research investigating a causal link. The results of the model show that this is an area that

needs further exploration, because even when a comparatively low level of voltage (1V) was used electropores were being created. While the effects of these electropores might not be as substantial as in the simulation, they could cause a noticeable change in impedance depending on the strength of the input signal used. This is further complicated by the difficulty of determining the effect of sweat and other forms hydration that are used during FES. The models show that representing skin with an equivalent circuit will only work for certain ranges of signals used. An input voltage of 0.1V and below will not create electropores, whilst substantially higher signals may cause irreversible damage to cells. This is an important finding as there is currently no other work showing the possible relationship between FES and electroporation and the results of the simulation suggests that electroporation will effect skin impedance.

8 Future Work

The main challenges in this field of research are a lack of experimental data and the highly specific focus within the literature due to interest in specialised applications. When considering experimentation the high number of influential factors in combination with the difficulty of creating controls for comparison would require extensive research.

The effect of the type of electrode used is very influential on the overall response of skin's impedance. However, due to the comparative size and complexity introduced when modelling an actual electrode there is much more that could be done to explore this. In order to do this the model would need to be scaled to a much larger degree, at least 30mm, to accommodate for even a small electrode. This would require a substantial level of computational power and perhaps be better suited to modelling the skin as distinct layers. In order to produce a model that would be able to more accurately determine whether electroporation, be it reversible or irreversible, does occur and also to what proportion of cells it might effect it would be beneficial to produce a model at the cellular level. This could aid in the selection of electrode as well as what hydrating solution should be used for FES.

The impact of sweat glands has been explored briefly in the sweat gland model that was created in Section 5.8 of this thesis. However, as discussed there are still a lot more factors that could be used to expand the model. The influence of sweat is a lot more complex than the impact of applying a hydrating solution to the skin. One of the main difficulties is that there are a lot of factors that influence what effect sweat will have on skin impedance and these vary not only between subjects, but also with time for any given subject. Some of these variables include the chemical composition of sweat, therefore changing its conductivity and the amount of sweat present in the sweat gland.

Time dependent effects would also be an area for further exploration. In the later set of models there was a move from using set frequencies to using an input pulse, mostly driven by the need to model the effects of electroporation on skin cells. The outcome was that using a pulse resulted in a change in the membrane impedance, suggesting that electropores may be formed with FES signals. What would be of interest would be creating further models exploring whether these electropores will remain reversible over time when exposed to pulses with a higher peak or pulses in rapid succession. This extension would require direct experimentation on skin cells to determine how long the cells found in the skin specifically take to recover from the signals typically used in FES, if indeed they undergo electroporation and whether it is reversible or irreversible electroporation.

Another time dependent factor is hydration; both in the form of sweat, as discussed previously, and applied hydrating solution. While applying a solution should be a comparatively constant effect of lowering skin impedance, the impact of a hydrating solution is temporary and will decrease over time. As suggested by the results of the hydration model there will be a non-linear impact on the impedance. With regards to clinical applications, it would be of benefit to conduct experimentation into the rate of hydration and dehydration of skin cells.

As an expansion to all the models created investigating the impact of using different parameters for the individual cells and cell shapes could provide more accurate results when considering skin cells in different areas of the body. Furthermore, if any of the models were to be expanded to include a larger number of cells it might be of interest to see the impact of changing the shapes of the cells to be more irregular. This would better represent the cells found in the skin, as well as trying to determine with greater accuracy if there are any changes in the membrane properties between cells across the skin layers. This might create signals which create electropores in some cells in the simulation, as opposed to the all cells or no cells undergoing electroporation that is currently simulated. The impact of electroporation on neighbouring cells has been explored in the literature; however no full analytical solution to describe the creation of electropores has yet been formulated.

8.1 Experiment

From the work done in this thesis there are two areas that would greatly benefit from further exploration and experimentation. The first of these would focus on the effect of hydration on skin impedance. This would be of greatest interest to clinicians and have direct biomedical applications, such as FES and NMES. The second would be primarily focused on whether electropores are formed during FES, and whether this is irreversible or reversible.

Useful information to extract from the hydration experiment would be the voltages of FES signals that are safe, comfortable and maintain the most consistent impedance possible. This would preferably avoid the need to reapply any sort of hydrating solution and as well as have the same strength of signal that could be applied across a variety of skin types. Because FES technology is expected to be used for long period of time it would be important to test these signals over the period of days or weeks to determine the long term effects of these signals.

It would be important to carry these experiments out on live participants in order to incorporate any effects for the body's normal functions and incorporate effects that might not otherwise be recorded. For the purposes of initial experimentation it would be preferable to test on healthy skin to reduce the number of variables, but having some participants with dry skin would be beneficial when determining the impact of hydration.

The simulations that have been designed and tested have shown the substantial impact of electroporation on the overall impedance of skin and the comparatively small impact of hydration. The electric field strength required to cause a collection of cells to undergo electroporation is not fully defined, the exact criteria for each individual is not known so a variety of signals strengths and waveforms would need to be used. Ideally this would be done without hydration as a variable to create a baseline set of results for comparison, but as discussed previously there is evidence that applying either a negative of positive electric field to the skin's surface will attract or repel sweat stored in the glands.

Also of particular interest for the model would be finding a more exact value for the electroporation threshold, the point at which electroporation occurs due to an applied

electric field as well as determining whether hydration has an impact on overall skin impedance both before and after electroporation occurs.

An important part of an experiment looking into the effect of electroporation is the time scale required for the formation of, and recovery from, electropores. In the literature it has been shown to potentially take hours between formation of electropores and recovery to the baseline dielectric properties of the cells. Furthermore, the converse issue of the small time required for electropores is also present, with electropores occurring after approximately 1µS of the voltage being applied, assuming that the voltage being applied is sufficient for an electropore to form. This is of particular importance for FES because, as mentioned previously, this technology is expected to be used over the course of days, and may therefore not allow for sufficient recovery time.

Appendix A: COMSOL®

COMSOL® Multiphysics uses the following equations when simulating the models produced in this work:

Electric Currents:

$$\nabla \cdot \mathbf{J} = Q_j$$

$$\mathbf{J} = (\sigma + j\omega\varepsilon_0\boldsymbol{\varepsilon_r})\mathbf{E} + \mathbf{J_e}$$

$$\mathbf{E} = -\nabla V$$

Electric Insulation:

$$\mathbf{n} \cdot \mathbf{J} = 0$$

Contact Impedance:

$$\mathbf{n} \cdot \mathbf{J_1} = \frac{1}{d_s}(\sigma + j\omega\varepsilon_0\boldsymbol{\varepsilon_r})(V_1 - V_2)$$

$$\mathbf{n} \cdot \mathbf{J_2} = \frac{1}{d_s}(\sigma + j\omega\varepsilon_0\boldsymbol{\varepsilon_r})(V_2 - V_1)$$

Where **J** is current density, Q is charge, E is the electric field, V is voltage, d_s is surface thickness, σ is conductivity, $\boldsymbol{\varepsilon_r}$ is relative permittivity, ε_0 is the permittivity of free space and V_1 and V_2 are the voltages on both sides of the boundary

The models do not include thermal or mechanical effects as reflected in the equations above. The initial condition necessary for the simulations to run is a value for V which is 0V unless otherwise stated.

Appendix B: Timings and example COMSOL® Multiphysics code

Typical run times for simulation:

Model	Typical run time	Average Mesh Density (μm^{-3})
Spherical cell model	10 mins	21.1
Epithelium cell model, one Frequency	15 mins	19.4
3 x 6 Cell model, one frequency	25 mins	18.4
Hydration model, 1 frequency all 10 SC conductivities	1 hr 05mins	17.5
Sweat gland model, one frequency	15 mins	5.6
Electroporation model 1 Voltage, all membrane and ITV Threshold values	1 hr 55 mins	18.2

These run times can vary sensationally due to changes in input parameters, particularly the electroporation model, and for some initial set ups a simulation would not converge but in most cases would vary by no more the 5% of the typical run times.

Computer Specifications:

CPU Brand: AMD FX(tm)-8350 Eight-Core Processor

Speed: 4018 MHz

8 logical processors

Operating System Version: Windows 10 (64 bit)

Driver: NVIDIA GeForce GTX 1060 6GB

Primary Bus: PCI Express 16x

Primary VRAM: 6143 MB

RAM: 16354 Mb

Example section of COMSOL code showing the set up for the geometry, materials used and the physics applied for the spherical cell model:

```
function out = model
%
% Block_Cell_single.m
%
% Model exported on Sep 21 2017, 07:50 by COMSOL 5.2.1.152.
```

```
import com.comsol.model.*
import com.comsol.model.util.*

model = ModelUtil.create('Model');

model.modelPath('D:\Google Drive\COMSOL');

model.modelNode.create('comp1');

model.geom.create('geom1', 3);

model.mesh.create('mesh1', 'geom1');

model.physics.create('ec', 'ConductiveMedia', 'geom1');

model.study.create('std1');
model.study('std1').feature.create('stat', 'Stationary');
model.study('std1').feature('stat').activate('ec', true);

model.geom('geom1').feature.create('blk1', 'Block');
model.geom('geom1').feature('blk1').setIndex('size', '30', 0);
model.geom('geom1').feature('blk1').setIndex('size', '15', 1);
model.geom('geom1').feature('blk1').setIndex('size', '15', 2);
model.geom('geom1').feature('blk1').setIndex('size', '30', 1);
model.geom('geom1').feature('blk1').set('base', 'center');
model.geom('geom1').run('blk1');
model.geom('geom1').run('blk1');
model.geom('geom1').feature.create('blk2', 'Block');
model.geom('geom1').lengthUnit([native2unicode(hex2dec({'00' 'b5'}),
'unicode') 'm']);
model.geom('geom1').run('fin');
model.geom('geom1').feature('blk2').setIndex('size', '1.5', 0);
model.geom('geom1').feature('blk2').setIndex('size', '.75', 1);
model.geom('geom1').feature('blk2').setIndex('size', '.75', 2);
model.geom('geom1').feature('blk2').set('base', 'center');
model.geom('geom1').run('blk2');
model.geom('geom1').feature('blk2').setIndex('size', '1.5', 1);
model.geom('geom1').run('blk2');
model.geom('geom1').run('blk2');
model.geom('geom1').feature.create('blk3', 'Block');
model.geom('geom1').feature('blk3').setIndex('size', '32', 0);
model.geom('geom1').feature('blk3').setIndex('size', '32', 1);
model.geom('geom1').feature('blk3').setIndex('size', '17', 2);
model.geom('geom1').feature('blk3').setIndex('size', '34', 0);
model.geom('geom1').feature('blk3').setIndex('size', '34', 1);
model.geom('geom1').feature('blk3').setIndex('size', '19', 2);
model.geom('geom1').feature('blk3').set('base', 'center');
model.geom('geom1').run('blk3');
model.geom('geom1').feature('blk1').name('Cytoplasm');
model.geom('geom1').feature('blk2').name('Nucleus');
model.geom('geom1').feature('blk3').name('Extracellular width');
model.geom('geom1').run('fin');

model.material.create('mat1');
model.material('mat1').propertyGroup('def').set('electricconductivity',
{'1.1[S/m]'});
model.material('mat1').propertyGroup('def').set('relpermittivity',
{'72'});
```

```
model.material('mat1').selection.set([1]);
model.material.create('mat2');
model.material.create('mat3');
model.material('mat1').name('Extracellular space');
model.material('mat2').name('Cytoplasm');
model.material('mat3').name('Nuclear interior');
model.material('mat2').selection.set([2]);
model.material('mat3').selection.set([3]);
model.material('mat2').propertyGroup('def').set('electricconductivity',
{'0.6'});
model.material('mat2').propertyGroup('def').set('relpermittivity',
{'86'});
model.material('mat3').propertyGroup('def').set('electricconductivity',
{'.8'});
model.material('mat3').propertyGroup('def').set('relpermittivity',
{'145'});

model.physics('ec').feature.create('dimp1', 'DistributedImpedance', 2);
model.physics('ec').feature.create('dimp2', 'DistributedImpedance', 2);
model.physics('ec').feature('dimp1').name('Distributed Impedance
Cmem');
model.physics('ec').feature('dimp2').name('Distributed Impedance
Nmem');
model.physics('ec').feature('dimp1').selection.set([6 7 8 9 10 17]);
model.physics('ec').feature('dimp1').set('ds', 1, '8[nm]');
model.physics('ec').feature('dimp1').set('sigmabnd_mat', 1, 'userdef');
model.physics('ec').feature('dimp1').set('sigmabnd', 1, '0.1[S/m]');
model.physics('ec').feature('dimp1').set('epsilonrbnd_mat', 1,
'userdef');
model.physics('ec').feature('dimp1').set('epsilonrbnd', 1, '31');
model.physics('ec').feature('dimp1').set('epsilonrbnd', 1, '9');
model.physics('ec').feature('dimp2').set('sigmabnd_mat', 1, 'userdef');
model.physics('ec').feature('dimp2').set('epsilonrbnd_mat', 1,
'userdef');
model.physics('ec').feature('dimp2').set('epsilonrbnd', 1, '31');
model.physics('ec').feature('dimp2').set('sigmabnd', 1, '2000[S/m]');
model.physics('ec').feature.create('pot1', 'ElectricPotential', 2);
model.physics('ec').feature('pot1').selection.set([1]);
model.physics('ec').feature.create('gnd1', 'Ground', 2);
model.physics('ec').feature('gnd1').selection.set([18]);
model.physics('ec').feature('pot1').set('V0', 1, '0.2');

model.mesh('mesh1').run;
model.mesh('mesh1').feature.create('ftet2', 'FreeTet');
model.mesh('mesh1').feature('ftet2').selection.geom('geom1', 3);

model.mesh('mesh1').feature('ftet2').selection.set([3]);
model.mesh('mesh1').feature('ftet2').feature.create('size1', 'Size');
model.mesh('mesh1').feature('ftet2').feature('size1').set('hauto',
'3');
model.mesh('mesh1').run('ftet2');
model.mesh('mesh1').run;
model.mesh('mesh1').feature('ftet2').feature('size1').set('hauto',
'2');
model.mesh('mesh1').run;
model.mesh('mesh1').feature('ftet2').feature('size1').set('hauto',
'1');
model.mesh('mesh1').run;
```

```
model.mesh('mesh1').feature('ftet2').feature('size1').set('hauto',
'4');
model.mesh('mesh1').run('ftet2');
model.mesh('mesh1').feature('ftet2').feature('size1').set('hauto',
'3');
model.mesh('mesh1').run('ftet2');
model.mesh('mesh1').feature('size').set('hauto', '4');
model.mesh('mesh1').run;
model.mesh('mesh1').run;
model.mesh('mesh1').feature('ftet2').feature('size1').set('hauto',
'4');
model.mesh('mesh1').feature('size').set('hauto', '1');
model.mesh('mesh1').run;
model.mesh('mesh1').run;
model.mesh('mesh1').feature('size').set('hauto', '5');
model.mesh('mesh1').run;
model.mesh('mesh1').feature('ftet2').feature('size1').set('hauto',
'2');
model.mesh('mesh1').run;
```

Appendix C: Parameter sweep results

Cytoplasm Conductivity Change:

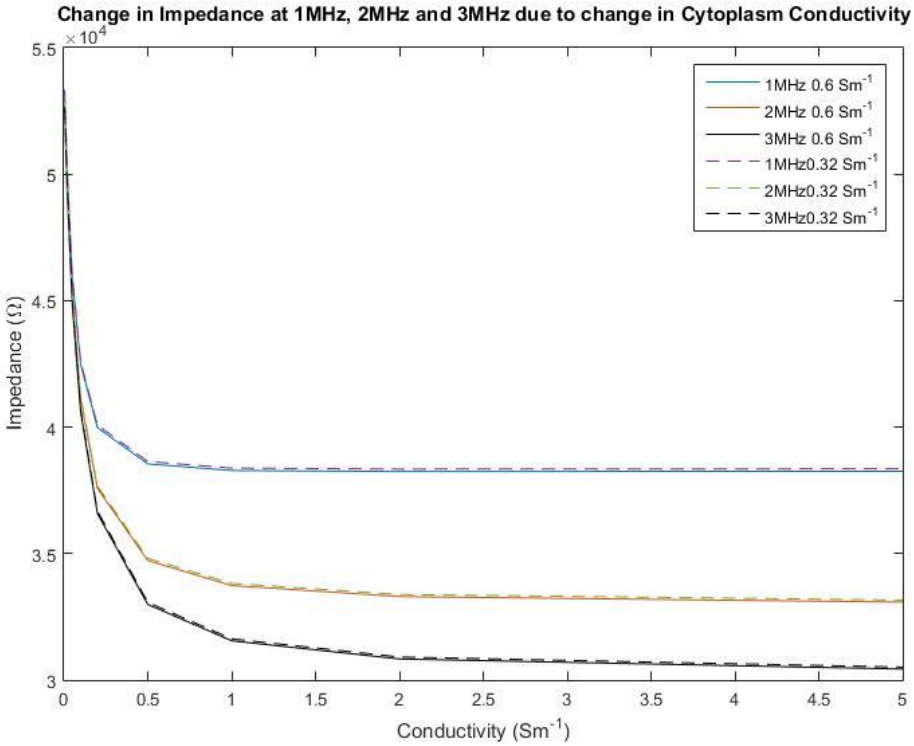

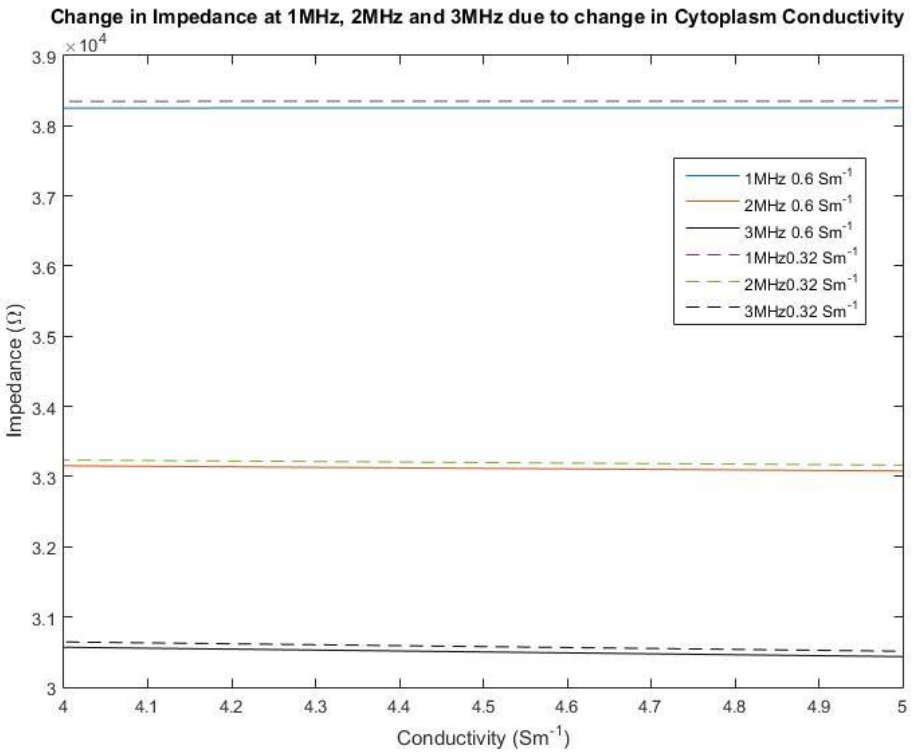

The results show a small variation due to changes in the cytoplasm conductivity but this is minor compared to the effect of hydration, frequency or electroporation.

References

[1] S. Verdier-Sévrain and F. Bonté, “Skin hydration: a review on its molecular mechanisms,” *J. Cosmet. Dermatol.*, vol. 6, no. 2, pp. 75–82, Jun. 2007.

[2] R. S. Son, K. C. Smith, T. R. Gowrishankar, P. T. Vernier, and J. C. Weaver, “Basic Features of a Cell Electroporation Model: Illustrative Behavior for Two Very Different Pulses,” *J. Membr. Biol.*, vol. 247, no. 12, pp. 1209–1228, Jul. 2014.

[3] O. G. Martinsen and S. Grimnes, *Bioimpedance and Bioelectricity Basics*. Academic Press, 2011.

[4] S. Gabriel, R. W. Lau, and C. Gabriel, “The dielectric properties of biological tissues: II. Measurements in the frequency range 10 Hz to 20 GHz,” *Phys. Med. Biol.*, vol. 41, no. 11, p. 2251, Nov. 1996.

[5] C. Gabriel, S. Gabriel, and E. Corthout, “The dielectric properties of biological tissues: I. Literature survey,” *Phys. Med. Biol.*, vol. 41, no. 11, p. 2231, Nov. 1996.

[6] C. Gabriel, A. Peyman, and E. H. Grant, “Electrical conductivity of tissue at frequencies below 1 MHz,” *Phys. Med. Biol.*, vol. 54, no. 16, p. 4863, 2009.

[7] I. Nicander, L. Emtestam, P. \AAberg, and S. Ollmar, “Twelve years evolution of skin as seen by electrical impedance,” in *Journal of Physics: Conference Series*, 2010, vol. 224, p. 012092.

[8] H. N. Mayrovitz, M. Bernal, and S. Carson, “Gender differences in facial skin dielectric constant measured at 300 MHz,” *Skin Res. Technol.*, vol. 18, no. 4, pp. 504–510, 2012.

[9] G. K. Johnsen, “Skin electrical properties and physical aspects of hydration of keratinized tissues,” PhD Thesis, University of Oslo, 2010.

[10] U. Birgersson, E. Birgersson, I. Nicander, and S. Ollmar, “A methodology for extracting the electrical properties of human skin,” *Physiol. Meas.*, vol. 34, no. 6, p. 723, Jun. 2013.

[11] S. R. Smith and K. R. Foster, “Dielectric properties of low-water-content tissues,” *Phys. Med. Biol.*, vol. 30, no. 9, p. 965, Sep. 1985.

[12] G. N. Stamatas, J. Nikolovski, M. C. Mack, and N. Kollias, “Infant skin physiology and development during the first years of life: a review of recent findings based on in vivo studies,” *Int. J. Cosmet. Sci.*, vol. 33, no. 1, pp. 17–24, Feb. 2011.

[13] C. Gabriel, “Dielectric properties of biological tissue: Variation with age,” *Bioelectromagnetics*, vol. 26, no. S7, pp. S12–S18, Jan. 2005.

[14] I. Nicander and S. Ollmar, “Electrical impedance measurements at different skin sites related to seasonal variations,” *Skin Res. Technol.*, vol. 6, no. 2, pp. 81–86, May 2000.

[15] M. A. Messerli and D. M. Graham, “Extracellular electrical fields direct wound healing and regeneration,” *Biol. Bull.*, vol. 221, no. 1, pp. 79–92, 2011.

[16] C. Jiang, R. V. Davalos, and J. C. Bischof, “A Review of Basic to Clinical Studies of Irreversible Electroporation Therapy,” *IEEE Trans. Biomed. Eng.*, vol. 62, no. 1, pp. 4–20, Jan. 2015.

[17] R. P. Joshi and K. H. Schoenbach, “Mechanism for membrane electroporation irreversibility under high-intensity, ultrashort electrical pulse conditions,” *Phys. Rev. E*, vol. 66, no. 5, p. 052901, Nov. 2002.

[18] A. P. Davie *et al.*, “Value of the electrocardiogram in identifying heart failure due to left ventricular systolic dysfunction,” *Bmj*, vol. 312, no. 7025, p. 222, 1996.

[19] E. Niedermeyer and F. L. da Silva, *Electroencephalography: basic principles, clinical applications, and related fields*. Lippincott Williams & Wilkins, 2005.

[20] E. Criswell, *Cram’s introduction to surface electromyography*. Jones & Bartlett Publishers, 2010.

[21] S. Ud-Din *et al.*, “Angiogenesis Is Induced and Wound Size Is Reduced by Electrical Stimulation in an Acute Wound Healing Model in Human Skin,” *PLOS ONE*, vol. 10, no. 4, p. e0124502, Apr. 2015.

[22] M. Osiri *et al.*, “Transcutaneous electrical nerve stimulation for knee osteoarthritis (Review),” *Cochrane Libr.*, no. 4, 2009.

[23] R. Butikofer and P. D. Lawrence, “Electrocutaneous Nerve Stimulation-I: Model and Experiment,” *IEEE Trans. Biomed. Eng.*, vol. BME-25, no. 6, pp. 526–531, Nov. 1978.

[24] C. L. Lynch and M. R. Popovic, “Functional Electrical Stimulation,” *IEEE Control Syst.*, vol. 28, no. 2, pp. 40–50, Apr. 2008.
[25] G. Alon, “Functional Electrical Stimulation (FES): Transforming Clinical Trials to Neuro-Rehabilitation Clinical Practice- A Forward Perspective,” *J. Nov. Physiother.*, Aug. 2013.
[26] J. L. Vargas Luna, M. Krenn, J. A. Cortés Ramírez, and W. Mayr, “Dynamic Impedance Model of the Skin-Electrode Interface for Transcutaneous Electrical Stimulation,” *PLoS ONE*, vol. 10, no. 5, May 2015.
[27] A.-M. R. Almalty, S. H. Hamed, F. M. Al-Dabbak, and A. E. Shallan, “Short-term and Long-term Effects of Electrical Stimulation on Skin Properties,” *Physiother. Res. Int.*, vol. 18, no. 3, pp. 157–166, Sep. 2013.
[28] K. S. Frahm, C. D. Mørch, W. M. Grill, N. B. Lubock, K. Hennings, and O. K. Andersen, “Activation of peripheral nerve fibers by electrical stimulation in the sole of the foot,” *BMC Neurosci.*, vol. 14, no. 1, p. 116, Oct. 2013.
[29] L. Davies, P. Chappell, and T. Melvin, “Modelling the effect of hydration on skin conductivity,” *Skin Res. Technol.*, pp. 363–368, Nov. 2016.
[30] L. Davies and P. Chappell, “The effects of electroporation on skin impedance,” *Biomed. Phys. Eng. Express*, vol. 4, no. 2, p. 025012, 2018.
[31] J. A. Bouwstra, “The skin barrier, a well-organized membrane,” *Colloids Surf. Physicochem. Eng. Asp.*, vol. 123–124, pp. 403–413, May 1997.
[32] L. Coderch, O. López, A. de la Maza, and J. L. Parra, “Ceramides and skin function,” *Am. J. Clin. Dermatol.*, vol. 4, no. 2, pp. 107–129, 2003.
[33] J. E. Lai-Cheong and J. A. McGrath, “Structure and function of skin, hair and nails,” *Medicine (Baltimore)*, vol. 37, no. 5, pp. 223–226, May 2009.
[34] Y. P. Guo, Y. Li, L. Yao, R. Liu, X. Y. Cao, and M. L. Cao, “Skin Temperature, Stratum corneum water content and transepidermal water loss distributions during running,” *J Fiber Bioeng Inf.*, vol. 4, no. 3, pp. 253–266, 2011.
[35] M. Harker, “Psychological sweating: a systematic review focused on aetiology and cutaneous response,” *Skin Pharmacol. Physiol.*, vol. 26, no. 2, pp. 92–100, 2013.
[36] S. Saeed, *Lookingbill & Marks’ Principles of Dermatology*. LWW, 2007.
[37] P. M. Elias, “The skin barrier as an innate immune element,” in *Seminars in immunopathology*, 2007, vol. 29, pp. 3–14.
[38] N. Kirschner, P. Houdek, M. Fromm, I. Moll, and J. M. Brandner, “Tight junctions form a barrier in human epidermis,” *Eur. J. Cell Biol.*, vol. 89, no. 11, pp. 839–842, Nov. 2010.
[39] G. K. Menon, G. W. Cleary, and M. E. Lane, “The structure and function of the stratum corneum,” *Int. J. Pharm.*, vol. 435, no. 1, pp. 3–9, Oct. 2012.
[40] T. Yamamoto and Y. Yamamoto, “Dielectric constant and resistivity of epidermal stratum corneum,” *Med. Biol. Eng.*, vol. 14, no. 5, pp. 494–500, Sep. 1976.
[41] U. Pliquett, R. Langer, and J. C. Weaver, “Changes in the passive electrical properties of human stratum corneum due to electroporation,” *Biochim. Biophys. Acta BBA - Biomembr.*, vol. 1239, no. 2, pp. 111–121, Nov. 1995.
[42] G. Yosipovitch, G. L. Xiong, E. Haus, L. Sackett-Lundeen, I. Ashkenazi, and H. I. Maibach, “Time-Dependent Variations of the Skin Barrier Function in Humans: Transepidermal Water Loss, Stratum Corneum Hydration, Skin Surface pH, and Skin Temperature,” *J. Invest. Dermatol.*, vol. 110, no. 1, pp. 20–24, Jan. 1998.
[43] R. Lu, S. K. Banerjee, and J. Marvin, “Effects of clay mineralogy and the electrical conductivity of water on the acquisition of depositional remanent magnetization in sediments,” *J. Geophys. Res. Solid Earth*, vol. 95, no. B4, pp. 4531–4538, Apr. 1990.
[44] H. N. Mayrovitz, M. Bernal, F. Brlit, and R. Desfor, “Biophysical measures of skin tissue water: variations within and among anatomical sites and correlations between measures,” *Skin Res. Technol.*, vol. 19, no. 1, pp. 47–54, 2013.

[45] T. S. Light, S. Licht, A. C. Bevilacqua, and K. R. Morash, “The Fundamental Conductivity and Resistivity of Water,” *Electrochem. Solid-State Lett.*, vol. 8, no. 1, p. E16, 2005.
[46] K. Wilke, A. Martin, L. Terstegen, and S. S. Biel, “A short history of sweat gland biology,” *Int. J. Cosmet. Sci.*, vol. 29, no. 3, pp. 169–179, 2007.
[47] C. Tronstad, H. avard Kalvøy, S. Grimnes, and Ø. G. Martinsen, “Improved Estimation of Sweating Based on Electrical Properties of Skin,” *Ann. Biomed. Eng.*, vol. 41, no. 5, pp. 1074–1083, 2013.
[48] “Three-dimensional cell shapes and arrangements in human sweat glands as revealed by whole-mount immunostaining.” [Online]. Available: http://journals.plos.org/plosone/article?id=10.1371/journal.pone.0178709. [Accessed: 19-Sep-2017].
[49] G. Liu *et al.*, “Real-time sweat analysis via alternating current conductivity of artificial and human sweat,” *Appl. Phys. Lett.*, vol. 106, no. 13, p. 133702, Mar. 2015.
[50] L. R. Arias, C. A. Perry, and L. Yang, “Real-time electrical impedance detection of cellular activities of oral cancer cells,” *Biosens. Bioelectron.*, vol. 25, no. 10, pp. 2225–2231, 2010.
[51] D. M. Bryant and K. E. Mostov, “From cells to organs: building polarized tissue,” *Nat. Rev. Mol. Cell Biol.*, vol. 9, no. 11, pp. 887–901, Nov. 2008.
[52] S. Elia, P. Lamberti, and V. Tucci, “A Finite Element Model for The Axon of Nervous Cells,” in *COMSOL Europe Conference*, 2009, pp. 14–16.
[53] T. Seyama, E. Y. Suh, and T. Kondo, “Three-dimensional culture of epidermal cells on ordered cellulose scaffolds,” *Biofabrication*, vol. 5, no. 2, p. 025010, Jun. 2013.
[54] L.-H. Gu and P. A. Coulombe, “Keratin function in skin epithelia: a broadening palette with surprising shades,” *Curr. Opin. Cell Biol.*, vol. 19, no. 1, pp. 13–23, Feb. 2007.
[55] S.-J. Bai and F. B. Prinz, “In vivo electrochemical impedance measurement on single cell membrane,” *Microelectron. Eng.*, vol. 88, no. 10, pp. 3094–3100, Oct. 2011.
[56] E. T. McAdams and J. Jossinet, “Problems in equivalent circuit modelling of the electrical properties of biological tissues,” *Bioelectrochem. Bioenerg.*, vol. 40, no. 2, pp. 147–152, 1996.
[57] C. B. Jeong, J. Y. Han, J. C. Cho, K. D. Suh, and G. W. Nam, “Analysis of electrical property changes of skin by oil-in-water emulsion components,” *Int. J. Cosmet. Sci.*, vol. 35, no. 4, pp. 402–410, 2013.
[58] M. Amin, P. P. Dey, and H. Badkoobehi, “A complete electrical equivalent circuit model for biological cell,” in *Proceedings of the 7th WSEAS International Conference on Applied Computer and Applied Computational Science*, 2008, pp. 343–348.
[59] M. R. Ahmad, M. Nakajima, T. Fukuda, S. Kojima, and M. Homma, “Single cells electrical characterizations using nanoprobe via ESEM-nanomanipulator system,” in *Nanotechnology, 2009. IEEE-NANO 2009. 9th IEEE Conference on*, 2009, pp. 589–592.
[60] A. di Biasio, L. Ambrosone, and C. Cametti, “Numerical simulation of dielectric spectra of aqueous suspensions of non-spheroidal differently shaped biological cells,” *J. Phys. Appl. Phys.*, vol. 42, no. 2, p. 025401, Jan. 2009.
[61] T. Schmid, M. Bogdan, and D. Günzel, “Discerning apical and basolateral properties of HT-29/B6 and IPEC-J2 cell layers by impedance spectroscopy, mathematical modeling and machine learning,” *PloS One*, vol. 8, no. 7, p. e62913, 2013.
[62] S. Huclova, D. Erni, and J. Fröhlich, “Modelling and validation of dielectric properties of human skin in the MHz region focusing on skin layer morphology and material composition,” *J. Phys. Appl. Phys.*, vol. 45, no. 2, p. 025301, Jan. 2012.
[63] Y. A. Chizmadzhev, A. V. Indenbom, P. I. Kuzmin, S. V. Galichenko, J. C. Weaver, and R. O. Potts, “Electrical properties of skin at moderate voltages: contribution of appendageal macropores.,” *Biophys. J.*, vol. 74, no. 2 Pt 1, pp. 843–856, Feb. 1998.
[64] R. Sharma, “Skin age testing criteria: characterization of human skin structures by 500 MHz MRI multiple contrast and image processing,” *Phys. Med. Biol.*, vol. 55, no. 14, p. 3959, 2010.
[65] S. Björklund *et al.*, “Skin Membrane Electrical Impedance Properties under the Influence of a Varying Water Gradient,” *Biophys. J.*, vol. 104, no. 12, pp. 2639–2650, Jun. 2013.

[66] M. Venus, J. Waterman, and I. McNab, “Basic physiology of the skin,” *Surg. Oxf.*, vol. 29, no. 10, pp. 471–474, 2011.
[67] H. N. Mayrovitz, “Local tissue water assessed by measuring forearm skin dielectric constant: dependence on measurement depth, age and body mass index,” *Skin Res. Technol.*, vol. 16, no. 1, pp. 16–22, 2010.
[68] I. H. Blank, “Factors Which Influence the Water Content of the Stratum Corneum1,” *J. Invest. Dermatol.*, vol. 18, no. 6, pp. 433–440, Jun. 1952.
[69] H. Tagami, “Location-related differences in structure and function of the stratum corneum with special emphasis on those of the facial skin,” *Int. J. Cosmet. Sci.*, vol. 30, no. 6, pp. 413–434, Dec. 2008.
[70] “Water conductivity - Lenntech.” [Online]. Available: http://www.lenntech.com/applications/ultrapure/conductivity/water-conductivity.htm. [Accessed: 10-Sep-2017].
[71] D. N. Rushton, “Functional electrical stimulation,” *Physiol. Meas.*, vol. 18, no. 4, p. 241, Nov. 1997.
[72] M. Handler, R. Nelson, D. Krapohl, and C. R. Honts, “An EDA primer for polygraph examiners,” *Polygraph*, vol. 39, no. 2, pp. 68–108, 2010.
[73] D. J. Hewson, J.-Y. Hogrel, Y. Langeron, and J. Duchêne, “Evolution in impedance at the electrode-skin interface of two types of surface EMG electrodes during long-term recordings,” *J. Electromyogr. Kinesiol.*, vol. 13, no. 3, pp. 273–279, 2003.
[74] A. Adamson, *A textbook of physical chemistry*. Elsevier, 1973.
[75] G. Liu *et al.*, “A wearable conductivity sensor for wireless real-time sweat monitoring,” *Sens. Actuators B Chem.*, vol. 227, pp. 35–42, May 2016.
[76] S. I. Birlea, N. M. Birlea, P. P. Breen, and G. ÓLaighin, “Identifying skin electrical properties using a standard neuromuscular electrical stimulation voltage pulse,” 2008.
[77] S. Huclova, D. Erni, and J. Fröhlich, “Modelling effective dielectric properties of materials containing diverse types of biological cells,” *J. Phys. Appl. Phys.*, vol. 43, no. 36, p. 365405, Sep. 2010.
[78] T. R. Gowrishankar and J. C. Weaver, “An approach to electrical modeling of single and multiple cells,” *Proc. Natl. Acad. Sci.*, vol. 100, no. 6, pp. 3203–3208, 2003.
[79] G. H. Markx and C. L. Davey, “The dielectric properties of biological cells at radiofrequencies: applications in biotechnology,” *Enzyme Microb. Technol.*, vol. 25, no. 3–5, pp. 161–171, Aug. 1999.
[80] E. C. Gregg and K. D. Steidley, “Electrical counting and sizing of mammalian cells in suspension,” *Biophys. J.*, vol. 5, no. 4, pp. 393–405, 1965.
[81] G. Pucihar, D. Miklavcic, and T. Kotnik, “A time-dependent numerical model of transmembrane voltage inducement and electroporation of irregularly shaped cells,” *Biomed. Eng. IEEE Trans. On*, vol. 56, no. 5, pp. 1491–1501, 2009.
[82] G. Pucihar, T. Kotnik, B. Valič, and D. Miklavčič, “Numerical determination of transmembrane voltage induced on irregularly shaped cells,” *Ann. Biomed. Eng.*, vol. 34, no. 4, pp. 642–652, 2006.
[83] G. Bonmassar, S. Iwaki, G. Goldmakher, L. M. Angelone, J. W. Belliveau, and M. H. Lev, “On the measurement of electrical impedance spectroscopy (EIS) of the human head,” *Int. J. Bioelectromagn.*, vol. 12, no. 1, p. 32, 2010.
[84] L. M. Broche, N. Bhadal, M. P. Lewis, S. Porter, M. P. Hughes, and F. H. Labeed, “Early detection of oral cancer – Is dielectrophoresis the answer?,” *Oral Oncol.*, vol. 43, no. 2, pp. 199–203, Feb. 2007.
[85] N. Pavšelj and D. Miklavčič, “Resistive heating and electropermeabilization of skin tissue during in vivo electroporation: A coupled nonlinear finite element model,” *Int. J. Heat Mass Transf.*, vol. 54, no. 11–12, pp. 2294–2302, May 2011.

[86] I. Meny, N. Burais, F. Buret, and L. Nicolas, “Finite-Element Modeling of Cell Exposed to Harmonic and Transient Electric Fields,” *IEEE Trans. Magn.*, vol. 43, no. 4, pp. 1773–1776, Apr. 2007.
[87] F. Apollonio, M. Liberti, P. Marracino, and L. Mir, “Electroporation mechanism: Review of molecular models based on computer simulation,” in *2012 6th European Conference on Antennas and Propagation (EUCAP)*, 2012, pp. 356–358.
[88] C. Chen, S. W. Smye, M. P. Robinson, and J. A. Evans, “Membrane electroporation theories: a review,” *Med. Biol. Eng. Comput.*, vol. 44, no. 1–2, pp. 5–14, Feb. 2006.
[89] C. Daniels and B. Rubinsky, “Electrical Field and Temperature Model of Nonthermal Irreversible Electroporation in Heterogeneous Tissues,” *J. Biomech. Eng.*, vol. 131, no. 7, pp. 071006–071006, Jul. 2009.
[90] A.-R. Denet, R. Vanbever, and V. Préat, “Skin electroporation for transdermal and topical delivery,” *Adv. Drug Deliv. Rev.*, vol. 56, no. 5, pp. 659–674, 2004.
[91] T. Kotnik, P. Kramar, G. Pucihar, D. Miklavcic, and M. Tarek, “Cell membrane electroporation-Part 1: The phenomenon,” *IEEE Electr. Insul. Mag.*, vol. 28, no. 5, pp. 14–23, Sep. 2012.
[92] A. Al-Khadra, V. Nikolski, and I. R. Efimov, “The Role of Electroporation in Defibrillation,” *Circ. Res.*, vol. 87, no. 9, pp. 797–804, Oct. 2000.
[93] T. Kotnik, F. Bobanović, and D. Miklavc˘ic˘, “Sensitivity of transmembrane voltage induced by applied electric fields—a theoretical analysis,” *Bioelectrochem. Bioenerg.*, vol. 43, no. 2, pp. 285–291, 1997.
[94] Øs. G. Martinsen, S. Grimnes, and E. Haug, “Measuring depth depends on frequency in electrical skin impedance measurements,” *Skin Res. Technol.*, vol. 5, no. 3, pp. 179–181, Aug. 1999.
[95] X. Huang, W.-H. Yeo, Y. Liu, and J. A. Rogers, “Epidermal differential impedance sensor for conformal skin hydration monitoring,” *Biointerphases*, vol. 7, no. 1, p. 52, 2012.
[96] S. Luebberding, N. Krueger, and M. Kerscher, “Skin physiology in men and women: in vivo evaluation of 300 people including TEWL, SC hydration, sebum content and skin surface pH,” *Int. J. Cosmet. Sci.*, vol. 35, no. 5, pp. 477–483, Oct. 2013.
[97] Ø. G. Martinsen and S. Grimnes, “Facts and myths about electrical measurement of stratum corneum hydration state,” *Dermatology*, vol. 202, no. 2, pp. 87–89, 2001.
[98] O. G. Martinsen *et al.*, “Gravimetric Method for in Vitro Calibration of Skin Hydration Measurements,” *IEEE Trans. Biomed. Eng.*, vol. 55, no. 2, pp. 728–732, Feb. 2008.
[99] H. Tagami, “Electrical measurement of the hydration state of the skin surface in vivo,” *Br. J. Dermatol.*, vol. 171, pp. 29–33, Sep. 2014.
[100] M. Hjouj and B. Rubinsky, “Electroporation,” in *Image-Guided Cancer Therapy*, D. E. Dupuy, Y. Fong, and W. N. McMullen, Eds. Springer New York, 2013, pp. 21–36.
[101] A. Meir and B. Rubinsky, “Electrical impedance tomographic imaging of a single cell electroporation,” *Biomed. Microdevices*, vol. 16, no. 3, pp. 427–437, Feb. 2014.
[102] M. Silk, D. Tahour, G. Srimathveeravalli, S. B. Solomon, and R. H. Thornton, “The State of Irreversible Electroporation in Interventional Oncology,” *Semin. Interv. Radiol.*, vol. 31, no. 2, pp. 111–117, Jun. 2014.
[103] L. Rittié, D. L. Sachs, J. S. Orringer, J. J. Voorhees, and G. J. Fisher, “Eccrine Sweat Glands are Major Contributors to Reepithelialization of Human Wounds,” *Am. J. Pathol.*, vol. 182, no. 1, pp. 163–171, Jan. 2013.
[104] Z. Ya-Xian, T. Suetake, and H. Tagami, “Number of cell layers of the stratum corneum in normal skin – relationship to the anatomical location on the body, age, sex and physical parameters,” *Arch. Dermatol. Res.*, vol. 291, no. 10, pp. 555–559, Nov. 1999.
[105] T. Uchiyama, S. Ishigame, J. Niitsuma, Y. Aikawa, and Y. Ohta, “Multi-frequency bioelectrical impedance analysis of skin rubor with two-electrode technique,” *J. Tissue Viability*, vol. 17, no. 4, pp. 110–114, 2008.

[106] E. Alanen, T. Lahtinen, and J. Nuutinen, “Measurement of dielectric properties of subcutaneous fat with open-ended coaxial sensors,” *Phys. Med. Biol.*, vol. 43, no. 3, p. 475, Mar. 1998.
[107] R. Merletti, “The electrode–skin interface and optimal detection of bioelectric signals,” *Physiol. Meas.*, vol. 31, no. 10, p. null, Oct. 2010.
[108] H. Morgan, T. Sun, D. Holmes, S. Gawad, and N. G. Green, “Single cell dielectric spectroscopy,” *J. Phys. Appl. Phys.*, vol. 40, no. 1, p. 61, Jan. 2007.
[109] D. C. Walker, “Modelling the electrical properties of cervical epithelium.,” PhD Thesis, University of Sheffield, 2001.
[110] M. S. Kim, Y. Cho, S.-T. Seo, C.-S. Son, H.-J. Park, and Y.-N. Kim, “A New Method for Non-Invasive Measurement of Skin in the Low Frequency Range,” *Healthc. Inform. Res.*, vol. 16, no. 3, p. 143, 2010.
[111] “X. The Organs of the Senses and the Common Integument. 2. The Common Integument. Gray, Henry. 1918. Anatomy of the Human Body.” [Online]. Available: http://www.bartleby.com/107/234.html. [Accessed: 10-Sep-2017].
[112] S. I. Birlea, N. M. Birlea, P. P. Breen, and G. O’Laighin, “Identifying changes in human skin electrical properties due to long-term NeuroMuscular Electrical Stimulation,” in *Engineering in Medicine and Biology Society, 2008. EMBS 2008. 30th Annual International Conference of the IEEE*, 2008, pp. 326–329.
[113] M. R. Prausnitz, V. G. Bose, R. Langer, and J. C. Weaver, “Electroporation of mammalian skin: a mechanism to enhance transdermal drug delivery.,” *Proc. Natl. Acad. Sci.*, vol. 90, no. 22, pp. 10504–10508, Nov. 1993.
[114] “Locally enhanced chemotherapy by electroporation: clinical experiences and perspective of use of electrochemotherapy,” *Future Oncol.*, vol. 10, no. 5, pp. 877–890, Apr. 2014.
[115] A. Denzi *et al.*, “Assessment of Cytoplasm Conductivity by Nanosecond Pulsed Electric Fields,” *IEEE Trans. Biomed. Eng.*, vol. 62, no. 6, pp. 1595–1603, Jun. 2015.